1-1-2015

Controlling Thermogenesis: Understanding the Role of PRDM16 in the Development and Function of Brown Fat

Matthew James Harms
University of Pennsylvania, matthew.j.harms@gmail.com

Controlling Thermogenesis: Understanding the Role of PRDM16 in the Development and Function of Brown Fat

Abstract
The alarming rise in the incidence of obesity found throughout the world has precipitated a need to look for novel methods to increase energy expenditure to counter weight gain. Recently it was discovered that adult humans possess a substantial mass of brown adipose tissue (BAT), a tissue that consumes stored lipid to produce heat. Although the primary physiologic role for BAT is to protect mammals from the cold, it is currently thought that enhancing BAT mass or activating BAT in humans is a novel way to decrease adiposity. However, before BAT can be effectively utilized for therapeutic purposes a better understanding of the transcriptional regulation underlying BAT function is required. Here, we investigated the role of the transcription factor PRDM16 in BAT. We found that PRDM16 is not required for BAT development, however it is required to maintain BAT identity in adult mice. The loss of PRDM16 in adult mice led to a loss of BAT functionality and an inability to produce heat. We found that PRDM16s ability to drive a thermogenic program is due to its recruitment of Med1/the Mediator Complex to BAT-selective genes. Without PRDM16 in BAT a loss of higher order chromatin structure and a corresponding loss of transcription takes place at genes required for BAT identity and function.

Degree Type
Dissertation

Degree Name
Doctor of Philosophy (PhD)

Graduate Group
Cell & Molecular Biology

First Advisor
Patrick Seale

Keywords
brown fat, Prdm16, thermogenesis, Ucp1

Subject Categories
Biology | Developmental Biology | Molecular Biology

CONTROLLING THERMOGENESIS: UNDERSTANDING THE ROLE OF PRDM16 IN THE DEVELOPMENT AND FUNCTION OF BROWN FAT

Matthew J. Harms

A DISSERTATION

in

Cell and Molecular Biology

Presented to the Faculties of the University of Pennsylvania
in
Partial Fulfillment of the Requirements for the
Degree of Doctor of Philosophy
2015

Supervisor of Dissertation:

_____

Patrick Seale, Ph.D.
Assistant Professor of Cell and Developmental Biology

Graduate Group Chairperson:

_____

Daniel S. Kessler, Ph.D.
Associate Professor of Cell and Developmental Biology

Dissertation Committee:

Paul J. Gadue, Ph.D., Assistant Professor of Pathology and Laboratory Medicine

Mitchell A. Lazar, MD, Ph.D., Sylvan H. Eisman Professor of Medicine and Genetics

Michael L. Atchison, Ph.D., Professor of Biochemistry

Kenneth S. Zaret, Ph.D., Joseph Leidy Professor of Cell and Developmental Biology

CONTROLLING THERMOGENESIS: UNDERSTANDING THE ROLE OF PRDM16 IN THE DEVELOPMENT AND FUNCTION OF BROWN FAT

ABSTRACT

CONTROLLING THERMOGENESIS: UNDERSTANDING THE ROLE OF PRDM16 IN THE DEVELOPMENT AND FUNCTION OF BROWN FAT

Matthew J. Harms

Patrick Seale, P.hD.

The alarming rise in the incidence of obesity found throughout the world has precipitated a need to look for novel methods to increase energy expenditure to counter weight gain. Recently it was discovered that adult humans possess a substantial mass of brown adipose tissue (BAT), a tissue that consumes stored lipid to produce heat. Although the primary physiologic role for BAT is to protect mammals from the cold, it is currently thought that enhancing BAT mass or activating BAT in humans is a novel way to decrease adiposity. However, before BAT can be effectively utilized for therapeutic purposes a better understanding of the transcriptional regulation underlying BAT function is required. Here, we investigated the role of the transcription factor PRDM16 in BAT. We found that PRDM16 is not required for BAT development, however it is required to maintain BAT identity in adult mice. The loss of PRDM16 in adult mice led to a loss of BAT functionality and an inability to produce heat. We found that PRDM16s ability to drive a thermogenic program is due to its recruitment of Med1/the Mediator Complex to BAT-selective genes. Without PRDM16 in BAT a loss of higher order chromatin structure and a corresponding loss of transcription takes place at genes required for BAT identity and function.

TABLE OF CONTENTS

LIST OF FIGURES

Chapter 1: Brown and beige fat: development, function and therapeutic potential

Published: Harms M, Seale P. (2013) Brown and beige fat: development, function and therapeutic potential. Nature Medicine. 2013 Oct; 19(10):1252-63.

Sedentary living and calorie dense food has precipitated a dramatic rise in obesity throughout the developed world. This is particularly alarming due to the vast array of associated diseases, including type 2 diabetes, heart disease, insulin resistance, hyperglycemia, dyslipidemia, hypertension and many types of cancer[1,2]. The result is an expanding population of chronically sick people, staggering health care expenses and a prediction that for the first time, the current generation will have a shorter life span than previous generations[3-5]. There is thus an urgent need for new weight loss-treatments. Brown adipose tissue (BAT) is a key site of heat production (thermogenesis) in mammals that has been considered for many decades as an attractive target to promote weight loss. The heat produced by BAT is essential for the survival of small mammals in cold environments and for arousal in hibernators. Brown adipocytes in BAT are packed with mitochondria that contain Uncoupling Protein-1 (Ucp1). Ucp1, when activated, short circuits the electrochemical gradient that drives ATP synthesis and thereby stimulates respiratory chain activity. Heat is generated from the combustion of available substrates[6] and is distributed to the rest of the body via the circulation.

Clusters of Ucp1-expressing adipocytes with thermogenic capacity also develop in white adipose tissue (WAT) in response to various stimuli[7]. These have been named beige, “brite” (**br**own **i**n whi**te**), iBAT (induced BAT), recruitable BAT, and wBAT (white adipose BAT). Like adipocytes in BAT, the beige cells in murine WAT are defined by

their multilocular lipid droplet morphology, high mitochondrial content, and expression of a core set of brown vs. white fat-specific genes (e.g. *Ucp1*, *Cidea*, *Pgc-1α*). Despite a common ability to undergo thermogenesis, brown and beige cells have many distinguishing characteristics and should be considered as distinct cell types (Figure 1).

	Immunohistochemistry with anti-Ucp1	Location in humans	Location in mice	Developmental origin in mice	Enriched markers	Key transcription factors	Activators
Brown	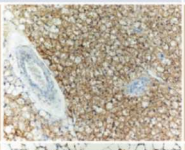	Neck Interscapular (newborns) (Perirenal?)	Interscapular Cervical Axillary Perirenal (Endocardial?)	Myf5^{+} cells (dermomyotome)	*Zic1* *Lhx8* *Eva1* *Pdk4* *Epsti1* *miR-206, miR-133b*	C/ebpβ Prdm16 Pgc-1α Ppar-α Ebf2 TR	Cold Thiazolidinediones Natriuretic peptides Thyroid hormone Fgf21, Bmp7, Bmp8b Orexin
Beige	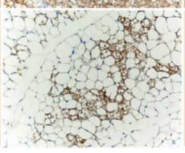	Supraclavicular (Paraspinal?)	Interspersed within WAT subcutaneous fat > visceral fat	Myf5^{-} cells Pdgfr-α^{+} (perigonadal)	*Cd137* *Tbx1* *Tmem26* *Cited1* *Shox2*	C/ebpβ Prdm16 Pgc-1α (Ppar-α?)	Cold Thiazolidinediones Natriuretic peptides (Thyroid hormone?) Fgf21 Irisin

Figure 1. Differences between Brown and Beige Adipocytes

Brown adipocytes express high levels of Ucp1 under basal conditions, whereas clusters of beige adipocytes can only be easily recognized in WAT after cold/β-adrenergic stimulation. Enriched markers of brown versus beige adipocytes have recently been identified, including: brown markers, Zic1, Lhx8[8,9], Eva1[10], Epsti1[11]; and beige markers, CD137, TMEM26[10], Tbx1[8,10], Cited1[11], Shox2[12]. Among the activators that have been studied in both compartments, Irisin is the only one that has selective actions in beige but not brown adipocytes.

Firstly, beige cells, at least those in the mouse subcutaneous depot, do not derive from the same embryonic (*Myf5*-expressing [see later]) precursors that give rise to brown adipocytes[13]. Secondly, a number of quantitative trait loci are associated with the induced development of beige but not brown adipocytes[14], suggesting that these cell types are differentially regulated. Thirdly, brown and beige adipocytes express distinct and distinguishing gene signatures[10,11]. Finally, a striking difference is that brown adipocytes express *high* levels of Ucp1 and other thermogenic genes under basal (unstimulated) conditions, whereas beige adipocytes only express these genes in response to activators, like β-adrenergic receptor or Pparγ agonists[8,15]. Importantly, this trait is fat cell-autonomous because brown fat cells turn on high levels of thermogenic

genes (e.g. Ucp1) during adipogenesis in culture from preadipocytes without addition of classical activators.

An obvious question is whether brown and beige fat cells have different functions. The answer to this is still unknown and has not been well studied. However, a recent study suggests that fully stimulated brown and beige adipocytes contain comparable levels of Ucp1, suggesting that their thermogenic capacities are similar[10]. Based on this, the name "beige" might be misleading and is more applicable to describe the **tissue** that has undergone "browning" rather than the Ucp1+ adipocytes themselves. Aside from thermogenesis, it seems highly likely that beige and brown adipocytes have other cell type-specific actions that have yet to be studied. For example, beige adipocytes may secrete certain factors that affect WAT function and/or systemic metabolism.

The biomedical interest in brown and beige adipocytes is centered on the capacity of these cell types to counteract metabolic disease, including obesity and type 2 diabetes. Indeed, increased brown and/or beige adipose activity is linked to obesity resistance in many mouse models (Table 1). In humans, it was assumed for many years that there was too little brown fat in adults to affect body weight. However, in 2009, imaging studies revealed the presence of substantial deposits of Ucp1-expressing adipocytes whose mass and/or activity are lower in obese and older subjects[16-20]. The key question now is whether reduced thermogenic activity in fat cells is a cause or consequence of weight gain in people. Regardless of its "natural" role, increasing brown/beige fat activity through drugs other methods holds tremendous promise for the treatment of metabolic disease.

Mitochondrial uncoupling has already been tried as a weight loss therapy. The chemical uncoupler, 2, 4-Dinitrophenol (DNP) allows protons to leak across the mitochondrial membrane, mimicking the effect of activated Ucp1[21]. In the 1930s, DNP was widely used as an effective diet pill to treat obesity, providing proof-of-concept for mitochondrial uncoupling as an approach for weight loss. However, at high doses (variable in different people), unregulated respiratory uncoupling in all cells causes dangerous side-effects including hyperthermia and death. Thus, the goal is to develop strategies that enhance respiratory uncoupling selectively in adipose tissue by exploiting the mechanisms that naturally evolved to do this in brown and/or beige fat cells.

Figure 2. Genetic Models Resistant to Weight Gain Through Enhanced Brown and Beige Fat Development

Gene	Induce Beige	Increase Brown	Gain of function models
Cox2[22]	X		Cox2 over-expressing mice have increased beige fat and are resistant to weight gain, demonstrating the role of prostaglandins in the recruitment of beige fat
FoxC2[23-25]	X	X	Overexpression of FoxC2 in adipose increases the expression of the R1α regulatory subunit of PKA, making the cells more sensitive to catecholamines
Prdm16[26]	X		Fat-selective Prdm16 transgenic mice have increased beige fat.
Pten[27]	X	X	Increases in Pten inhibits PI3K, which drives a thermogenic program
Ucp1[28,29]	X		Transgenic expression of Ucp1 increases thermogenesis in WAT and prevents weight gain
Loss of function models			
4E-BP1[30]	X		4E-BP1 KO mice have an increased metabolic rate, an induction of thermogenic genes in WAT depots, and an increases in eIF4F phosphorylation
4E-BP2[31]		X	Treatment with a antisense oligo. caused weight loss and an increase of the β3-adrenergic receptor in both WAT and BAT. BAT showed a PGC-1α independent increase in Ucp1
ActRIIB[32,33]		X	Neutralizing antibodies show an increase in BAT mass without affecting WAT. Loss of ActRIIB activates Smad3 signaling to increase thermogenic genes
Aldh1a1[34]	X		KO results in a buildup of Retinaldehyde. This activated the retinoic acid receptor – which recruited PGC-1α to the Ucp1 promoter
Arrdc3[35]	X	X	Arrdc3 interacts directly with β-adrenergic receptors. Loss of Arrdc3 sensitized adipocytes to catecholamines and thus increased thermogenic programs in BAT and WAT
ATG7[36]	X	X	BAT from KO mice showed an increase in thermogenic proteins, and WAT had an increase in thermogenic signatures. Studies demonstrate role of autophagy in adipose development
ATF4[37]	X	X	WAT showed an increase of PGC-1α and Ucp2, while BAT was enriched for Ucp1 and Ucp3
Bace1[38]		X	An increase in Ucp1 in BAT and Ucp2/3 in skeletal muscle
Cidea[39]		X	KO mice are lean, have increased oxygen consumption, and defend core temperature against a cold challenge. Direct interactions with Ucp1 could explain Cidea's repressive effect
Cnr1[40]	X		Mice are lean. In vitro, Cannaboid receptor type 1m antagonists are able to induce Ucp1 transcription in white adipocytes

Crfr2[41]		X	An increase in glucose tolerance and a further increase of Ucp1 in BAT
Ffar2[42]		X	Mice resist weight gain and have increased core temperature
FoxO1[43]		X	Adipose specific dominant negative mice had increased oxygen consumption and a BAT specific increase in thermogenesis
Fsp27[44]	X		Mice have increased BAT specific genes and mitochondrial in WAT. The mechanism is thought to involve a loss of pRb and RIP140.
Ghsr[45]		X	Mice are protected from the age-associated decline of thermogenesis
Grk2[46]	X		Knockout mice have an increased core temperature and thermogenic program in BAT and WAT. Interestingly, the phenotype appears to be age related.
Id1[47]		X	Increased oxygen consumption and an increase in thermogenic genes in BAT
Ikbke[48]	X		WAT has increased Ucp1 transcript and protein
Lipe[49]	X		The Increase in Ucp1 is attributed to a decrease in RIP140 and pRb
LPR6[50]	X		KO animals gain less weight and a diminished mTORC1 activity in BAT causes an increase in thermogenic proteins
LXRα[51]	X		Recruitment of RIP140 to displace PPARγ/PGC-1α
Mstn[52]	X		Increase of thermogenic program in WAT
Nprc[53]	X	X	Loss of the natriuretic peptide (NP) clearance receptor causes increased circulating NPs which increase thermogenic activity
Oprd1[54]		X	Mice are resistant to weight gain and have enhanced thermogenesis in BAT
p107[55]	X		Loss of p107 causes a loss of pRb and increased browning of WAT.
Pctp[56]		X	BAT showed enlarged mitochondrial and an increase thermogenic genes
pRb[57]	X		pRB binds to and represses the PGC-1a promoter.
Pref-1[58]		X	BAT has increased PGC-1α and Ucp1. C/EBPδ binds and activates the Pref-1 promoter
Prkar2b[59]	X		The loss causes a compensatory increase in RIα, which binds cAMP with higher affinity, causing increased basal PKA activity –increasing thermogenesis
Prkcb[60]	X		WAT had increased β1 and β3 adrenergic receptors. This resulted in a p38/MAPK mediated increase of PGC-1α and Ucp1
Prlr[61]	X		Prolactin receptor KO mice have increased thermogenic genes and altered pRb/Foxc2 levels in WAT. This indicates a novel paracrine or endocrine role of prolactin
Rip140[62-64]	X		RIP140 directly interacts with PGC-1a to inhibit its transcriptional activity ; Recruits DNMTs and HMTs to silence Ucp1
Scd1[65]	X	X	Skin-specific KO mice result in increased thermogenesis in BAT and WAT, indicating cross talk between the different tissues
Sfrp5[66]	X		KO mice are resistant to weight gain and isolated KO adipocytes have increased oxidative respiration
Smad3[67]	X		Smad3 represses PGC-1α expression. Loss of Smad3 induces transcripts that correspond to increased thermogenesis
Them1[52]		X	An increase in thermogenic genes in brown fat and a decrease in markers of inflammation in white adipose
Tif2[68]	X		Tif2 competes with the activator Src2 for PGC-1a binding. Tif2 binding prevents PGC-1α from interacting with PPARγ
Tnrf1[69]		X	Knockout of tumor necrosis factor-alpha receptor 1 results in increased Ucp1 in BAT and Ucp3 in muscle resulting in increased O2 consumption
Trpv4[70]	X		KO mice are resistant to weight gain and have increased thermogenic gene expression in WAT, mediated by a loss of ERK1/2 effects on Pgc-1α
Twist-1[71]		X	Twist-1 binds to and inhibits PGC-1α activity at target genes.
Vegfa[72]	X		An induction of the thermogenic program in WAT with associated resistance to weight gain
Vgf[73]		X	Knockout of secreted protein VGF caused increased Ucp1 expression in BAT. Unclear if the effect is cell autonomous.

The Development of Brown/Beige Adipocytes

Brown adipocytes

BAT forms during embryonic development, before other fat depots, and is assumed to contain a uniform population of adipocytes. The major BAT depots in rodents are in the interscapular region (interscapular, axillary and cervical pads), embedded in and around deep back muscles. An interscapular BAT depot has also been noted in human infants, which regresses and is absent in adults[12,74]. Most brown fat cells originate from precursor cells in the embryonic mesoderm that also give rise to skeletal muscle cells and a subpopulation of white adipocytes[13,75,76]. These precursors transiently express *Myf5* and *Pax7*, two genes that were previously thought to selectively mark skeletal myogenic cells in the mesoderm (Figure 2A)[13,76]. Consistent with a developmental relationship between brown fat and muscle, brown fat precursor cells express a muscle-like gene signature[77], and brown fat and muscle have related mitochondrial proteomes[78]. However, whether *Myf5*+ cells are multipotent or whether there are separate pools of *Myf5*+ precursors that contribute to muscle, brown fat and white fat remains to be tested.

Beige Adipocytes

The embryonic origin and cell hierarchy of beige adipocytes is less clear. Beige and brown adipocytes likely come from distinct cell lineages, given that beige cells, at least in the subcutaneous depot, do not have a history of *Myf5* expression[13,75]. In formed WAT, an important question is whether beige adipocytes come from white adipocytes via “transdifferentiation” or arise through *de novo* differentiation/maturation of precursors. Over a decade ago, Himms-Hagen *et al*. found that most beige adipocytes arise from pre-existing (non-dividing) cells that they presumed were mature adipocytes[79].

Since then, Cinti and others have provided substantial evidence in support of the idea that large unilocular "white" adipocytes transform into beige adipocytes in response to cold/β3-adrenergic agonists[7].

A new study from the Scherer lab used a pulse-chase fate-mapping technique in mice to revisit this issue. Wang *et al.* pulse labeled the mature adipocytes in WAT with LacZ expression[80]. This labeling is indelible and heritable such that LacZ is constitutively expressed in the pulsed adipocytes and any of their descendents. After being "pulsed", the mice were exposed to cold or treated with β3-adrenergic agonists to induce the formation of beige adipocytes. The results were clear- the large majority of newly acquired Ucp1+ adipocytes in the subcutaneous inguinal depot are ***not*** marked by LacZ. This proves that most, if not all, beige adipocytes, at least in this subcutaneous depot, arise from a precursor population rather than from pre-existing adipocytes (Figure 2B).

The thermogenic profile of beige adipocytes is reversible. Beige adipocytes acquired in WAT during cold-exposure lose Ucp1 and are retained after mice are moved back to warmer conditions (Figure 2B)[80,81]. When these animals are re-exposed to cold, the same (marked) cells again induce Ucp1[81]. Interestingly though, the cells marked by prior Ucp1 expression were not the only source of beige adipocytes during the second round of cold exposure. This suggests that beige adipocytes are retained, and may function like white fat cells, for a certain period of time in animals that were previously cold. These beige adipocytes are presumably depleted via the normal mechanisms that control tissue turnover.

Another important question is whether beige and white adipocytes arise from different types of precursors. Petrovic *et al*., found that a subset of adipocytes differentiated *in vitro* from the stromal vascular fraction (SVF, an enriched source of preadipocytes) of WAT activate Ucp1 expression in response to treatment with Pparγ activators[8]; this suggests that some but not all preadipose cells are thermogenically competent. Recently, the Spiegelman lab used limited dilution to clone preadipocyte cell lines from the stromal vascular fraction of subcutaneous (inguinal) WAT[10]. Through global gene profiling and differentiation analyses, two types of preadipocytes were identified - white and beige. Both types of committed precursors differentiate into lipid-laden adipocytes that lack thermogenic characteristics under standard adipogenic conditions. However, only beige cells induce a thermogenic gene program when treated with β-adrenergic agonists. Notably, Cd137 and Tmem26 were identified as cell surface markers for native beige precursors, thus enabling the direct purification of these cells from fat tissues. In considering the studies discussed above, the data suggest that cold (via β-adrenergic agonists) triggers the differentiation of Cd137+:Tmem26+ precursor cells into Ucp1+ beige adipocytes and that beige cells require constant stimulation to maintain their thermogenic programming. In light of these recent studies, there does not seem to be much/any direct transformation of white into beige adipocytes, at least under physiological conditions.

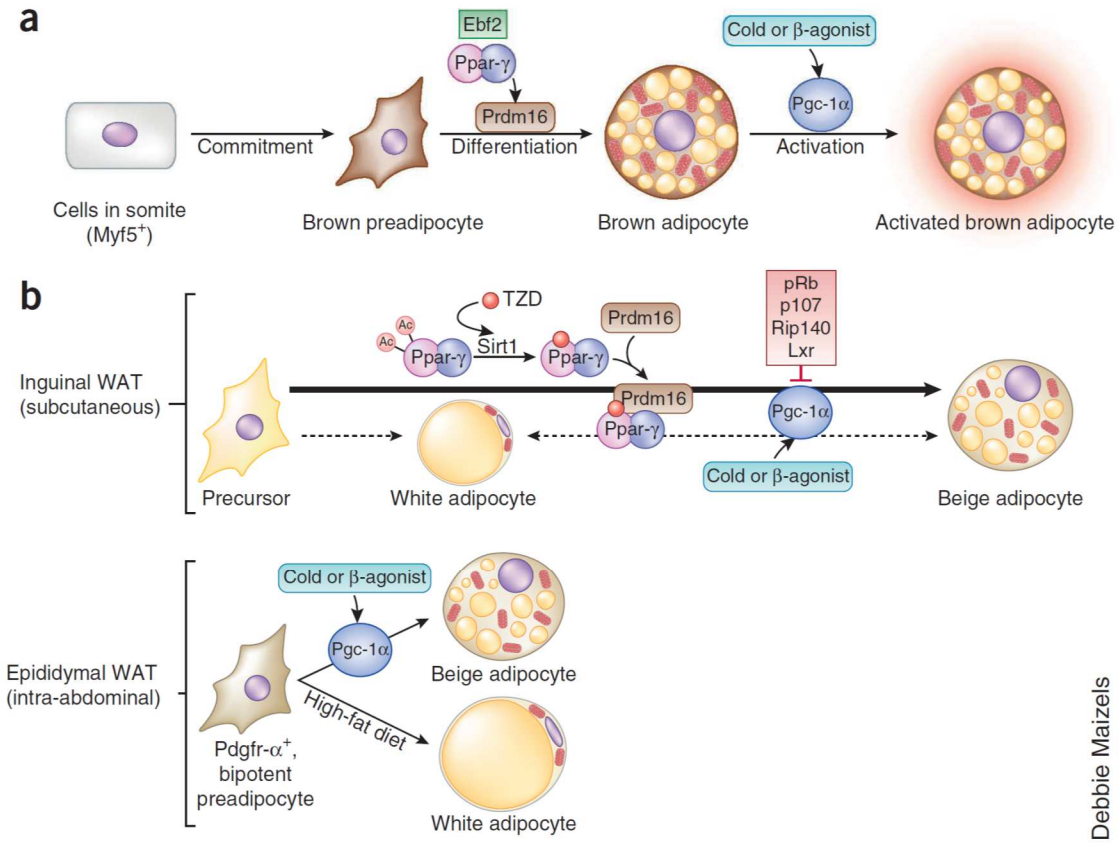

Figure 3. Transcriptional Regulation of Brown and Beige Adipocyte development

(A) Brown adipocytes are derived from a *Myf5*-expressing progenitor population. Ebf2 cooperates with Pparγ to promote the expression of Prdm16, which drives a brown fat cell fate. Thermogenesis in mature brown adipocytes is activated by norepinephrine (NE) released from sympathetic neurons. NE signals through β-adrenoreceptors to increase the expression and activity of Pgc-1α, a transcriptional co-activator that coordinates gene programming in response to activation. **(B)** In inguinal fat, β-adrenergic stimulation predominately triggers *de novo* differentiation of precursor cells (large arrow). We leave open the possibility that under some conditions, mature white fat cells can transdifferentiate into beige cells (small dashed arrow). In epididymal WAT, caloric excess causes bi-potent progenitors to differentiate into white adipocytes, while β-adrenergic activators stimulate beige adipocyte development. TZD agonists of Pparγ promote beiging by both increasing the stability of Prdm16, and through the Sirt1-dependent deacetylation of Pparγ, which recruits Prdm16 to Pparγ target genes. β-adrenergic signaling drives the expression and activity of Pgc-1α in beige adipocytes. Pgc-1α is targeted by numerous repressors to block beige adipocyte development.

Beige adipocytes are most abundant in the inguinal WAT, a major subcutaneous depot in rodents[7]. However, Ucp1-expressing adipocytes are evident in most (if not all) WAT depots in response to cold exposure[7,79,82]. In peri-gonadal (visceral) fat of male mice, beige adipocytes develop from a population of precursors that also differentiates into white adipocytes (Figure 2B)[83]. These bi-potent white/beige precursors express Platelet-derived growth factor receptor-α (Pdgfrα) and are closely associated with blood vessels. Upon treatment of mice with β3-adrenergic agonists, these precursor cells proliferate, then lose Pdgfrα expression and differentiate into Ucp1+ adipocytes. Conversely, high fat diet stimulates the differentiation of Pdgfrα+ cells into white adipocytes[83]. This is consistent with the finding that most/all white adipocytes are descendent from Pdgfrα-expressing cells[84]. Importantly, cell culture analyses shows that single Pdgfrα+ cells give rise to both Ucp1- and Ucp1+ (beige) adipocytes.

In the mature adipocyte tracing studies of Wang *et al*. (discussed above), very little beige fat recruitment but a surprising amount of white adipogenesis was detected in the perigonadal WAT of mice exposed to cold for 1-3 days or treated with β-agonist for 7 days[80]. Why new white fat cells develop during cold exposure is unclear. It is also surprising that so few Ucp1+ cells were detected. Perhaps the exposure was too short to elicit a full beige recruitment in the newly developed adipocytes? It would be interesting to examine the effect of chronic cold in these mice, since this is known to extensively brown the WAT depots.

The prevalence of beige adipocytes within different human WAT depots has not been carefully evaluated. However, it is known that human WAT contains precursor cells that are capable of expressing Ucp1 and other brown/beige characteristics, particularly in response to Pparγ activation (see section on Pparγ below)[85]. Additionally,

it was (and still is) unclear whether the deposits of Ucp1-expressing adipocytes identified by Fluorodeoxyglucose - Positron Emission Topography (FDG-PET) in adult humans are analogous to beige or brown fat. Wu *et al*. and Sharp *et al*., reported that supraclavicular tissue, the largest FDG-PET+ depot, expresses selective markers of rodent beige versus brown fat cells [10,11]. By contrast, Jesperson *et al*., found that tissue and *in vitro* differentiated adipocytes from this depot expresses both brown- and beige-specific markers[9]. A different depot in the neck region was shown to possess the molecular characteristics of murine brown fat[86]. Typing these depots as "brown" or "beige" based on the expression levels of a few mouse marker genes that have no known function(s) has not been conclusive thus far. Functional marker genes or assays are needed to better categorize the different human (as well as mouse) depots/cell types. The field must continue to study the biology and therapeutic potential of both the classic/developmental BAT and (inducible) beige fat.

Developmental regulation of brown and beige adipocytes by Prdm16

Prdm16 (PRDI-BF1 and RIZ homology domain containing protein-16) is a large zinc-finger containing transcriptional factor that is expressed at high levels in murine BAT relative to visceral WAT[87]. Prdm16 expression is also substantially enriched in human "BAT" relative to adjacent subcutaneous WAT[20,88]. Ectopic Prdm16 expression converts myoblasts and white fat precursors into thermogenic, Ucp1-containing adipocytes. Mechanistic studies suggest that Prdm16 acts primarily through binding to, and modulating the activity of, other transcriptional factors, including c/EBPβ, Pparγ, Pparα and Pgc-1α[13,87,89,90]. Knockdown of Prdm16 ablates the thermogenic

characteristics of brown fat cells while also causing an increase in the expression of white fat- and muscle-specific genes. Together, these studies have strongly suggested that Prdm16 is a key driver of brown fat cell fate.

The importance of Prdm16 in brown fat cell differentiation prompted us to examine whether Prdm16 also played a role in the development of beige adipocytes. Upon analyzing various murine WAT depots, we noted that Prdm16 was expressed at higher levels in the depots that are most prone to beiging, especially the inguinal WAT[26]. Importantly, reduction of Prdm16 blocks the induction of a thermogenic program in cultured subcutaneous adipocytes and decreases the recruitment of beige adipocytes in WAT in response to β-adrenergic or Pparγ agonists[26,91]. Conversely, transgenic expression of Prdm16 in adipose tissues of mice stimulates beige adipocyte development to counteract high fat diet-induced weight gain and improve glucose tolerance[26].

Several factors have been shown to regulate brown/beige adipocyte differentiation by modulating Prdm16 expression/activity. Notable among these is Bone morphogenic protein-7 (Bmp7), an essential signal for brown fat development, which increases *Prdm16* mRNA levels in brown and white fat precursor cells[92-94]. Additionally, thiazoledinediones (TZDs), which agonize Pparγ, induce thermogenic gene expression in fat cells through effects on Prdm16 (see later). Interestingly, the muscle-enriched microRNA, miR-133 directly targets and reduces Prdm16 levels to block both brown and beige adipose development[95-46]. Notably, cold-exposure suppresses miR-133 expression in fat cells, which leads to increased levels of Prdm16 and downstream thermogenic target genes[95]. Mice lacking miR-133 express higher levels of Prdm16 in WAT and develop more beige adipocytes[96]. Intriguingly, miR-133 is also present at high

levels in adult muscle stem cells where it suppresses Prdm16 expression[97]. Reduction of miR-133 in regenerating muscle causes the ectopic development of brown adipocytes and an associated increase in energy expenditure.

Role of brown/beige fat in regulating weight and metabolism

BAT has long been viewed as a critical tissue for defending body temperature in response to cold. In 1979, Rothwell and Stock first reported that BAT was also activated in rodents when they overeat as a mechanism to preserve energy balance and limit weight gain- so called *diet-induced thermogenesis* (DIT)[98]. Consistent with this, mice genetically engineered to have less BAT gain more weight than control animals[99]. However, for many years it was unclear why *Ucp1*-deficient mice, which are cold intolerant (and thus have defective BAT), resisted rather than developed obesity[100].

An important study by the Cannon and Nedergaard group in 2009 revealed that Ucp1-deficient mice gain more weight than wildtype controls, but only when they are housed under thermoneutral (28-30ºC) conditions[101]. At room temperature (20-22ºC), mice are cold and must therefore expend extra energy to defend their body temperature. Ucp1-deficient mice, which can't use BAT, activate alternative thermogenic mechanisms[102,103]. This is thought to conceal the effect of brown fat/Ucp1 on energy balance. Consistent with this, old Ucp1-deficient animals, that are larger and less cold-sensitive than younger mice, become obese even at ambient temperature[104]. The dramatic impact of temperature on physiology has been overlooked by much of the mouse/rodent research community. In the area of metabolism, cold stress and its effects have undoubtedly confounded many studies. Since people tend to live at

thermoneutrality with the aid of clothing, heating, etc., a compelling argument could be made that all/most metabolic studies in mice should be conducted under thermoneutral conditions.

The obesogenic effect of Ucp1-deficiency in warm mice indicates that BAT/beige fat activity ***can*** affect energy balance, but the magnitude (and significance) of this effect in free-living mice or humans is uncertain. It should also be noted that previous studies in rats housed at thermoneutrality failed to find any significant contribution of BAT activity to diet-induced thermogenesis[105]. Moreover, Kozak and colleagues did not observe changes in adiposity in their studies of Ucp1-knockout animals when housed under varying temperature conditions[106]. Finally, increases in BAT/Ucp1 activity in response to high fat feeding are not consistently observed[107]. These divergent findings may provide an opportunity to identify modifying factors that affect BAT/Ucp1 activity and energy balance. Are there specific dietary components that are needed to recruit BAT efficiently? What are the genetic/strain-specific effects? Does the microbiome or other environmental factors in different vivariums play a role?

Regardless of whether BAT plays a major physiological role in body weight regulation in mice or humans, there is no question that expanding BAT/beige fat activity in mice, through genetic manipulation, drugs, or transplantation suppresses metabolic disease (Table 2 and [26,28,108,109-112]) This implies that counter-regulatory mechanisms (e.g. increased food intake), which might have been predicted to offset the effects of expanded BAT activity to preserve energy balance, are not fully effective in mice. Notably, in some cases, the beiging of WAT and a highly correlated anti-obesity effect happens without evidence of increased BAT function. For example, the hormone, Irisin (see below) raises energy expenditure via selective actions in beige adipocytes[108].

Similarly, transgenic expression of Prdm16 in all fat tissues promotes beiging of WAT and resistance to obesity without increasing BAT mass or *Ucp1* mRNA levels[26,28]. Finally, transgenic expression of Ucp1 in adipocytes suppresses obesity in spite of a reduction in BAT mass[28]. These results raise an obvious question - do beige adipocytes play a more important physiological role in fighting obesity? This seems unlikely, given that high fat diet generally decreases the levels of thermogenic genes in WAT, coincident with increases in WAT mass[107].

Mice with increased brown and/or beige fat activity resist weight gain, but also display improvements in systemic metabolism, including improved glucose tolerance and increased insulin sensitivity. Along these lines, activated brown fat takes up and metabolizes large quantities of lipid from the bloodstream[113], which has beneficial effects on metabolism. In models where beige fat appears to be selectively increased, such as Prdm16 fat transgenics[26] and Irisin-treated animals[108], the improvement in glucose tolerance seems disproportional to the modest effects on body weight. We speculate that the increased proportion of beige to white adipocytes in WAT modulates systemic insulin action through non-thermogenic mechanisms, perhaps via altering the secretome of adipose tissue. Additionally, thermogenic fat cells, not yet classified as brown or beige, that surround blood vessels (perivascular adipose) have been suggested to protect against the development of atherosclerosis[114]. Thus, the potential therapeutic uses of brown/beige fat go beyond obesity and should be considered for various metabolic disturbances, including type 2 diabetes, insulin resistance, atherosclerosis, lipid disorders, etc.

Sympathetic nerve control of brown/beige fat

Cold is a dominant regulator of many aspects of BAT biology. Mice lacking BAT activity are cold intolerant due to defective non-shivering thermogenesis[100]. Cold, sensed by various mechanisms, including through thermoreceptors in the skin, elicits sympathetic outflow to BAT through an intricate neural circuitry (reviewed in [115]). In addition to nerve terminals, alternatively activated macrophages in BAT produce catecholamines in response to cold[116]. Norepinephrine (NE) agonizes adrenergic receptors on adipocytes which triggers a signal transduction cascade leading to adaptive increases in the expression of thermogenic genes (Figure 3)[117]. Prolonged cold exposure also stimulates the proliferation and differentiation of brown precursor cells to expand BAT mass and increase thermogenic capacity[118]. Conversely, at warmer housing temperatures or in surgically denervated BAT, Ucp1 and other thermogenic factors are dramatically reduced[119,120].

Sympathetic nerve activity also acutely stimulates heat production by activating Ucp1 function. Classic studies showed that fatty acids, rapidly released from lipid droplets in response to nerve activity, increase proton leak through Ucp1 (reviewed by [121]). Fedorenko *et al*. recently discovered that long chain fatty acids generated in the inner mitochondrial membrane by a phospholipase A2 (PLA2) bind directly to Ucp1 and are required for proton transport[122] (Figure 3). An important, but often overlooked tenet is that Ucp1 does not increase the respiratory activity of cells under basal conditions[123,124]. Therefore, therapeutic approaches which expand brown and/or beige adipocytes without also promoting activation could be unproductive. Though, in many

people, an expanded BAT/beige fat compartment may be sufficiently activated by daily "tonic" stimuli (e.g. food, cold, exercise, etc.) to achieve therapeutic effect.

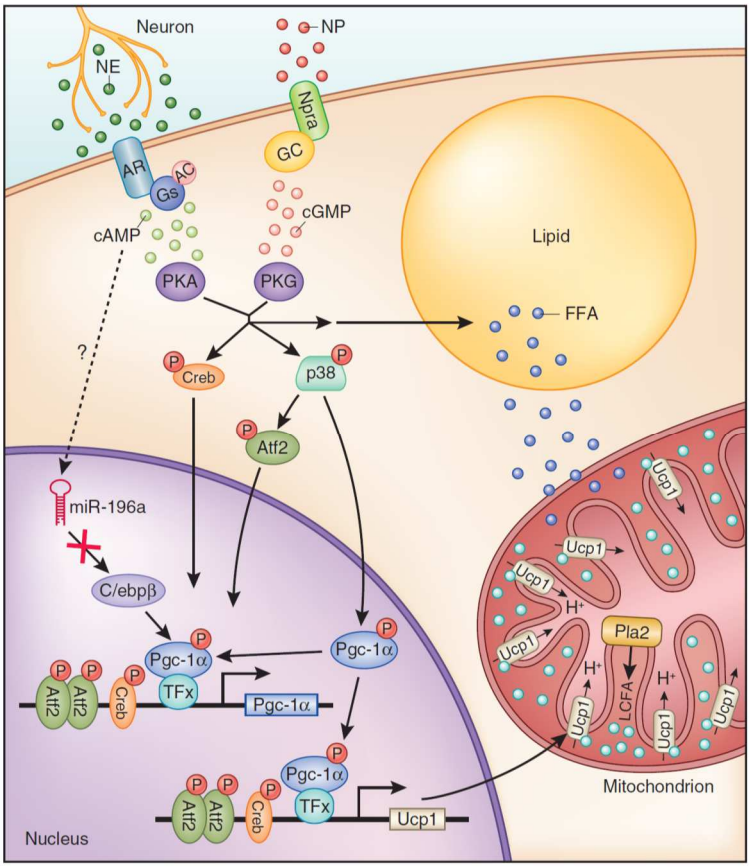

Figure 4. Catecholamine and Natriuretic induction of Thermogenesis

Sympathetic neurons exocytose catecholamines (dark green ovals), which bind to β-adrenoreceptors leading to activation of Adenylyl Cyclase (AC), increased cAMP (light green ovals) levels and enhanced PKA activity. Natriuretic Peptides (red ovals) bind the NPRA receptor which activates Guanylyl Cyclase to increase cGMP (pink ovals) levels, leading to activation of PKG. Activated PKA and PKG use similar mechanisms to drive transcriptional responses in brown adipocytes through the activity of phosphorylated CREB and 38MAPK. Specifically, p38MAPK phsophorylates and activates ATF2 and Pgc-1α which induce the transcription of downstream thermogenic genes including Ucp1. Pgc-1α binds to DNA through interactions with Pparγ, Pparα, RXR and Thyroid Receptor (TFx). Additionally, catecholamines elevate miR-196a levels, resulting in increased C/EBPβ expression, which helps drive the thermogenic gene program. Importantly, PKA and PKG activation also acutely induce lipolysis. The fatty acids released from lipid droplets are oxidized by mitochondria to produce heat. Proton leak through Ucp1 is activated by long chain fatty acids (LCFA) released from the mitochondrial membrane by PLA2.

Cold is also the classic activator of beige adipocyte development and function. Animals housed in the cold undergo a dramatic remodeling of their WAT, characterized by an accumulation of beige adipocytes - this can be mimicked by treating animals with β3-adrenergic activators like CL 316,243[7,79,109,110,125-128]. Interestingly, the propensity of WAT depots to undergo beiging is highly correlated with the density of sympathetic nerve fibers[129]. However, other adipose cell/tissue autonomous factors must be involved because systemic β3-agonist administration (thus bypassing the central nervous system) causes certain depots to beige more than others. Many of the effects of chronic cold on adipose tissues are recapitulated in mice that express elevated levels of FoxC2 in adipocytes[23] Specifically, FoxC2 increases BAT mass, induces beige fat cell development, drives mitochondrial biogenesis and promotes angiogenesis in fat tissue[25,130,131]. FoxC2 functions in fat cells, to a large extent, by driving the expression of the R1α regulatory subunit of PKA (*Prkar1a*)[23,24], thus sensitizing adipocytes to the effects of catecholamines. These results suggest that the adipocytes instigate most of the tissue remodeling that occurs in response to NE.

The discovery of the murine β3-adrenergic receptor (β3-AR), which is expressed mainly in fat and whose agonism activates thermogenesis, generated tremendous excitement for therapeutic possibilities in humans. However, treatment of humans with β3-AR agonists never lived up to the forecasted predictions[132]. Difficulties appear to be due to receptor differences between mice and humans - leading to off-target effects in humans, as well as poor pharmacokinetic properties and oral bioavailability[133]. These problems, compounded with the previously held tenet that adults had very little BAT caused many companies to abandon their development of β3-AR agonists for obesity. Future studies should consider whether β3-ARs could be used in combination with

BAT/beige fat recruiters. Alternatively, it would be worth considering whether prescribed cold exposure could be used to activate BAT/beige fat after augmentation via other pathways.

Cold exposure, which induces thermogenic features in adipose cells, also affects the developmental programs of other cell types in adipose tissue to coordinate and optimize heat production. For example, and as noted above, cold activates alternatively activated macrophages in BAT to produce catecholamines[116]. Cold also stimulates sympathetic nerve branching/recruitment during the browning response of WAT[129]. Finally, cold exposure induces the sprouting and growth of blood vessels in adipose to facilitate oxygen delivery and heat exchange[118,120,134]. This angiogenic effect is regulated through increased production of Vascular endothelial growth factor (Vegf), through a mechanism that does not involve hypoxia[135-137]. Interestingly, Vegf secreted by adipose tissue also enhances the recruitment of brown and beige adipocytes via an unknown mechanism (Figure 4). In cultured brown adipocytes, Vegf enhanced cell survival and proliferation whereas Vegf neutralizing antibodies caused apoptosis[138]. Strikingly, overexpression of Vegf in adipose tissues of mice increases BAT mass, stimulates beiging and promotes a healthy metabolic profile[139,140]. Curiously, Vegf-inhibition has also been shown to reduce metabolic disease in mice, though this is in the context of already dysfunctional obese WAT[72,140]. Further studies are needed to elucidate the mechanism(s) by which Vegf manipulates the fate of adipose tissue under different metabolic states.

Pparγ Coactivator-1α (Pgc-1α) controls the thermogenic activation of adipocytes

Pgc-1α was discovered as a cold-induced interacting partner of Pparγ in brown fat[141]. Based on hundreds of studies, Pgc-1α is now recognized as a master regulator of mitochondrial biogenesis and oxidative metabolism in many cell types. In adipocytes, Pgc-1α also induces the expression of Ucp1 and other thermogenic components[141,142]. Surprisingly however, BAT develops normally without Pgc-1α[143], probably due to compensation by the related family member, Pgc-1β. Although not required for tissue development, Pgc-1α is essential for the cold/β-agonist-induced thermogenic activation of brown adipocytes[144,145] and for the expression of thermogenic genes in WAT[146] (Figure 2). Thus, Pgc-1α is a central transcriptional effecter of adrenergic activation in thermogenic adipocytes.

Pgc-1α expression levels and activity are directly regulated by the β-adrenergic signaling pathway[147], providing a link between the physiological activator of brown fat thermogenesis and the transcriptional machinery in brown adipocytes (Figure 3). Specifically, Pgc-1α is phosphorylated and thereby activated by p38 MAPK in response to sympathetic stimulation[147,148]. Activated Pgc-1α regulates thermogenic gene levels through its interaction with Pparγ, Pparα, Thyroid Receptor and other factors, though a detailed mechanism to account for its selective effects at brown fat-specific genes is lacking. *Pgc-1α* transcription also rises in response to β-adrenergic agonists through increases in the function of Activating transcription factor-2 (Atf2)[147].

Several transcription factors suppress thermogenesis by interfering with Pgc-1α activity (Figure 2). For example, Retinoblastoma (Rb) family members, pRb and p107 repress Pgc-1α transcription to block the expression of brown genes in white

adipose[55,57]. Notably, pRb activity declines during the β-adrenergic-induced beige conversion of WAT[57]. The nuclear co-repressor, RIP140 binds to Pgc-1α and blocks its transcriptional activity at certain target genes[149]. The nuclear receptor, LXRα also blocks Ucp1 expression by recruiting RIP140 and displacing Pgc-1α at an LXR binding site[51].

Brown/beige-specific functions for the general adipogenic machinery

Pparγ and members of the C/EBP protein family orchestrate the general differentiation program in all adipose lineages[150], but are also deployed to activate specific thermogenic genes in brown/beige adipocytes. For example, C/EBPβ is present at higher levels in BAT relative to WAT and protein levels increase further in response to cold [90]. In WAT, β-adrenergic agonists increase C/EBPβ levels through miRNA-mediated degradation of Hoxc8, a repressor of C/EBPβ transcription (Figure 3)[151]. Loss of C/EBPβ is associated with defective thermogenesis, whereas increasing the levels of C/EBPβ in white fat cells triggers a brown fat transcriptional profile[90,152-154].

The master adipogenic factor, Pparγ also controls the expression of brown fat-specific genes, including Ucp1, particularly in response to β-adrenergic activators [147,148,155]. Genome-wide analyses demonstrate that Pparγ binds and regulates distinct target genes in brown and white fat cells[156,157]. We recently discovered that Ebf2, a helix-loop-helix transcription factor, regulates Pparγ activity to drive the expression of Prdm16 and a brown fat fate[156,157] (Figure 2). Ebf2 appears to function, at least in part, by facilitating the recruitment of Pparγ (and likely other factors) to brown fat-specific genes. Ebf2-deficient mice develop fatty tissue with the molecular and morphological characteristics of white fat in the areas where brown fat normally forms.

Activation of Pparγ by synthetic Thiazolidinedione (TZD) agonists enhances thermogenic gene expression in both white and brown adipocytes[8,158-162]. TZDs induce Ucp1 expression and increase mitochondrial biogenesis in adipocytes from mice and humans[8,85,163]. This enables TZD-treated adipocytes to undergo Ucp1-mediated increases in respiration in response to β3-adrenergic activators[8,85,91]. Mechanistically, TZDs appear to act, in large part, through Prdm16 to activate a thermogenic program. In particular, TZD treatment stabilizes Prdm16 protein to increase its levels in fat cells[91] and also enhances the interaction of Prdm16 with Pparγ (Figure 2). SirT1 plays a role in this TZD-driven process by deacetylating Pparγ to facilitate the docking of Prdm16. *In vivo*, activation of SirT1 promotes browning of WAT and resistance to obesity[112], suggesting that SirT1 activators might have a use as weight loss agents.

In the clinic, TZDs, though associated with unwanted side effects, are highly effective in the treatment of type 2 diabetes through enhancing insulin action. Given that beige adipocytes improve insulin sensitivity, it is reasonable to speculate that TZDs may act, at least in part, by inducing beige fat development. However, non-TZD Pparγ modulators, like MRL24, promote insulin sensitivity but have little effect on Ucp1 expression[91,164]. Moreover, TZDs are associated with weight gain and increased adipocyte development in rodents and humans rather than weight loss. This may be due to a blunting effect that TZDs have on the sympathetic activation of adipocytes[165,166] which would block Ucp1 function. As mentioned earlier, it would be worth exploring treatments that combine TZDs with Ucp1-activators, like β3-selective adrenergic agonists.

Novel BAT/beige fat recruiters/activators

Sympathetic nerve activity was widely believed to be the primary or only physiological signal which activates BAT thermogenesis and induces beige adipocyte development. Though β-AR signaling is undoubtedly a central regulator of these processes, several other hormones and factors have now been shown to regulate energy expenditure in adipose tissue (Figure 3); these have been discussed comprehensively in recent reviews [15,167,168]. Here, we comment on secreted/systemic factors that affect brown/beige fat and appear particularly promising for therapeutic development.

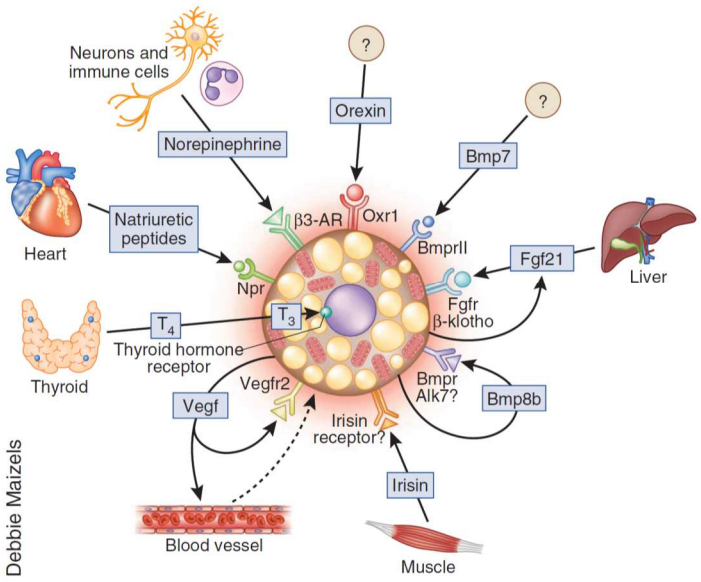

Figure 5. Secreted factors that recruit brown/beige adipocytes

In rodents, a number of tissues and cell types have been found to secrete factors that regulate brown and beige adipose activity through systemic, autocrine and paracrine mechanisms. Neurons and alternatively activated macrophages secrete norepinephrine (NE); cardiac tissue – natriuretic peptides; liver and BAT – Fgf21; muscle- Irisin, thyroid hormone- T_4. BAT also produces Bmp8b, and Vegf which increase thermogenic function in an autocrine manner. Additionally, Orexin and Bmp7 promote brown fat development but their cellular source is unknown.

Irisin

In skeletal muscle, Pgc-1α orchestrates the adaptive response to exercise, including increased mitochondrial biogenesis, fast to slow muscle fiber switching, and angiogenesis[169]. Unexpectedly however, raising Pgc-1α levels in muscle protects sedentary animals against obesity [170]. In a search for effectors of the enhanced energy expenditure in these animals, Spiegelman and colleagues discovered that the WAT of Pgc-1α transgenic mice contained more beige adipocytes[108]. They identified FNDC5 (Fibronectin type III domain containing 5) as a Pgc-1α target gene that was secreted from myocytes in the form of a novel hormone, named Irisin. Irisin stimulates the browning of WAT through specific actions on the beige preadipocyte population[10](Figure 4). Circulating Irisin levels increase in rodents and humans by exercise training. Remarkably, a modest increase in the serum levels of Irisin in mice stimulates beige fat development leading to enhanced glucose tolerance and suppressed weight gain[108]. Irisin is thus a very compelling hormone for clinical development since it has marked beneficial effects when used at near-physiological levels in mice.

Of course, as with any new hormone, there are many outstanding questions. What is the Irisin receptor(s) in beige fat precursors and how does it signal to the transcriptional machinery? Is the cleavage of FNDC5 into Irisin a regulated process? And, what effects does Irisin have on other tissues?

Fibroblast Growth Factor 21 (Fgf21)

Fgf21 is a circulating hormone that regulates systemic energy levels and has become a focus of clinical trials for obesity, diabetes and cardiovascular disease. In BAT, Fgf21 expression is increased by cold exposure and plays an important role in

thermogenesis[171,172]. Interestingly, there is a dramatic burst of Fgf21 production from the neonate liver in response to suckling- this is likely to be critical for activating BAT thermogenesis, at a time when animals are especially vulnerable to hypothermia[173]. Consistent with this, administration of Fgf21 to fasted neonates augments the thermogenic gene program in BAT. In WAT, Fgf21 increases Pgc-1α protein levels to drive beige adipocyte recruitment in response to cold[174,175].

Fgf21 has many desirable effects on metabolism in fed animals, including increased glucose uptake into peripheral tissues, improved insulin sensitivity and weight reduction[174,176,177]. Some of these actions may be mediated, at least in part, by stimulating fatty acid oxidation and energy dissipation pathways in adipocytes. Unfortunately however, Fgf21 has also been shown to cause bone loss, which will need to be overcome for clinical applications in obesity[178].

Natriuretic Peptides (NPs)

The natriuretic peptides, atrial NP (ANP) and brain-type NP (BNP) are released by the heart in response to heart failure or pressure overload. These factors reduce blood volume, blood pressure and cardiac output by dilating blood vessels and by promoting salt and fluid excretion from the kidneys. ANP was also known to promote lipolysis in adipocytes. Notably, high circulating levels of NPs had also been associated with weight loss in humans[179,180].

Bordicchia *et al*. recently discovered that increased levels of NPs in mice promotes beige adipocyte development in WAT and increases thermogenic gene levels in BAT[53]. This effect is due to a direct effect of NPs on adipose cells. Mechanistically, NPs trigger lipolysis and browning through activation of cGMP-dependent protein kinase

(PKG). PKG works in parallel with the more familiar β-adrenergic/PKA pathway to trigger lipolysis and stimulate thermogenesis (Figure 3).

The effect of NPs on brown and beige adipogenesis suggests that the control of adaptive thermogenesis is more complex than is currently appreciated. Cardiomyocytes, a cell type thought to have little cross-talk with adipocytes can dramatically alter gene expression and function of adipose through the secretion of potent cardiometabolic hormones. Importantly, cold increases NP levels, suggesting that this browning system may have evolved, perhaps in epidcardial fat, to safeguard cardiac function in animals during cold exposure. Systemic elevation of NPs would likely have a large number of undesirable off-target effects, but pharmacological targeting of this pathway in adipocytes could be considered.

BAT activators with central and peripheral actions

Bmp8b is produced by mature brown fat cells and functions to amplify the thermogenic response of brown adipocytes to adrenergic activators[181] (Figure 4). Interestingly, Bmp8b is also expressed in certain hypothalamic nuclei. Central treatment with Bmp8b increases sympathetic outflow to BAT but not other tissues and leads to weight loss. More studies are needed to assess the effect of Bmp8b on other tissues. But, at this stage, Bmp8b is a very promising target for therapeutics.

Other factors have been shown to augment BAT activity through both central and peripheral actions. For example, thyroid hormone directly induces thermogenic genes in brown adipocytes via the action of Thyroid receptors and also functions centrally to activate BAT[182-184]. Along similar lines, the neurotransmitter, Orexin augments BAT function via regulating sympathetic outflow and through directly promoting brown fat

precursor differentiation (Figure 4)[185,186]. Targeting molecules like Bmp8b, Orexin and Thyroid hormone that both recruit and activate brown fat may be particularly effective in promoting energy expenditure and weight loss.

Outlook and challenges

There is persuasive evidence from animal models that enhancement of brown and/or beige adipose function in humans could be very effective for treating type 2 diabetes and/or obesity. Moreover, there is now an extensive variety of factors and pathways that could potentially be targeted for therapeutic effect. In particular, the discoveries of circulating factors like Irisin, Fgf21 and NPs that enhance brown and beige fat function in mice has garnered tremendous interest. However, there are several challenges/issues to consider with regard to brown/beige fat-targeted therapies.

First, many of the thermogenic inducers, like Irisin, Bmp8b, Orexin, NPs, Sirt1, etc. were identified very recently as having effects on brown/beige fat biology. While the early findings are very promising, many more studies are needed to assess the potency of these factors on brown/beige fat under a variety of experimental conditions. On a related point, very few studies have explored the mechanisms of brown/beige adipocyte recruitment in human cells/tissues. Given the depot-specific mechanisms of beige fat recruitment in mice, this trait is likely to be highly variable amongst human fat depots. Defining the cell type(s) within human fat depots that can undergo efficient thermogenic activation and examining which pathways promote this process will be an important avenue of future research.

Secondly, even if thermogenic tissue can be pharmacologically expanded in humans, it still must be efficiently activated. Most available studies have used mice

housed below their thermoneutrality, which consequently have increased sympathetic outflow to fat. Thus, brown/beige fat-based therapies will likely need to expand the number of thermogenic fat cells(s) and/or activate them. Molecules like Bmp8b that increase the sensitivity of brown fat cells to adrenergic stimuli could be particularly valuable.

Finally, energy balance is tightly controlled by homeostatic mechanisms. Despite enormous fluctuations in food intake and physical activity, the average person is relatively weight stable over long periods of time. By virtue of this, most individuals that lose weight tend to gain it back. Even if brown fat thermogenesis can be ramped up to increase calorie consumption, the body may compensate for the calorie "deficit" by increasing hunger or increasing the metabolic efficiency of other tissues, like muscle.

Acknowledgements

Due to space limitations, we respectfully note that we were unable to comprehensively cite many worthy contributions to the field. We would like to thank members of the Seale lab for helpful comments and discussion. This work is supported by a NIGMS/NIH award DP2OD007288 and a Searle Scholars Award to P.S.

CHAPTER 2: Prdm16 is required for the maintenance of brown adipocyte identity and function in adult mice

Published: Matthew J. Harms[1,2], Jeff Ishibashi[1,2], Wenshan Wang[1,2], Hee-Woong Lim[1,3], Susumu Goyama[4], Tomohiko Sato[4], Mineo Kurokawa[4], Kyoung-Jae Won[1,3], Patrick Seale[1,2,*] (2014) Prdm16 is required for the maintenance of brown adipocyte identity and function in adult mice. Cell Metabolism, 2014 Apr 1;19(4):593-604. 33(19):8534-40.

Abstract

Prdm16 is a transcription factor that regulates the thermogenic gene program in brown and beige adipocytes. However, whether Prdm16 is required for the development or physiological function of brown adipose tissue (BAT) *in vivo* has been unclear. By analyzing mice that selectively lacked Prdm16 in the brown adipose lineage, we found that Prdm16 was dispensable for embryonic BAT development. However, Prdm16 was required in young mice to suppress the expression of white fat-selective genes in BAT through recruitment of the histone methyltransferase Ehmt1. Additionally, Prdm16-deficiency caused a severe adult-onset decline in the thermogenic character of interscapular BAT. This resulted in BAT dysfunction and cold sensitivity but did not predispose the animals to obesity. Interestingly, the loss of brown fat identity due to ablation of Prdm16 was accelerated by concurrent deletion of the closely related Prdm3 gene. Together, these results show that Prdm16 and Prdm3 control postnatal BAT identity and function.

Introduction

The global rise in obesity and type-2 diabetes has precipitated the need for novel approaches to reduce adiposity. Obesity is caused by prolonged periods of positive energy balance in which energy taken in from food exceeds energy expenditure. Brown and beige adipose cells expend chemical energy in the form of heat and can thus oppose obesity in mice. Higher levels of brown and/or beige adipose activity are also correlated with reduced adiposity in people [18].

Brown adipocytes reside in discrete brown adipose tissue (BAT) depots whereas beige adipocytes are intermingled with white adipocytes in white adipose tissue (WAT). Both cell types have a multilocular morphology, large numbers of mitochondria, and express a common set of brown fat (versus white fat)-selective genes such as *Uncoupling protein-1* (*Ucp1*) [187]. Upon activation, Ucp1 dissipates the mitochondrial proton gradient, which results in loss of respiratory control and the production of substantial amounts of heat from the combustion of available substrates [120]. The heat produced by brown and/or beige fat is necessary for the survival of small mammals in the cold and also reduces fat deposition in animals fed a high fat/low protein diet [98,101,120].

The development of therapies aimed at increasing the amount of brown or beige adipocytes will require a detailed mechanistic understanding of how these cell types are formed. PR (PRD1-BF1-RIZ1 homologous)-domain containing 16 (Prdm16) is a transcriptional co-regulator that has been shown to powerfully regulate the differentiation of brown and beige fat cells [187]. Notably, increased expression of Prdm16 in mouse WAT promotes beige adipocyte development and suppresses metabolic disease [26]. By contrast, deletion of Prdm16 in adipocytes causes a profound loss of beige adipocyte function in mice, leading to aggravated metabolic disease upon exposure to high fat diet

[188]. Surprisingly, the deletion of Prdm16 in adipocytes, at relatively late stages of their differentiation, does not affect BAT function [188].

BAT forms during embryonic development before other fat depots, and is an essential source of heat production in neonates. Lineage analyses indicate that brown adipocytes and skeletal myocytes originate from precursor cells in the somite that express *Engrailed-1*, *Pax7* and *Myf5* [13,76,189]. Previous studies showed that Prdm16 controls a bidirectional cell fate switch between brown fat and skeletal muscle in this somite-derived lineage [13,90,97,190,191]. However, the requirement for Prdm16 in regulating brown adipocyte development and function *in vivo* had not been thoroughly assessed.

In this study, we used the *Myf5*^{Cre} mouse strain to delete Prdm16 in the progenitors for brown adipocytes and muscle but not beige adipose cells. BAT developed normally in the absence of Prdm16, without evidence of a cell fate switch into muscle. In BAT from young mice, Prdm16-deficiency had little effect on the expression of key BAT-selective genes but elicited a dramatic rise in expression of many WAT-selective genes. As the knockout animals aged, however, there was a striking loss of thermogenic character in the interscapular BAT (iBAT). This collapse of iBAT identity was accelerated by concurrent deletion of the closely related Prdm3 gene. Importantly, adult mice with Prdm16-depleted BAT had severely reduced BAT function but did not gain more weight than wildtype animals. Altogether, our results indicate that Prdm16 and Prdm3 play a critical role in the postnatal maintenance and function of BAT.

Results

Prdm16 is dispensable for embryonic BAT development

To investigate the genetic requirement for Prdm16 in BAT development and function, we deleted *Prdm16* in the brown fat lineage by intercrossing *Myf5*^{Cre} mice [192] with *Prdm16*$^{flox/flox}$ mice (Figure S1A). *Myf5*^{Cre} is activated in the somitic precursors that give rise to brown adipocytes. The resulting *Myf5*$^{Cre/+}$;*Prdm16*$^{flox/flox}$ (*Myf5-ΔPrdm16*) mice were born in normal Mendelian ratios and were grossly indistinguishable from their wildtype (WT) littermates. Prdm16 mRNA and protein expression were almost completely ablated in *Myf5-ΔPrdm16* BAT (Figure 1A).

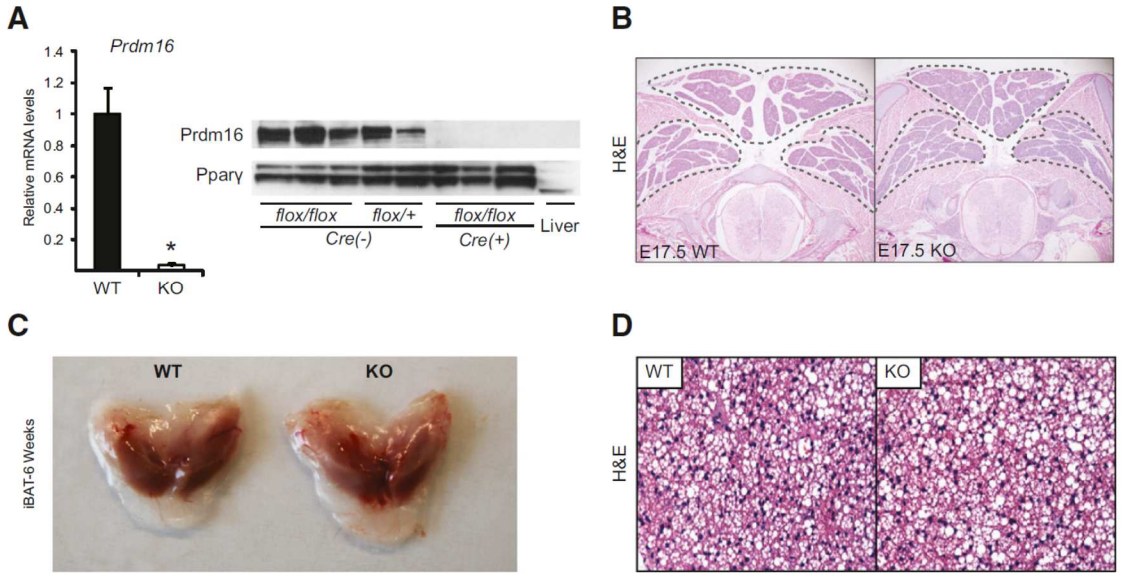

Figure 1: *Prdm16* is dispensable for embryonic BAT development

(A) *Prdm16* mRNA and protein levels from wildtype (WT) and *Myf5ΔPrdm16* (KO) mice (mean ± SEM; n=5, 8 (WT, KO); *p<0.05). **(B)** Hematoxylin and eosin (H&E) staining of representative sections from the interscapular regions of E17.5 WT and KO embryos. **(C)** Interscapular brown adipose tissue (iBAT) from 6-week-old WT and KO mice. **(D)** H&E staining of representative sections from the iBAT of 6-week-old WT and KO mice.

Surprisingly, there were no differences in the morphology or size of BAT depots between WT and *Myf5-ΔPrdm16* mice at E17.5 of development (Figure 1B). At 6 weeks of age, WT and *Prdm16*-deficient iBAT depots were also grossly and histologically similar (Figures 1C, D). The other major site of *Myf5*^{Cre}-mediated DNA recombination during development is skeletal muscle where *Prdm16* mRNA is not normally detected [87]. Consistent with this, *Prdm16* mRNA levels were equivalent in WT and *Myf5-ΔPrdm16* muscles (Figure S1B). Previous studies indicated that Prdm16 can suppress the expression of certain muscle-specific genes [13]; however, we did not observe elevated expression of muscle-specific genes in the iBAT of *Myf5-ΔPrdm16* mice (Figure S1C). Taken together, these results indicate that Prdm16 is dispensable for BAT formation in mice.

Figure S1. *Prdm16* deficiency in BAT does not increase the expression of skeletal muscle genes.

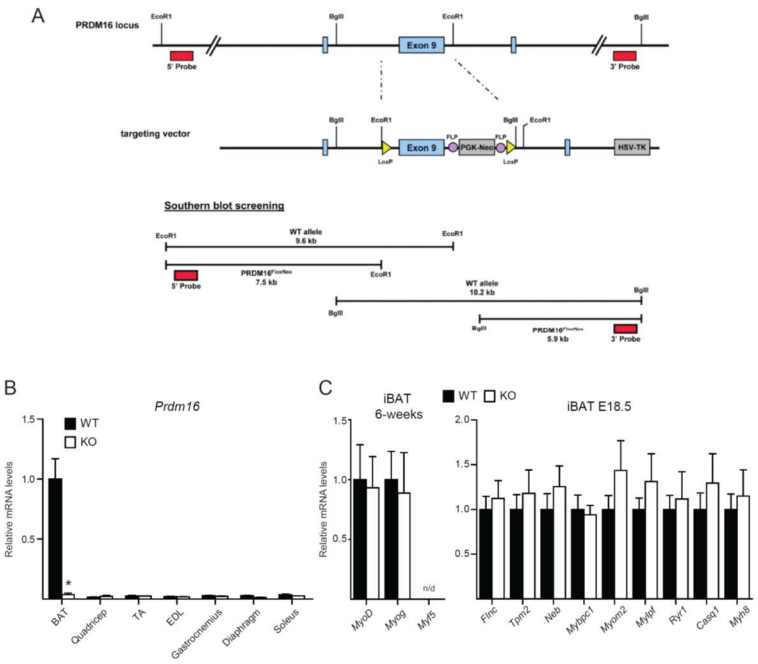

(A) Gene targeting strategy for creating *Prdm16*^{flox} mice. **(B)** *Prdm16* mRNA levels in interscapular brown adipose tissue (iBAT) and several skeletal muscles (quadricep, tibialis anterior [TA], extensor digitorum longus [EDL], gasterocnemius, diaphragm and soleus) of wildtype (WT) and *Myf5-ΔPrdm16* mice. **(C)** mRNA levels of skeletal muscle-selective genes from the iBAT of 6-week-old and E18.5 WT and KO mice. (**B,C**: mean ±SEM, n=6-11. *p,0.01).

Prdm16 recruits Ehmt1 to repress the expression of white fat-selective genes

We next analyzed the molecular phenotype of iBAT from 6-week-old WT and *Myf5-ΔPrdm16* mice. Pan-adipocyte genes like *Fabp4* and *Adipoq* were equivalently expressed in WT and Prdm16 knock-out (KO) iBAT (Figure 2A), although KO tissue expressed higher levels of *Pparγ2*, the adipose-selective isoform of *Pparγ*. The levels of brown fat-selective (*Pgc1α*, *Ucp1* and *Cidea*) and mitochondrial (*Cycs*, *Cox5b*, *Cox7a1*) genes were mildly but not significantly decreased in Prdm16 KO tissue (Figure 2A).

To search for genes/pathways that were sensitive to Prdm16 levels in BAT, we compared the global gene expression profiles of iBAT from 6-week-old WT and *Myf5-ΔPrdm16* mice using cDNA microarrays. Gene ontology analysis revealed that genes involved in lipid-metabolism, including "lipid biosynthetic process" and "lipid metabolic process", were increased in the absence of Prdm16 (Figure S2A). This suggested that loss of Prdm16 shifted adipocyte metabolism to favor a white fat-like energy storage phenotype. We thus specifically analyzed the impact of Prdm16-deficiency on the complete set of BAT- and WAT-selective genes (Figure 2B). Consistent with qPCR analysis, most typical brown-selective genes (e.g. *Ucp1*, *Cidea, Cox5b*) were only slightly reduced in Prdm16-deficient BAT. However, the expression of a few BAT-selective genes were dramatically diminished in KO BAT, including *Dio2* (*deiodinase, iodothyronine, type II*), an important regulator of brown adipocyte function [182] (Figure 2B, C). In line with the mRNA data, western blots showed that Prdm16-deficient BAT expressed higher levels of Pparγ and Agt and slightly reduced levels of Ucp1 protein (Figure 2D). Additionally, the global expression analyses revealed a broad increase in the expression of white fat-selective genes in KO BAT (Figure 2B). Real-time PCR analysis validated the increased expression of many of these genes, including a 20-fold

increase in *Agt*, and 6- to 8-fold increases in *Retn, Gpr64, Nnmt and Trim14* (Figure 2C). These results reveal that Prdm16 is required in BAT to suppress the expression of many white fat-selective genes.

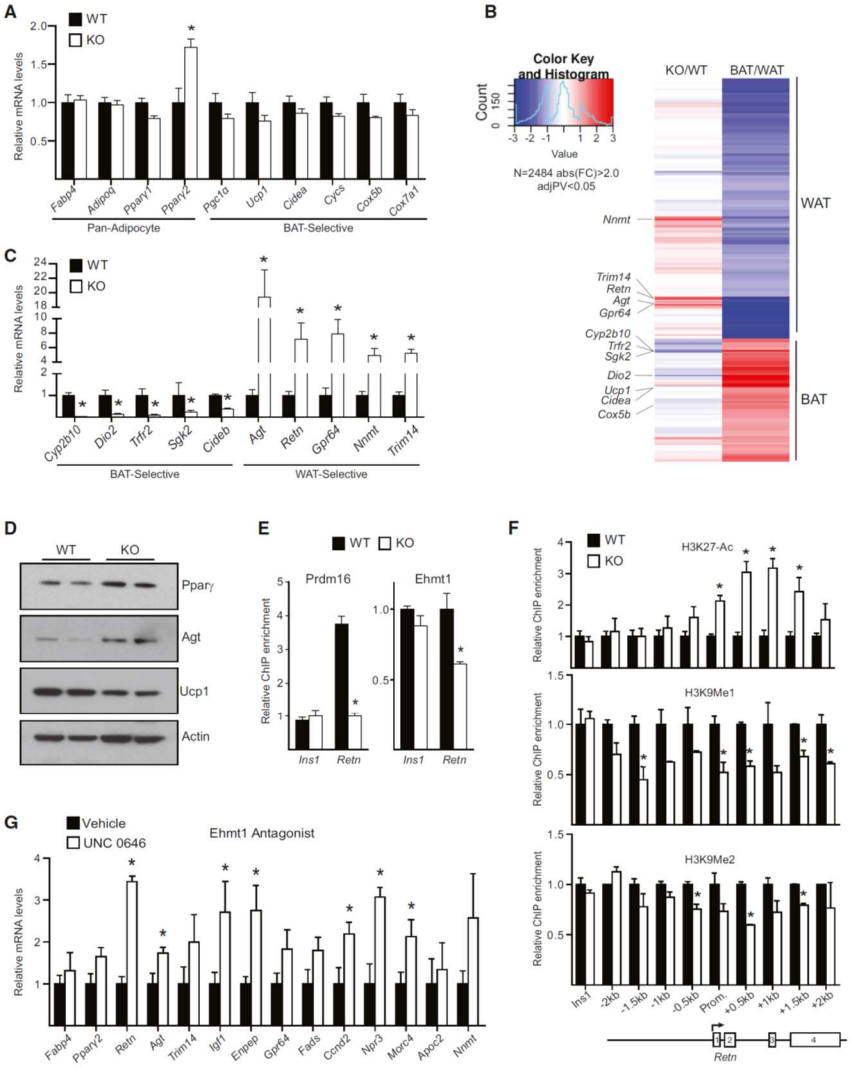

Figure 2: Prdm16 represses the expression of white fat-selective genes (A) mRNA levels of pan-adipocyte and BAT-selective genes in BAT from 6-week-old wildtype (WT) and *Myf5ΔPrdm16* (KO) mice (mean ± SEM, WT n=5, KO n=4, *p<0.05). (B) Heat map depicting the mRNA levels of white and brown fat-selective genes (WAT/BAT) in BAT from 6-week-old WT and KO mice (KO/WT) (n=4). (C) qPCR validation of BAT- and WAT-selective mRNAs identified in (B) from WT and KO BAT (mean ± SEM, WT n=5, KO n=4, *p<0.05. (D) Western blot analysis of Pparγ, Agt, Ucp1 and Actin (loading control) protein levels in BAT from 6-week-old WT and KO mice. (E) ChIP-qPCR analysis of endogenous Prdm16 and Ehmt1 binding at the *Retn* promoter (mean ± SEM; n=3; *p<0.05). (F) ChIP-qPCR analysis of H3K27-Ac, H3K9-Me1 and H3K9-Me2 enrichment in a 4 kb region spanning the transcriptional start site of *Retn*. *Ins1* was used a non-specific control binding site (mean ± SEM; n=3; *p<0.05). (G) mRNA levels of WAT-selective genes in brown adipocytes treated with Ehmt1 antagonist UNC 0646, or vehicle control (mean ± stdev; n=3; *p<0.05).

We used *Retn* as a model locus to investigate the mechanism by which Prdm16 represses white fat-selective genes. Chromatin immunoprecipitation (ChIP) for Prdm16 in WT and KO BAT showed that it was specifically enriched at the *Retn* promoter relative to non-specific control sites (Figure 2E). The repressive chromatin modifier, Ehmt1 (G9a-like protein), an interacting partner of Prdm16 [90,190], was also bound to the *Retn* promoter in BAT and its binding there was reduced by ~40% in Prdm16 KO BAT relative to WT BAT (Figure 2E). Importantly, the loss of Prdm16 and Ehmt1 binding at *Retn* was associated with increased levels of H3K27-Ac, a histone mark correlated with active transcription; and decreased levels of H3K9-Me1 and H3K9-Me2, modifications laid down by Ehmt1 and associated with gene repression (Figure 2F). Ehmt1 binding at the *Agt* promoter was also significantly decreased in *Myf5-ΔPrdm16* BAT (Figure S2B). These data suggest that Prdm16 recruits Ehmt1 to certain white fat-selective genes to decrease their transcription. In accordance with this, treatment of cultured brown adipocytes with UNC 0646, an Ehmt1 antagonist, increased the expression of many white fat-selective genes, including *Retn* and *Agt* (Figure 2G).

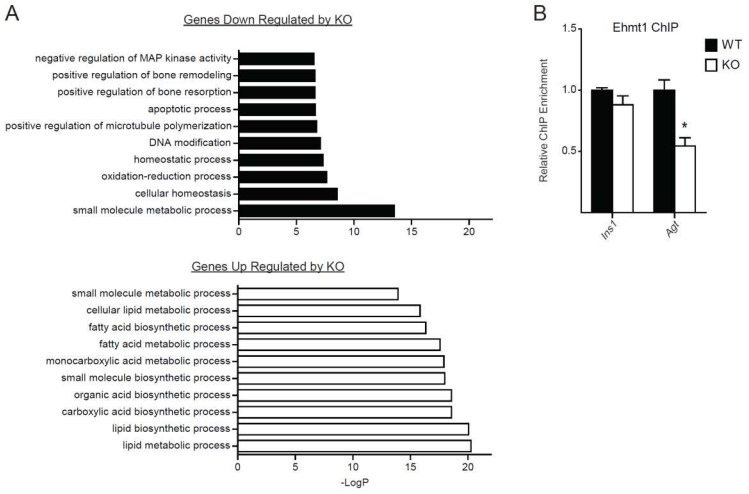

Figure S2. *Prdm16* deficient iBAT expressed a white fat-related gene profile.
(A) Gene Ontology (GO) analysis of genes thar are differentially expressed betweeb wildtype (WT) and *Prsm16*-deficient BAT (KO) of 6-week-old mice. **(B)** Relative ChIP enrichment for Ehmt1 at the *Ins1* (control) and *Agt* promoter in WT and KO iBAT. (mean± stdev, n=3,*p<0.05).

Prdm16 maintains iBAT identity during aging

In contrast to juvenile mice, we noticed that older (>6 months of age) *Myf5-ΔPrdm16* animals exhibited a profound morphological "whitening" of their iBAT. This included a ~50% increase in the size of the tissue, a switch from multilocular to unilocular morphology, and increased lipid content (Figures 3A, S3A). To determine when this phenotype emerged, we analyzed gene expression in iBAT from WT and *Myf5-ΔPrdm16* mice at 3 and 6 months of age. In 3-month-old animals, Prdm16-deficiency resulted in a modest decline in the expression of brown fat-selective genes, including ~30-40% reductions in the levels of *Ucp1*, *Pparα* and many mitochondrial genes (Figure 3B). The reduction of brown fat-specific gene expression in KO BAT was much more pronounced in 6-month-old mice. At that age, *Ucp1* mRNA levels were decreased by >90% and *Cidea* and *Pparα* levels were reduced by ~70% (Figure 3B). Hematoxylin and eosin staining showed that lipid droplet size increased dramatically in the KO BAT from 3 to 6 months of age (Figure S3B). Microarray analyses revealed that *Myf5-ΔPrdm16* iBAT from 11-month-old mice expressed substantially reduced levels of a broad brown fat-selective program (Figure 3C). The elevation of white fat-selective gene expression caused by *Prdm16*-deficiency was further exaggerated in older mice (Figure 3C). Immunohistochemical analysis showed that Ucp1 protein levels decreased dramatically in the iBAT of *Myf5-ΔPrdm16* animals between 3 and 6 months of age (Figure 3D). Western blot analysis confirmed that Ucp1 protein levels were much lower in KO relative to WT iBAT at 6 months of age, coincident with elevated levels of Pparγ and Agt (Figure 3E). DNA isolated from the iBAT of 11-month-old *Myf5-ΔPrdm16* mice was >90% recombined at the *Prdm16* locus (ie. exon 9-deleted) (Figure S3C), indicating that the "whitened" KO tissue was composed of *Myf5*^{Cre} lineage-derived adipocytes.

We next examined the consequences of *Prdm16*-deficiency on mitochondrial mass and function. Using a Clark electrode, we measured oxygen consumption in isolated iBAT from 9-month-old WT and *Myf5-ΔPrdm16* mice. Remarkably, basal (unstimulated) respiration in the KO iBAT was ~85% lower than in WT tissue (Figure 3F), indicative of a loss of mitochondrial mass. Indeed, PCR analysis revealed that KO BAT had 50% less mitochondrial DNA than WT tissue (Figure 3G). Transmission electron microscopy studies showed that WT adipocytes were packed with mitochondria containing well-ordered cristae, whereas KO adipocytes had a paucity of mitochondria, of which the remainder had poorly organized cristae and exhibited signs of degeneration (Figure 3H). Taken together, these data establish an important role for Prdm16 in maintaining brown adipocyte identity (including high levels of mitochondria) in adult mice.

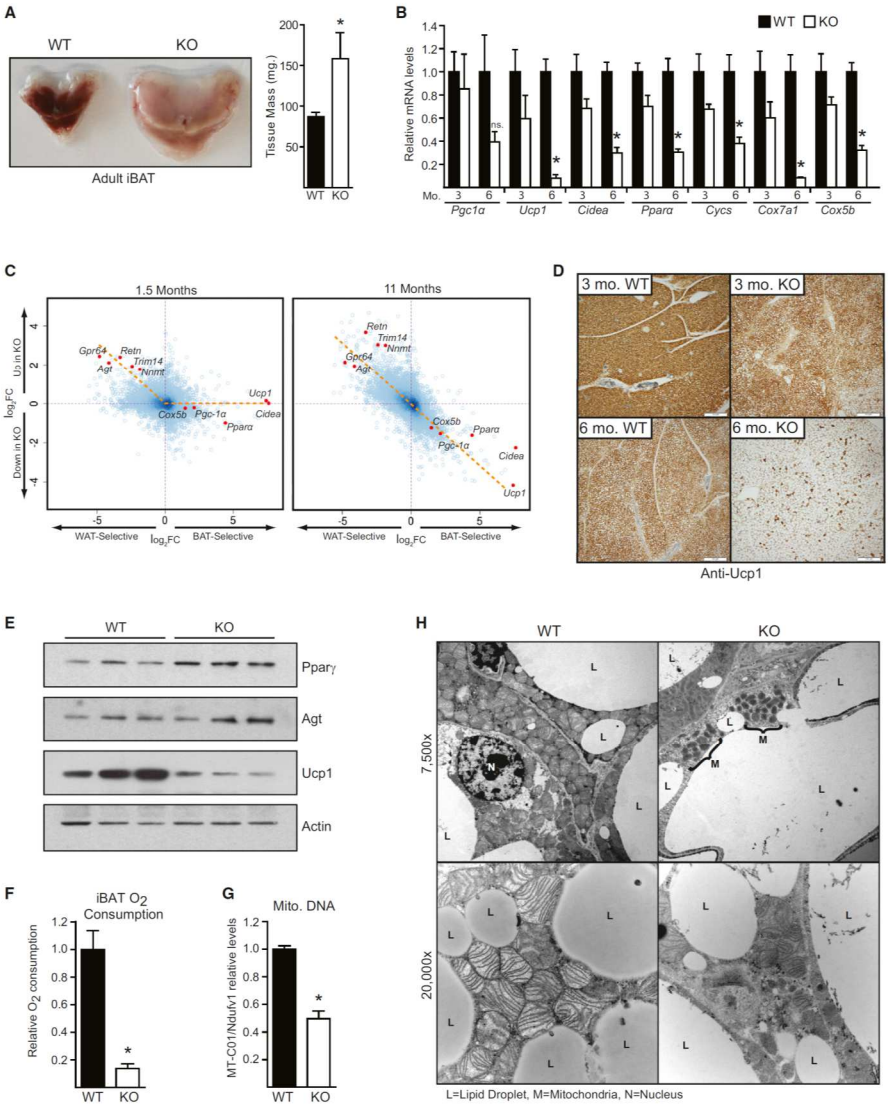

Figure 3: Prdm16 is required for the maintenance of iBAT fate in adult animals **(A)** Gross morphology and mass of iBAT depots from one-year-old wildtype (WT) and *Myf5*Δ*Prdm16* (KO) mice (mean ± SEM, n=7, *p<0.05). **(B)** mRNA levels of BAT-selective genes in BAT from 3- and 6-month-old WT and KO mice (mean ± SEM, n=4, *p<0.05). **(C)** Global analysis of BAT- and WAT-selective mRNA levels in BAT from 6-week-old and 11-month-old mice. Dashed orange line illustrates the change in gene expression pattern. Data is presented as a $\log_2$FC scatter plot. (n=4). **(D)** Immunohistochemical staining for Ucp1 protein in sections of BAT from 3- and 6-month-old WT and KO mice. **(E)** Western blot analysis of Pparγ, Agt, Ucp1 and Actin (loading control) protein levels in BAT from 11-month-old WT and KO mice. **(F)** Oxygen consumption of isolated and minced BAT from 9-month-old WT and KO mice. Data is presented as nmol of oxygen consumed per minute per mg of tissue (mean ± SEM, WT n=4, KO n=3, *p<0.05). **(G)** Mitochondrial DNA levels in BAT from 9-month-old WT and KO mice (mean ± SEM, WT n=4, KO n=3, *p<0.05. **(H)** Transmission electron micrographs of BAT from 9-month-old WT and KO mice (L=lipid droplet; M=mitochondria; N=nucleus).

The interscapular depot is the largest BAT depot in adult mice and was the focus of our study. However, we also investigated the impact of *Prdm16*-deficiency on the axillary and cervical BAT (aBAT and cBAT). The aBAT and cBAT depots in 6-month-old *Myf5-ΔPrdm16* appeared paler than those in WT mice, but there was no difference in aBAT or cBAT mass between WT and *Myf5-ΔPrdm16* mice (Figure S3D). Interestingly, the white fat-selective genes were markedly elevated in Prdm16-deficient aBAT and cBAT but brown fat-specific gene levels were not affected (Figure S3E). These results suggest that interscapular BAT is particularly reliant on Prdm16 for maintaining the expression of brown fat-selective genes during aging.

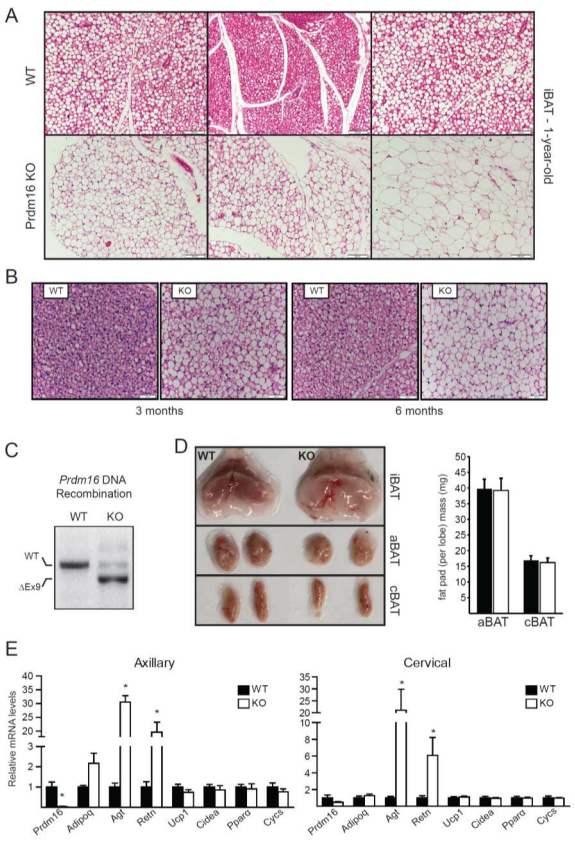

Figure S3. Prdm16-deficiency causes a loss of interscapular brown adipose tissue identity in adult mice

(A) Hematoxylin and eosin (H&E) staining of sections from the interscapular brown adipose tissue (iBAT) of one-year-old WT and Myf5-ΔPrdm16 (Prdm16 KO) mice. **(B)** H&E staining of WT and Myf5-ΔPrdm16 (KO) iBAT from 3 and 6 month-old-mice. **(C)** Myf5-Cre driven DNA recombination of the Prdm16 locus in iBAT from 9-month-old WT and KO mice. **(D)** Gross morphology and mass of dissected axillary and cervical BAT depots from WT and KO mice. **(E)** mRNA levels of brown and white fat-related genes in the axillary and cervical BAT depots of 6-month-old WT and KO mice (mean ± stdev, n=4, *p<0.05).

Prdm16 is required for induction of the brown fat gene program in isolated precursors

The aging-associated decline of iBAT identity in *Myf5-ΔPrdm16* mice raised the question of whether Prdm16 was required cell autonomously for proper brown adipocyte differentiation in this depot. To study this, we isolated primary brown adipocyte precursors from the iBAT of WT and *Myf5-ΔPrdm16* mice and examined their differentiation into adipocytes under defined culture conditions. WT and KO precursor cells from newborn iBAT differentiated with equivalent efficiently into mature lipid droplet-containing adipocytes that expressed similar levels of pan-adipocyte genes, including *Fabp4* and *Adipoq* (Figure 4A, S4A). KO cultures displayed a >90% reduction in Prdm16 mRNA and protein levels (Figure 4B, D), indicating that most or all of the precursor cells in BAT descend from *Myf5*^{Cre}-expressing cells. Strikingly, Prdm16-deficient cultures expressed dramatically lower levels of brown adipocyte-specific genes as compared to WT cultures, including 90-95% reductions in the mRNA levels of *Ucp1*, *Cidea* and *Dio2*; and 60-80% decreases in *Pgc1α, Pparα, Cox7a1, Cycs,* and *Errγ* (Figure 4B). WT adipocytes also had four times more mitochondrial DNA than KO cells (Figure 4C). Western blot analysis showed that Ucp1 protein, like its mRNA, was dramatically lower in KO adipocytes (Figure 4D). Importantly, retroviral expression of Prdm16 in KO preadipocytes efficiently activated the expression of thermogenic genes like *Ucp1* and *Cidea* (Figure 4E), indicating that the KO cells were competent to induce the brown-selective gene program. Immortalized brown fat cell lines from newborn BAT of *Myf5-ΔPrdm16* mice displayed a similarly severe defect in activating the differentiation-linked brown fat-specific gene program (Figure S4B).

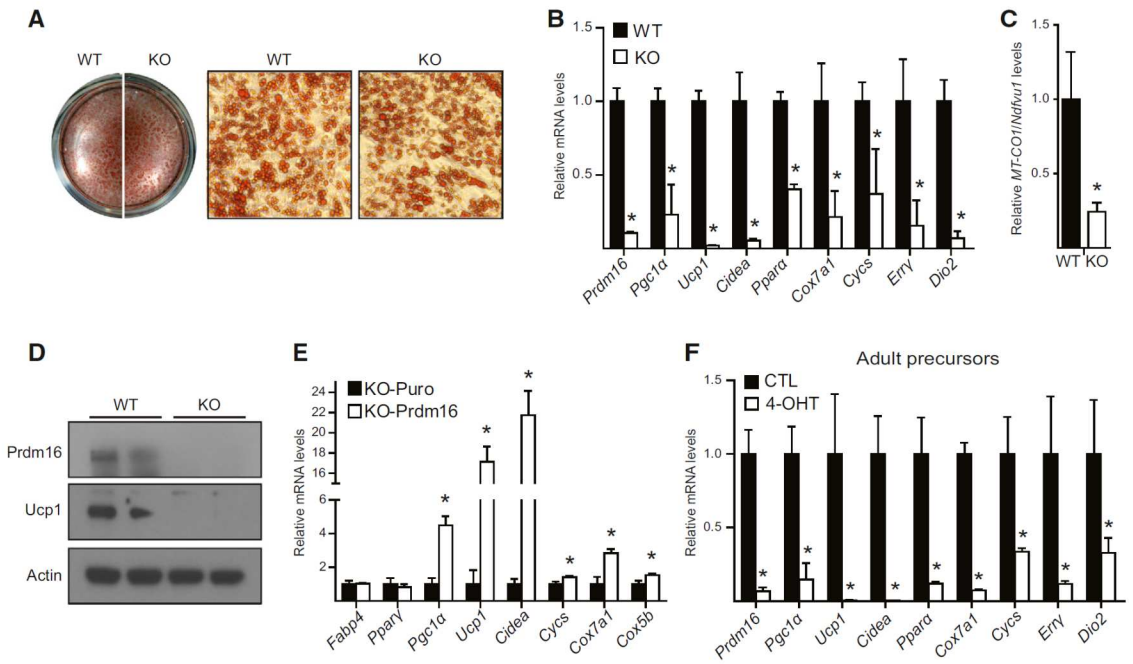

Figure 4: Prdm16 is required for activation of the brown fat-selective gene program in cultured brown fat precursors

(A,B) Primary precursor cells from the iBAT of newborn wildtype (WT) and *Myf5ΔPrdm16* (KO) mice induced to differentiate into adipocytes and stained with Oil-red-o (A) or analyzed by qPCR for their expression of brown fat-selective genes (mean ± stdev, n=3, *p<0.05) (B). **(C)** Mitochondrial DNA levels in WT and KO adipocytes from immortalized brown fat-derived precursor cells (mean ± SEM, n=6, *p<0.05). **(D)** Western blot analysis of Prdm16, Ucp1 and Actin (loading control) in WT and KO adipocytes from immortalized brown fat-derived precursor cells. **(E)** Primary precursor cells from iBAT of newborn KO mice infected with puromycin (KO-puro; control) or Prdm16 (KO-Prdm16) retrovirus, were induced to differentiate into adipocytes. Gene expression analysis for general adipocyte (*Fabp4*, *Pparγ*) and brown fat-selective genes (mean ± stdev, n=3, *p<0.05). **(F)** Primary precursor cells from the iBAT of adult *Rosa26*$^{Cre/+}$;*Prdm16*$^{flox/flox}$ mice were treated with 4-hydroxytamoxifen (4-OHT) to delete Prdm16 or vehicle (ethanol) (CTL) before being induced to undergo adipocyte differentiation. Adipocyte cultures were analyzed for their expression of brown fat-selective genes (mean ± stdev, n=3, *p<0.05).

We also tested whether acute *Prdm16* deletion affected the brown fat differentiation program of preadipocytes isolated from adult animals. To this end, brown fat precursor cells were isolated from 8-week-old *Prdm16*$^{flox/flox}$;*Rosa26*^{CreERT} mice that ubiquitously express a tamoxifen-inducible Cre recombinase. Precursor cells from the

iBAT of these mice were isolated and then treated with 4-hydroxytamoxifen (4-OHT) or vehicle (ethanol). The acute loss of Prdm16 caused by 4-OHT treatment completely blocked the differentiation-linked induction of brown-selective genes (including *Ucp1* and *Cidea*) while leaving the general adipogenic program intact (Figure 4F).

The brown-specific gene program was not significantly affected by loss of *Prdm16* in BAT from embryos and young mice. This raised the possibility that the embryonic precursors may not require *Prdm16* to execute a normal brown fat differentiation program. To investigate this, we purified brown adipocyte precursors from the dorsal body walls of WT and *Myf5-ΔPrdm16* mouse embryos at E14.5 days post-coitum - a stage when differentiated brown adipocytes are first appearing. Precursor cells were purified by flow cytometry based on cell-surface expression of platelet-derived growth factor receptor alpha (Pdgfrα), which enriches for adipogenic precursors in BAT and other tissues[193].

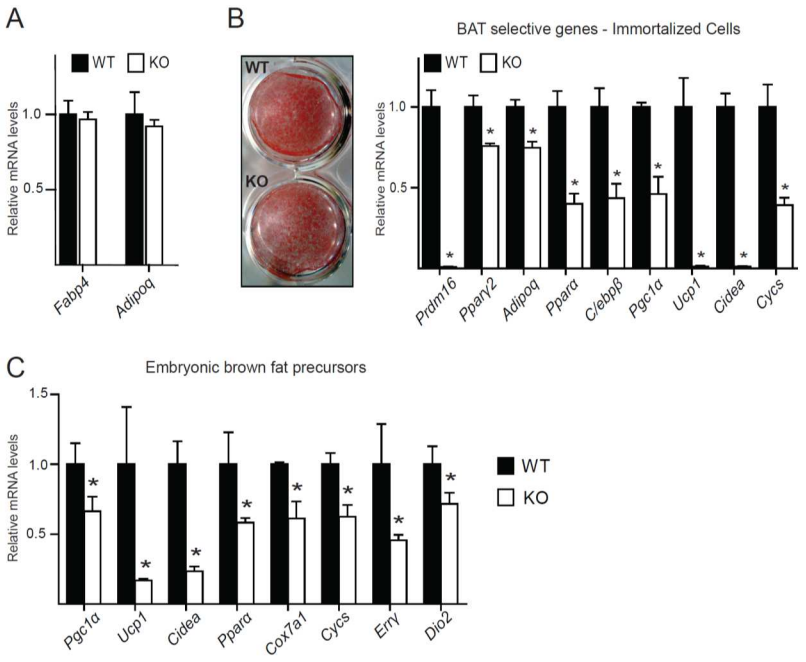

Figure S4 - Prdm16 is required cell automously
(A) Fabp4 and Adipoq mRNA levels in adipocytes derived from newborn WT and Myf5-ΔPrdm16 (KO) brown adipocyte precursors. **(B)** Differentiated immortalized WT and KO brown precursor cells. Oil-red-O staining (left); mRNA expression (mean ± stdev, n=3) (right). **(C)** Gene expression in FACS purified Pdgfrα+ precursors from the body wall of E14.5 WT and KO embryos induced to differentiated for 8 days (mean ± SEM, n=3, *p<0.05).

The *Prdm16*-deficient embryonic cells, like the cells from newborn and adult BAT, displayed an *ex vivo* deficit in brown fat-specific gene expression during adipogenesis (Figure S4C). Taken together, these data demonstrate that Prdm16 is required to activate the brown-specific adipogenic program in isolated BAT precursors.

Reduced BAT function in *Myf5-ΔPrdm16* mice

A key question is whether the loss of Prdm16 in BAT has physiological consequences for the animals. To assess BAT function in mice, we surgically implanted temperature probes subcutaneously in the interscapular region of 10-month-old WT and *Myf5-ΔPrdm16* mice. After allowing the animals to recover for one week, we exposed them to cold (4°C) and monitored tissue temperature over a period of 3 hours. Under room temperature conditions (at T=0 prior to cold exposure), WT and *Myf5-ΔPrdm16* mice had similar core and interscapular temperatures (Figure 5A; S5A). However, upon cold exposure, tissue temperature dropped precipitously in *Myf5-ΔPrdm16* mice, declining >1°C more than in WT animals after 3 hours (Figure 5A). Since mice rely substantially on shivering thermogenesis during acute cold exposure [195], we further analyzed *in vivo* BAT function by measuring whole-animal oxygen consumption before and at several time points after injection of norepinephrine (NE), the classic activator of BAT-mediated thermogenesis. As evidenced through the study of Ucp1 KO animals, this method provides a more stringent measurement of BAT activity [195,196]. In WT mice, oxygen consumption increased by ~4-fold in response to NE (Figure 5B). By contrast, NE only marginally raised the oxygen consumption of *Myf5-ΔPrdm16* mice, which diverged significantly from than that of WT mice by 24 minutes post-NE treatment (Figure 5B). Taken together, these data demonstrate that *Prdm16* is required for the

thermogenic function of BAT *in vivo*.

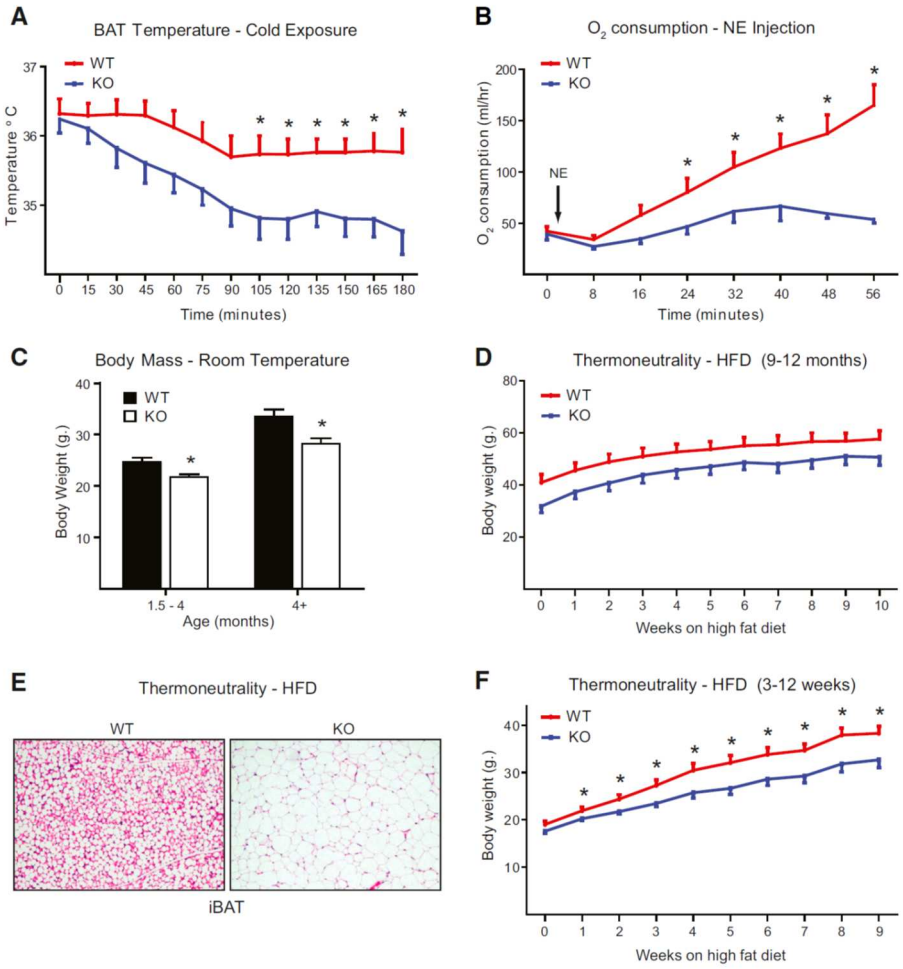

Figure 5: *Myf5-*Δ*Prdm16* mice have severely deficient BAT function but are not prone to obesity or metabolic disease

(A) Temperature recordings from probes implanted into the interscapular (subcutaneous) region of 1-year-old WT and *Myf5*Δ*Prdm16* (KO) mice. Data was collected over 3 hours after moving animals from room temperature (~22°C) to 4˚C (T=0) (mean ± SEM, n=10, *p<0.05). **(B)** Whole-body oxygen consumption in 1-year-old WT and KO mice before and after treatment with 1 mg/kg norepinephrine (NE) (mean ± SEM, n=10, *p<0.05). **(C)** Body weights of WT and KO mice at different ages maintained under standard housing conditions and fed a regular chow diet (mean ± SEM, n=10-22, *p<0.05). **(D)** Body weights of 9-month-old WT and KO mice that were housed at 28°C and fed a high fat diet (HFD) for ten weeks (mean ± SEM, n=5, *p<0.05). **(E)** Hematoxylin and eosin (HE) staining of sections from the interscapular BAT of 3-week-old mice housed at 28°C on HFD. **(F)** Body weights of WT and KO mice that were kept at 28°C and fed a high fat diet for 9 weeks starting at weaning (3-weeks-old) (mean ± SEM, WT n=6, KO n=8, *p<0.05).

The reduced thermogenic capacity of *Myf5-ΔPrdm16* mice suggested that these animals may be susceptible to weight gain and metabolic disease. However, contrary to our expectation, *Myf5-ΔPrdm16* mice weighed less than their WT counterparts at all ages studied (Figure 5C). MRI examination revealed that *Myf5-ΔPrdm16* mice had less lean and fat mass than WT mice (Figure S5B). Unexpectedly, *Myf5-ΔPrdm16* mice were also slightly, but significantly shorter than WT animals (Figure S5C) – this likely explains their proportional reduction in lean and fat mass. Consistent with their reduced fat mass, *Myf5-ΔPrdm16* mice also had improved glucose tolerance as compared to WT mice (Figure S5D).

The contribution of BAT thermogenesis to energy balance can be masked at room temperature in mice due to the cold-mediated activation of other thermogenic pathways [101,195]. We therefore placed 9-month-old WT and *Myf5-ΔPrdm16* mice at 28°C to exempt them from cold stress, and fed them a high fat diet for 10 weeks. Under these conditions, the weight gained by WT and *Myf5-ΔPrdm16* mice was remarkably similar (Figure 5D). We also placed 3-week-old WT and *Myf5-ΔPrdm16* mice on a high fat diet and housed them at 28°C for 10 weeks. Under these conditions, *Myf5-ΔPrdm16* iBAT developed a severe loss of normal brown adipocyte morphology (Figure 5E) and reduced levels of brown fat-specific genes (Figure S5E). Despite this, the KO mice gained less weight than WT mice (Figure 5F), although the percent weight gained by WT and KO mice per week and overall was very similar. Consistent with this, oxygen consumption (Figure S5F) and food intake (Figure S5G) was not significantly different between WT and KO mice.

The loss of BAT function in adult *Myf5-ΔPrdm16* mice was not accompanied by increased browning of WAT depots. Specifically, there was: (1) no increase in the expression levels of *Ucp1* or other brown fat-selective gene markers in the inguinal or

epididymal WAT of *Myf5-ΔPrdm16* KO mice (Figure S5H,I); and (2) no difference between the morphology of WT and KO WAT in mice housed at 22°C (not shown) or 28°C (Figure S5J). Altogether, these data show that loss of Prdm16 activity in BAT does not impair diet-induced thermogenesis in mice.

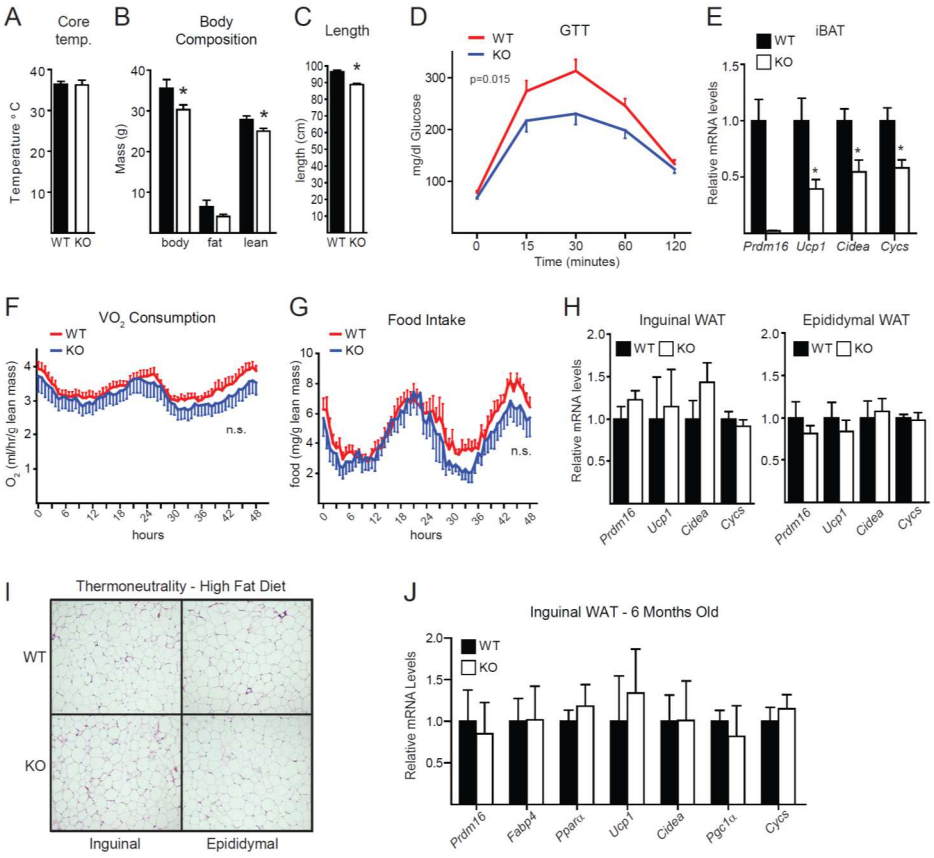

Figure S5 - Myf5-ΔPrdm16 mice do not have metabolic defects. **(A)** Core body temperatures of 3-month-old WT and Myf5-ΔPrdm16 (KO) mice, n=4. **(B)** Body compositions (fat and lean mass) of 11-month-old WT and KO mice by MRI, n=10. **(C)** Body length of 11-month-old WT and KO mice, n=10. **(D)** Glucose tolerance tests on 11-month-old chow-fed WT and KO mice after an overnight fast. Blood glucose levels measured at the indicated times following an intraperitoneal injection of glucose (T0), n=10. **(E)** mRNA expression levels of BAT-enriched genes from BAT of 3-month-old WT and KO mice at thermoneutrality and fed a high-fat diet, n=8. **(F,G)** Oxygen consumption and food intake over 48 hours in individually housed 11-month-old WT and KO mice housed at 22°C. Data are normalized to lean body mass. Oxygen consumption is presented as V(O2)/mouse/hour, n=10. **(H)** mRNA expression of BAT-enriched genes in inguinal WAT from 6-month-old WT and KO mice housed at standard housing conditions, n=4. **(I,J)** Hematoxylin and eosin staining (I) and mRNA expression levels of BAT nriched genes (J) in inguinal and epididymal WAT from 3-month-old mice at thermoneutrality and fed a high-fat diet for 9 weeks, n=8. Values are mean ± SEM; *$p < 0.05$.

Prdm3 compensates for the loss of Prdm16 to preserve brown fat fate in young mice

Prdm16 is most closely related in sequence and structure to Prdm3 (also called Mecom [Mds1 and Evi1 complex locus]) [197]. We previously reported that Prdm3 regulates white adipocyte differentiation through its association with C/EBPβ[198]. To test whether Prdm3 could induce brown fat-selective genes, we used retrovirus to ectopically express Prdm16, Prdm3 (Evi1 isoform), or empty vector (MSCV-Puro) in C2C12 cells (Figure 6A). In this context, both Prdm16 and Prdm3 robustly induced adipocyte differentiation and the expression of *Adipoq*, a general adipocyte marker (Figure 6A). Prdm16 and Prdm3 also potently activated *Ucp1* and *Pgc1α* expression (Figure 6A). Interestingly, we also noted that *Prdm3* expression in iBAT was higher in E18 embryos compared to 1.5-, 3- and 6-month-old mice (Figure S6A). *Prdm3* mRNA levels were also somewhat reduced in 6-month-old BAT relative to 3-month-old BAT. Together, these data suggested that Prdm3 might be compensating for the loss Prdm16 during brown fat development.

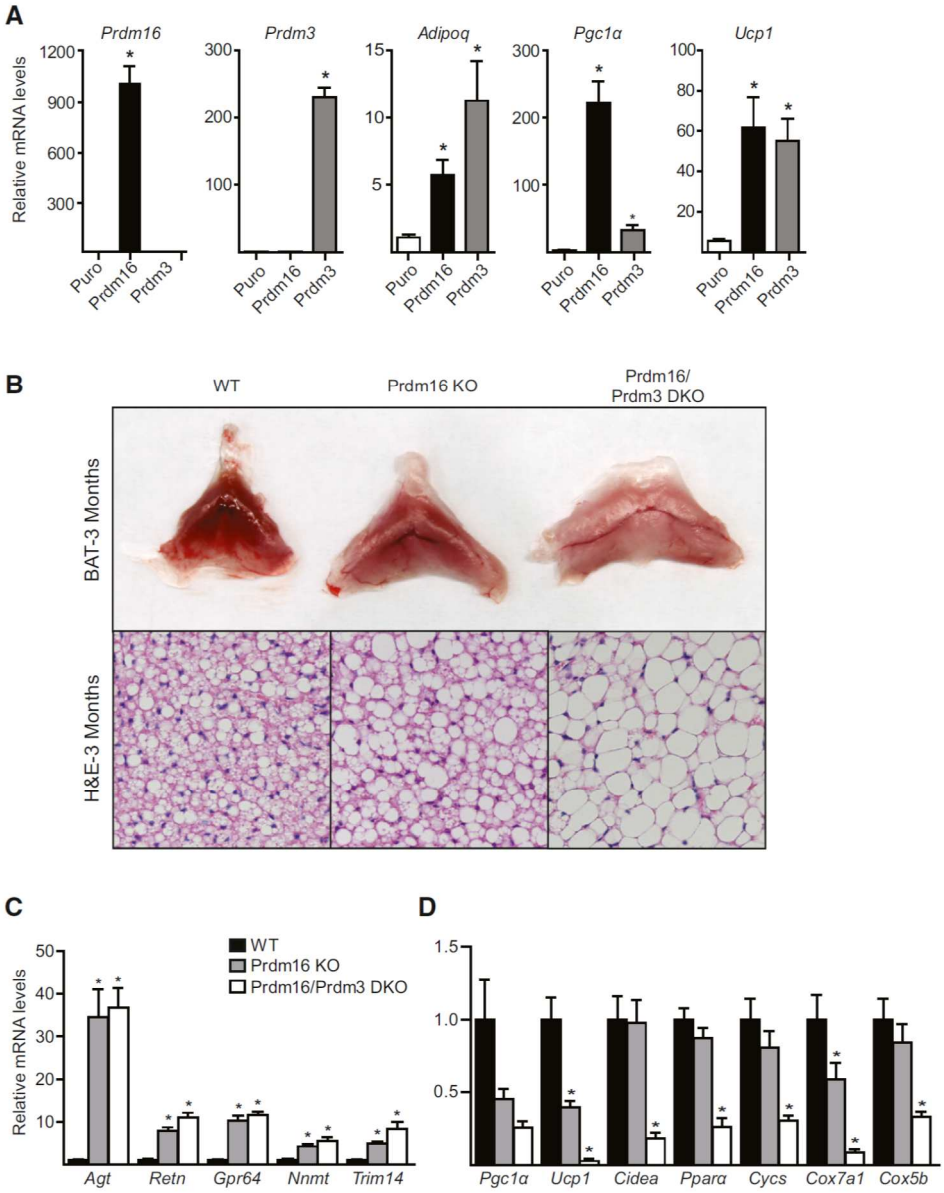

Figure 6: Prdm3 compensates for the loss of Prdm16 in juvenile BAT

(A) C2C12 muscle cells were transduced with retrovirus expressing puromycin (ctl), Prdm3 or Prdm16 and induced to undergo adipocyte differentiation. Cultures were then analyzed by qPCR for their expression levels of *Adipoq* (adipocyte marker) and brown fat-selective genes (*Pgc1α*, *Ucp1*). **(B)** Gross appearance (top) and hematoxylin/eosin (HE) staining (bottom) of interscapular BAT from 3-month-old WT, *Myf5-ΔPrdm16* (KO) *and Myf5-ΔPrdm16/Prdm3* (DKO) mice. **(C,D)** Expression analysis of WAT-selective (C) and BAT-selective (D) transcripts in WT, KO, and DKO BAT (mean ± SEM, n=5-7, *p < 0.01).

To explore this possibility, we created mice lacking both Prdm16 and Prdm3 in the brown fat lineage by intercrossing *Myf5-ΔPrdm16* mice with *Prdm3*^{flox} mice [199]. At 3 months of age, the iBAT of *Myf5-ΔPrdm16/Prdm3* double knockout (DKO) mice was visibly paler than Prdm16-KO, Prdm3-KO or WT BAT (Figure 6B, S6B). H&E staining of iBAT sections revealed that DKO adipocytes had larger lipid droplets than adipocytes in WT or Prdm16 KO tissue (Figure 6B). Gene expression analysis showed that white fat-selective genes were increased to a similar extent in KO and DKO iBAT relative to their levels in WT iBAT (Figure 6C). However, the levels of brown fat-selective genes (including *Pgc1α*, *Ucp1*, *Cidea*, and *Pparα)* were dramatically reduced in DKO BAT at this age while only modestly reduced in Prdm16 KO BAT relative to WT controls. We did not detect any changes in the expression of brown or white genes in Prdm3 KO relative to WT iBAT (Figure S6C). Skeletal muscle-enriched genes were not significantly increased in DKO relative to WT BAT (Figure S6D). Notably, at two weeks of age, WT and DKO iBAT expressed nearly equivalent levels of most brown fat-selective genes, including *Ucp1* (Figure S6D). These results indicate that, while both factors are dispensable for establishing a BAT-specific gene program during embryonic development, Prdm16 or Prdm3 is required for the postnatal/adult expansion and maintenance of iBAT.

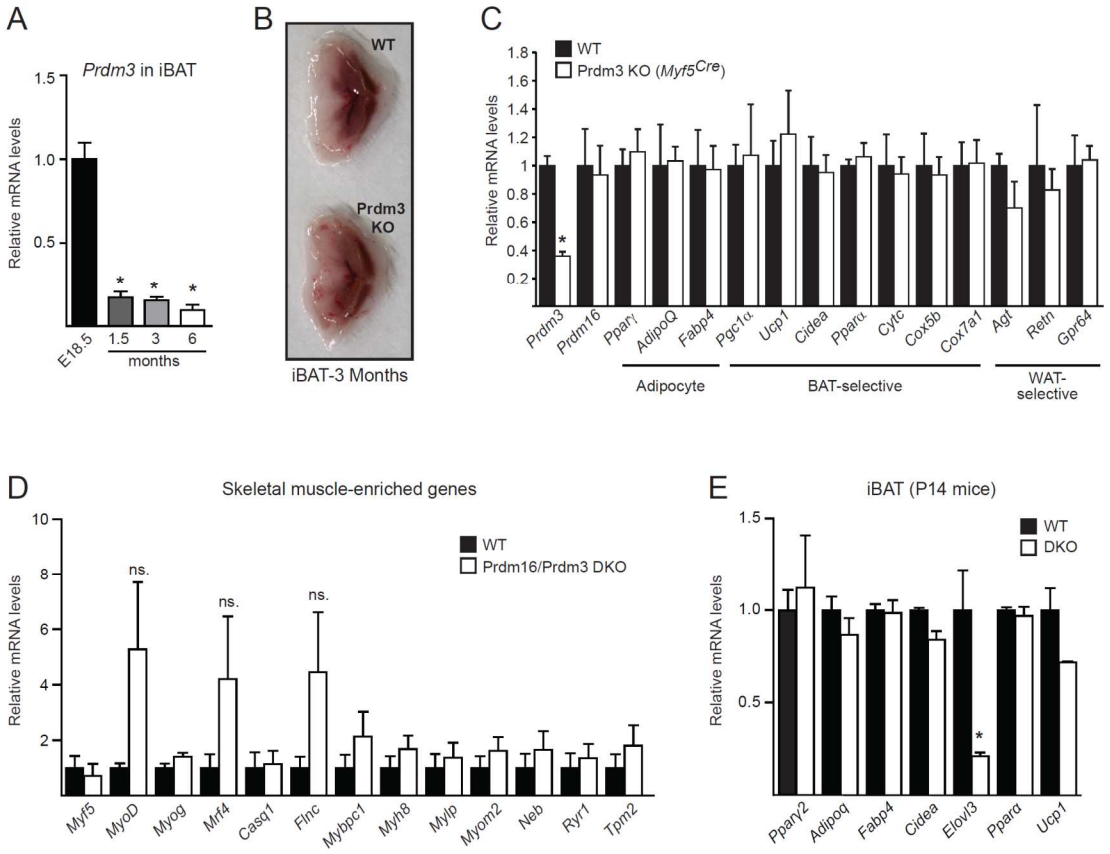

Figure S6. Prdm16 or Prdm3 are required for the postnatal maintenance of brown fat fate

(A) Prdm3 mRNA levels in interscapular brown adipose tissue (iBAT) of E18.5 embryos (n=5) and 1.5 to 6 month-old mice (as indicated (n=4/group). **(B)** iBAT depots from WT and Prdm3 Knockout (KO) (Myf5Cre) mice. **(C)** mRNA levels of Prdm3, Prdm16 and various adipocyte, BAT-selective and WAT-selective markers in the iBAT of 3-month-old WT (n=3) and Prdm3 KO animals (n=4). **(D)** mRNA levels of skeletal muscle-selective genes in iBAT of 3-month-old WT (n=7) and Myf5-ΔPrdm16/Prdm3 (DKO, n=5) mice. **(E)** mRNA levels of adipocyte and BAT-selective genes in iBAT of p14 (2-week-old) WT (n=7) and DKO (n=4) mice. All mRNA expression values are mean ± SEM, *$p < 0.05$.

Discussion

A detailed understanding of the mechanisms that control brown adipocyte development may reveal new approaches to reduce obesity and associated disorders. Prdm16, a zinc-finger containing transcription factor, is a key regulator of brown fat cell development and function. Using conditional knockout mice, we found that Prdm16 is required for suppressing a white fat-selective gene profile in all BAT depots and for maintaining the brown fat-specific attributes of iBAT in adult animals. As a result, animals lacking Prdm16 in BAT have a dramatically reduced capacity to produce heat.

The major BAT depots in mice arise from a multipotent cell population in the somites that expresses *Myf5*, *Pax7* and *En1* at early stages of development [13,76,189]. Surprisingly, deletion of Prdm16 in this early embryonic precursor pool caused an adult-onset loss of brown fat-specific characteristics in the interscapular depot, with little effect on the embryonic and early postnatal tissue. BAT is a critical source of heat in eutherian mammals and, as such, is required for the survival of newborn and young mice in the cold. Consequently, redundant mechanisms have likely evolved to safeguard early BAT development.

Prdm16 is most closely related in sequence and structure to Prdm3. Notably, Prdm3, like Prdm16, activates the expression of brown fat-selective genes when expressed in C2C12 muscle cells (Figure 6). Importantly, simultaneous loss of both Prdm16 and Prdm3 in the *Myf5*^{Cre}-descendent brown fat lineage caused a profound loss of iBAT fate in young mice, much earlier and more completely than observed with Prdm16-deficiency alone (Figure 6). Loss of Prdm3 alone had no detectable impact on BAT development, suggesting that Prdm3 has no non-redundant functions in BAT. Altogether, our results suggest that Prdm16 or Prdm3 is required for the function of

brown fat stem/precursor cells that mediate tissue expansion after birth. In other words, as BAT grows and undergoes turnover postnatally, the differentiation of new brown adipocytes requires the presence of Prdm3 or Prdm16. The distinctive requirement for Prdm16 in iBAT maintenance, which is revealed as animals get older, correlates with a decline in *Prdm3* levels (Figure S6). Brown fat precursor cells also appear to lose *Prdm3* expression after their isolation into culture (not shown), which could explain why Prdm16-deficient brown fat precursor cells display such a profound differentiation deficit *ex vivo* (Figure 4).

The precursor cells in the embryo that give rise to brown adipocytes and skeletal muscle are developmentally related[13,76,189]. Interestingly, Prdm16 and several other factors have been shown to regulate a muscle/brown fat cell fate switch[13,90,190,191,200-202]. In particular, ectopic expression of Prdm16 in myogenic precursor cells promotes brown fat differentiation[13,90,202], whereas knockdown of Prdm16 in brown preadipose cells increases muscle differentiation[13]. Consistent with this, loss of the Ehmt1, a histone methyltransferase that mediates Prdm16 action in BAT, leads to the ectopic expression of a broad set of muscle-specific genes in iBAT[190].

Unexpectedly, we found that deletion of Prdm16 and Prdm3 in the brown adipose lineage did not elevate muscle-specific gene expression. These results diverge from those of earlier studies in demonstrating that Prdm16 is, in fact, not required in brown fat cells to repress the expression of muscle genes. The increased expression of muscle genes observed in other models of Prdm16-depleted brown adipocytes may be related to differences in mouse strain used, off-target effects of the shRNA, non-brown fat cell-autonomous functions of Prdm16 or variable levels of muscle contamination during dissection. While it will be important to investigate these possible explanations, our current findings using cell-type selective genetic ablation *in vivo* provide compelling

evidence that Prdm16 and Prdm3 are dispensable for the determination of brown fat versus muscle cell identity. Given this, we speculate that there is additional redundancy in the Prdm16/Prdm3 pathway that activates the brown-selective program whilst suppressing skeletal muscle gene expression during the first wave of brown fat differentiation in the embryo. Future studies should thus consider whether another Prdm family member or functionally related protein can participate in the same complexes as Prdm16/Prdm3 to recruit Ehmt1 during embryonic BAT development.

Prdm16 is uniquely required at all stages of BAT development to repress the transcription of many WAT (versus BAT)-selective genes. Deletion of Prdm16, but not Prdm3, caused a large increase in the expression of these genes in all the BAT depots we examined and at all ages. It makes sense that Prdm3 lacks this repressive function since it is also expressed in all WAT depots [198]. Our data suggest that Prdm16 represses the transcription of "white" genes (eg. *Retn, Agt*) by binding to their promoters and recruiting Ehmt1 to cause histone methylation (Figure 2). The consequences of having these genes over-expressed in BAT remain unknown.

A key question was whether the selective loss of Prdm16 activity in BAT had physiological consequences for the animals. Indeed, we found that *Myf5-ΔPrdm16* mice had a severely crippled thermogenic response to norepinephrine, the dominant physiological activator of BAT. Despite this, *Myf5-ΔPrdm16* mice did not gain more weight than their WT counterparts under a variety of conditions. By contrast, mice lacking Prdm16 in all adipose cells (*AdipoQ-ΔPrdm16*) display a selective loss of beige fat activity, gain more weight and become much more severely insulin resistant than WT mice [188]. Taken together, these results suggest that beige fat cells play a larger role than BAT in high fat diet-induced thermogenesis and in modulating systemic insulin sensitivity.

However, it is important to consider that alternative thermogenic mechanisms may be recruited in *Myf5-ΔPrdm16* animals to compensate for their diminished iBAT function. While there was no compensatory browning of WAT in *Myf5-ΔPrdm16* mice, future studies should examine whether adaptive decreases in skeletal muscle efficiency could compensate for loss of BAT function as has been observed in other models of BAT-insufficiency [103]. Additionally, it is conceivable that BAT depots which express normal levels of Ucp1 in the absence of Prdm16 are recruited under the influence of high fat diet to compensate for defective iBAT function. In this regard, surgical removal of iBAT has been shown to promote expansion of the remaining BAT depots in animals exposed to a low protein diet [203,204]. On the other hand, the aBAT and cBAT in adult *Myf5-ΔPrdm16* mice is pale and expresses high levels of white fat-specific genes, so it is not clear that these depots are functional even though they have normal amounts of Ucp1.

The body weight and metabolic studies led us to discover that *Myf5-ΔPrdm16* mice are smaller than controls, involving proportionate decreases in fat mass, lean mass, and body length. We do not know if the reduced stature of *Myf5-ΔPrdm16* mice is secondary to the BAT defects. Interestingly, BAT has been suggested to affect bone development and metabolism [205]; the relevance of this will require further study. It is also incumbent upon us to note that *Myf5*^{Cre} activity traces to tissues other than BAT, including muscle (where *Prdm16* is not expressed) and also regions in the developing brain [206,207]. Prdm16 may therefore regulate stature directly through its expression in non-adipose tissues.

In conclusion, our analyses of *Myf5-ΔPrdm16* and *-ΔPrdm16/Prdm3* mice have revealed that Prdm16 and Prdm3 control the postnatal growth and maintenance of BAT. Moreover, genetic loss of iBAT activity in adult mice is not necessarily associated with

obesity or metabolic disease. However, ectopically increasing BAT function remains likely to have therapeutic value, and our observation that Prdm16 and Prdm3 maintain brown fat identity will be important for designing persistent thermogenesis-based treatments.

Materials and Methods

Animals

Myf5^{Cre} (stock no. 010529) and *Rosa26*^{Cre} (stock no. 004847) mice were obtained from the Jackson Laboratory. *Prdm16*^{flox} (Figure S1A) and *Prdm3*^{flox} [199] conditional-null mice were generated by standard gene-targeting techniques. *Myf5*^{Cre}*;Prdm16*^{flox} mice were backcrossed for 10 generations into the C57Black6 strain. The *Myf5*^{Cre}*;Prdm16*^{flox};*Prdm3*^{flox} mice studied were on a mixed 129Sv/C57Black6 genetic background. Mice in weight-gain studies were fed a 45% high-fat diet (Research Diets). For norepinephrine injections, mice were first placed in metabolic chambers at 22°C, then sedated with 75 mg/kg Nembutal, followed 15 min later by injection with 1 mg/kg norepinephrine. Data were collected until mice recovered from barbituate sedation. Temperature probes (IPTT 300; BioMedic Data Systems) were implanted into a subcutaneous position on top of the BAT of sedated mice. All animal experiments were approved by the University of Pennsylvania's Institutional Animal Care and Use Committee.

Histology

For immunohistochemistry, BAT was fixed in 4% PFA overnight, dehydrated, and embedded in paraffin for sectioning. Sections were stained with hematoxyin and eosin; or were probed with antibodies for Ucp1 (R&D Systems; MAB6158). For transmission

electron microscopy, tissues were fixed with 2.5% glutaraldehyde, 2.0% paraformaldehyde in 0.1M sodium cacodylate buffer, pH7.4, overnight at 4°C; then post-fixed with 2.0% osmium tetroxide for 1 hour at room temperature. Thin sections were stained with uranyl acetate and lead citrate and examined with a JEOL 1010 electron microscope.

Cell culture

Primary brown preadipocytes were isolated as described previously (Seale et al., 2007). Preadipocytes were immortalized through retroviral expression of SV40 large-T antigen. For differentiation assays, confluent preadipocytes were treated with medium containing 10% FBS, 0.5 mM isobutylmethylxanthine, 125 nM indomethacin, 1 μM dexamethosone, 20 nM insulin, and 1 nM T3. After 48 hrs, cells were switched to medium containing 10% FBS, 20 nM insulin, and 1 nM T3. Thermogenesis was stimulated by treatment with 10 μM isoproterenol. Recombination in $R26^{Cre}$/$Prdm16^{floxEx9}$ adipocytes was induced by treating cells with 1 μM of 4-hydroxy-tamoxifen (Sigma) for 3 days in growth phase. The GLP antagonist UNC 0646 (Tocris Bioscience) was added to medium throughout differentiation at 1 μM. Oil-red-o staining and retrovirus production was performed as decribed previously [87].

Real-Time PCR and Western blot analysis

Total RNA was extracted by TRIzol (Invitrogen) followed by purification using PureLink RNA columns (Invitrogen). Isolated mRNA was reverse transcribed using the High-Capacity cDNA Synthesis kit (Applied Biosystems) and used in real-time PCR reactions with SYBR Green master mix (Applied Biosystems) on a 7900 HT (Applied Biosystems). *Tata-binding protein* (*Tbp*) was used as an internal normalization control. Primer

sequences are in Table S1. Protein extracts were prepared as previously described[208]. Proteins were separated in 4-12% Bis-Tris NuPAGE gels (Invitrogen), and transferred to PVDF membranes. Primary antibodies were: anti-Prdm16 [87], anti-Pparγ (E8; Santa Cruz Biotechnology; sc-7273), anti-Agt (IBL; 28101), anti-Ucp1 (R&D Systems; MAB6158), and anti-pan-actin (Chemicon; MAB1501).

Chromatin Immunoprecipitation (ChIP)

For ChIP, fat depots from WT and KO mice (6 weeks old) were dissected and washed with PBS. Chromatin was purified from the isolated fat tissue and immunoprecipitated as previously described [208]. Target enrichment was calculated as percent input and normalized to WT. Primer sequences are in Table S1. Anti-Prdm16 for ChIP was produced by inoculating rabbits with a Prdm16 peptide (RMDKRPEIQDLDSNPPC) to generate a polyclonal antiserum (Pierce). Commercial antibodies were anti-GLP (Abcam; ab41969), anti-H3K27-Me3 (Abcam; ab6002), anti-H3K9-Me1 (Millipore; 17 680) or anti-H3K9-Me2 (Abcam; ab1220).

Microarray Analyses

We used Agilent cDNA microarrays to profile gene expression in WT and Prdm16-deficient BAT from young (6-week-old) and old mice (11-month-old) (GSE55080). To identify depot-specific genes for BAT and WAT, we compared data sets from epididymal WAT and iBAT (GDS2813) [87]. Gene expression comparisons were performed using Linear Models for Microarray Data [209]. Genes with fold-changes >2 and FDR <0.05 in each direction were selected as brown or white depot-specific genes. Hierarchical clustering was done by Euclidean distance and Ward's criterion using Fastcluster [210].

Gene ontology analysis was performed on differentially expressed genes in *Myf5*Δ*Prdm16* BAT from 6-week-old mice using HOMER [211].

Mitochondrial DNA Quantification

BAT was isolated and digested overnight in a buffer containing 100 mM Tris pH 8, 5 mM EDTA, 200 mM NaCl, 0.5% SDS, and 100 µg/ml proteinase K. DNA was ethanol precipitated and resuspended in TE. DNA was quantified by real-time PCR by comparing the ratios of *Mt-Co1* and *Ndufv1* [212]. Primer sequences are in Table I.

Tissue O_2 Consumption

BAT was isolated, weighed, and 15-25 mg of tissue was minced in a buffer comprised of 2% BSA, 1.1 mM sodium pyruvate, and 25 mM glucose in PBS. Samples were placed in an MT200A Respirometer Cell (Strathkelvin) and oxygen consumption was measured for approximately 5 minutes. Oxygen consumption was normalized to minced tissue weight.

Fluorescence Activated Cell Sorting

Excised tissue was digested as described above. Cells were resuspended in DMEM with 5% FBS, and stained with Pdgfrα-APC (Biolegend, 135907) for 30 min at 4 °C in the dark. Stained cells were sorted with BD FACS Aria. Debris and dead cells were excluded by forward scatter, side scatter and DAPI gating. The purity was greater than 95%. Data analysis was performed using FlowJo.

Statistical Analysis

All data derived from tissues are reported as mean ± SEM. Data from cells are reported as mean ± standard deviation. Student's t-test was used to calculate significance (*p < 0.05) using Excel or Prism software packages. Data from mice in metabolic chambers was tested for significant differences using a Two-Way Anova (Prism).

Accession Numbers

The Gene Expression Omnibus (GEO) accession number for the mRNA expression data reported in this paper is: GSE55080.

Primers used for real-time PCR and ChIP-PCR analysis

mRNA	Fwd	Rev
Adipoq	GCACTGGCAAGTTCTACTGCAA	GTAGGTGAAGAGAACGGCCTTGT
Agt	AAGACCCTGCATGATCAGCTC	CTTCCTGCCTCATTCAGCATC
Casq1	ATGAGGTGCTGGCCCTCCTCT	GAGTCCACCAGGCCAAAGCCA
Cidea	TGCTCTTCTGTATCGCCCAGT	GCCGTGTTAAGGAATCTGCTG
Cideb	ATGGTGCTTGAGCAGGGCCAG	ATCGAAGGTGATGCGGGCGAT
Clstn3	AGCCGTGAGGTCATCGAGTGC	CCTCCAGGGTGAGCAGGGACT
Cox5b	GCTGCATCTGTGAAGAGGACAAC	CAGCTTGTAATGGGTTCCACAGT
Cox7a1	CAGCGTCATGGTCAGTCTGT	AGAAAACCGTGTGGCAGAGA
Cycs	GCAAGCATAAGACTGGACCAAA	TTGTTGGCATCTGTGTAAGAGAATC
Cyp2b10	TGCCCCTCTTGGGGAACCTCT	CACAGGCCTTGGTCCCAGGTG
Dgat1	CGGGACAAAGACGGGCGGAC	AGGATCAGCATCACCACACACCA
Dio2	CAGTGTGGTGCACGTCTCCAATC	TGAACCAAAGTTGACCACCAG
Errg	TGGCTGACCGAGAGTTGGTGG	AGCGATCGGTACACAACGCCG
Fabp4	ACACCGAGATTTCCTTCAAACTG	CCATCTAGGGTTATGATGCTCTTCA
Flnc	ATGCCAGAGAGGCCATGCAGC	CGGGTTTGAGCTTGGCCTTGG
Fosl1	GAGACGCGAGCGGAACAA	CTTCCAGCACCAGCTCAAGG
Fosl2	AGCCTCCCGAAGAGGACAG	AGGACATTGGGGTAGGTGAAG
Gpr64	CCACACCAGCCCCATCTGTCC	TCCATCTGGGATACTTGGGCTTCC
Hsph1	ACGGACCTGCCGCTGAACATC	TGCAGGAGCTCAGCACACAGT
Krt19	ACCATCGAGGACTTGCGCGAC	GCTCAGACGCAAGGCGTGTTC
Limk1	GACCTGGGTCGCTCCGAATCC	CCTTGCCCAGCACTTCCCCAT
Mybpc1	CGCAGGGAATTATAGGTGTGAGGTC	CCTGCATCCTCTTGACCTTCTCCA
Myf5	CAGCCCCACCTCCAACTG	GGGACCAGACAGGGCTGTTA
Myh8	CTCCATGAGCCCGGAGTGCTG	CGGCAGCCACTTGTAGGGGTT
Mylpf	GAGAAGGGCAGGAGCGGAAGG	TGGCTGCAAAGGTGTCCCGAA
Myod	CGCCACTCCGGGACATAG	GAAGTCGTCTGCTGTCTCAAAGG
Myogenin	AGCGCAGGCTCAAGAAAGTGAATG	CTGTAGGCGCTCAATGTACTGGAT
Myom2	CGGTCACAGGCTCGGGACAAG	GGGCCCTGCTCATTCGGTCTT
Neb	AGGCAAAGGCTTCTTCCCCCA	GGGCTTGCACCAGGACAGGAG
Nnmt	GGAGCCTTTGACTGGTCCCCA	CCTGCTTGATTGCACGCCTCA
Pck1	TGGCCATGATGAACCCCAGCC	GAGGTGCCAGGAGCAACTCCA
Pgc-1a	CCCTGCCATTGTTAAGACC	TGCTGCTGTTCCTGTTTTC
Ppara	GCGTACGGCAATGGCTTTAT	GAACGGCTTCCTCAGGTTCTT
Pparg1	TGAAAGAAGCGGTGAACCACTG	TGGCATCTCGTGTCAACCATG
Pparg2	TGGCATCTCTGTGTCAACCATG	GCATGGTGCCTTCGCTGA

Prdm3	AACAAAACCTGGAGAGTGAGAG	AATGCCTTGGGACACTGATC
Prdm16	CAGCACGGTGAAGCCATTC	GCGTGCATCCGCTTGTG
Retn	CTGTCCAGTCTATCCTTGCACAC	CAGAAGGCACAGCAGTCTTGA
Ryr1	GCACTCATGCCCGCTCCCTAT	GGCCTTGGTCCTCAGTGAGCC
Sgk2	GGTGGTGCTTAGGGGCAGTCC	GAGGTCACAGGCAGCCACTGT
Tbp	GAAGCTGCGGTACAATTCCAG	CCCCTTGTACCCTTCACCAAT
Thbd	CAGGGGCCCAATCCATGTCCC	CGGATCCAGAAGCTCCACGCA
Tpm2	GGGGACAGAGGACGAGGTGGA	GGCGGTTCAGAGAGGCCACAT
Trfr2	GAGCGACCTCCAGGCCATGTT	TGGCGCGAGAGCTTATCGAGG
Trim14	TTGGAAGACGCCGGGGAAAGG	GGCCAGTACTTCCTCTTCATCCAGG
Tubb2a	GTGAGGTCGGGACCATTCGGC	GACAGAGTCCACCAGCTCGGC
Ucp1	ACTGCCACACCTCCAGTCATT	CTTTGCCTCACTCAGGATTGG
Ugdh	GCCGATGTGGAAGAGGTGGCA	CGGGCAGATTCAGAGCCTCACA
ChIP		
Ins	GGACCCACAAGTGGAACAAC	GTGCAGCACTGATCCACAAT
Retn -2kb	AGCACAAAGGTGGGGGATGGT	AACCACAGAACAGGAGGCCCAT
Retn -1.5kb	TGGACAGAGGGGTGTCAGGGG	GCATTGCTGGAGACCTGAGGTGA
Retn -1kb	CAGGAGTTCAAGGTCGTTCTTGGC	GCTGTTACACTGGCCTCGATGT
Retn -0.5kb	CTCTTGCTTAGCCCCACCCCC	ACCACACCACCAGACCCTCAC
Retn P.	AGACAACGTCCTGAGAAGACAATC	CCATCCTGCCTTGGATAATAAGTA
Retn 0.5kb	GGAACAGACCCGCCCAGCTAC	GGGGCCTTTTGGAGTGAGGGG
Retn 1.0kb	ATGGGTGCCCCTACACCATGC	GCAGGGGGCGATCTTTGGGT
Retn 1.5kb	CATCTCTGCCTCCCACCTGCC	GCGGGCTGCTGTCCAGTCTAT
Retn 2kb	TGGACCTTGGCAGGACTGAGGT	ATCCTCTGCCCCAGGTGGTGT
Agt P.	CTTGGTCAAGCCTGGATTCTC	CCAACCTAGACAAGCACAGCTATC
Mito DNA		
Ndufv1	CTTCCCCACTGGCCTCAAG	CCAAAACCCAGTGATCCAGC
MT-CO1	TGCTAGCCGCAGGCATTAC	GGGTGCCCAAAGAATCAGAAC

Acknowledgements

We thank Dr. Bruce Spiegelman for generously sharing the *Prdm16*^{flox} animals; Dr. Mitch Lazar and Dr. Rex Ahima for their expert guidance; Matthew Brown, Li Huang and Jim Davis for technical help; Min Min Lu, Lan Cheng and the Histology and Gene Expression Core of the Penn Cardiovascular Institute for immunohistochemistry; and Ray Meade in the electron microscopy core. We are grateful to the Functional Genomics Core and the Mouse Metabolic Phenotyping Core of the Penn Diabetes and Endocrinology Research Center (DK19525) for microarray studies and mouse metabolic analyses, respectively. This work was supported by NIGMS/NIH award DP2OD007288, and a Searle Scholars Award to P.S.

CHAPTER 3: PRDM16 binds MED1 and controls chromatin architecture to determine a brown fat transcriptional program

Published: Matthew J. Harms[1,2,4], Hee-Woong Lim[1,3,4], Yugong Ho[3], Suzanne Shapira[1,2], Jeff Ishibashi[1,2], Sona Rajakumari[1,2], David J. Steger[1], Mitchell A. Lazar[1], Kyoung-Jae Won[1,3], Patrick Seale[1,2,*]

PRDM16 binds MED1 and controls chromatin architecture to determine a brown fat transcriptional program.

Genes and Development, Feb 1, 2015; 29 (3)

Abstract

PRDM16 drives a thermogenic gene program in fat cells, but the mechanism by which PRDM16 activates genes was unknown. Through ChIP-seq analyses in brown adipose tissue (BAT), we reveal that PRDM16 is strongly enriched at a broad set of BAT-selective genes. Importantly, PRDM16 physically binds to MED1, a component of the Mediator complex, and recruits it to BAT-selective super-enhancers. Loss of PRDM16 reduces MED1 and RNA Pol II binding at PRDM16-target sites; this is associated with a fundamental change in chromatin architecture at key BAT genes. Together, these data indicate that PRDM16 controls chromatin architecture and super-enhancers in BAT.

Introduction

Obesity is a leading cause of preventable death in the U.S. due to its link to many diseases, including type 2 diabetes, cardiovascular disease, stroke and certain cancers [2]. White adipose tissue (WAT), which expands in obesity, is specialized to store energy in the form of lipid whereas brown and beige adipose tissue expend energy as heat [187]. High levels of brown/beige fat activity protect animals against many of the harmful effects of a high fat diet, including obesity and insulin resistance. In humans, brown/beige fat activity levels also correlate with reduced adiposity. Thus, elucidating the molecular pathways that regulate brown/beige fat activity may reveal new approaches to treat obesity and related diseases.

PR (PRD1-BF1-RIZ1 homologous)-domain containing 16 (PRDM16), a zinc-finger containing transcription factor, is a critical molecular determinant of brown/beige fat cell fate. Ectopic expression of PRDM16 in fibroblasts or muscle precursors drives brown fat cell differentiation [26,87,90,213]. PRDM16 is also required for beige fat differentiation and for the maintenance of BAT fate in adult mice [188,214]. PRDM16 induces genes that are expressed at higher levels in brown relative to white adipocytes (BAT-selective) such as *Ucp1*, *Pparγ* and *Ppargc1a*, while also suppressing white fat- (versus brown fat- selective genes (WAT-selective) [214,215]. However, the mechanism(s) by which PRDM16 stimulates BAT-selective gene expression was unknown.

We show here that PRDM16 binds strongly to a broad set of BAT-selective genes in BAT. Genetic loss of PRDM16 reduced RNA Polymerase II (Pol II) levels at BAT-selective genes and caused an associated decrease in gene expression levels. PRDM16-deficiency did not affect PPARγ or C/EBPβ binding at BAT-selective genes and caused only a mild decrease in the levels of H3K27-Acetylation (H3K27-Ac), a

chromatin mark that is associated with active transcription. By contrast, PRDM16 was critically required for the binding of MED1, a component of the Mediator complex, to BAT-selective genes. Notably, PRDM16 binds directly to MED1 through its zinc-finger domains. Loss of PRDM16/MED1 in brown fat cells disrupted the chromatin architecture at *Ppargc1a* and *Pparγ*, two crucial PRDM16-target genes. Finally, we found that PRDM16 marks and regulates the activity of super-enhancers (SE), large clusters of transcriptional binding sites that drive the expression of cell identity genes [216]. Taken together, our results reveal that PRDM16 recruits MED1 to SE in the control of BAT identity.

Results and Discussion

PRDM16 binding is enriched at BAT-selective genes

PRDM16 stimulates BAT-selective gene expression, but whether PRDM16 acts directly at these genes was unknown. To investigate this, we analyzed the genome-wide binding profile of PRDM16 in BAT using chromatin immunoprecipitation followed by deep sequencing (ChIP-Seq) (Figure S1A). A majority of the PRDM16-binding sites identified in wildtype (WT) BAT were lost in *Prdm16*-knockout (KO) tissue (Figure S1B), indicating that the ChIP antibody was specific. The genomic distribution of PRDM16 binding was typical for transcription factors with a large proportion of binding sites located within intergenic and intronic regions (Figure S1C).

There were numerous PRDM16 binding sites at classic BAT-selective genes, such as *Ucp1*, *Pparγ*, *Cidea* and *Ppargc1a* (Figure 1A). These PRDM16-bound sites also displayed enriched levels of the activating histone mark H3K27-Ac in BAT relative to WAT. As previously reported, PRDM16 was also bound at certain WAT-selective

genes, including *Agt* and *Retn* [214,215] (Figure S1D). Upon genome-wide analysis, we found that PRDM16 binding was, in general, more highly enriched at BAT-selective genes than at WAT-selective or common genes (Figure 1B). BAT-selective genes also contained more PRDM16 binding sites and these sites were located closer to the transcriptional start site (TSS) (Figure 1C and 1D). Consistent with these findings, PRDM16-binding levels were positively correlated with RNA Pol II levels at BAT-selective genes (Figure S1E). Finally, PRDM16-binding was globally enriched at BAT-selective regions of H3K27-Acetylation (Figure S1F). These results suggest that PRDM16 acts directly in chromatin to regulate the transcription of BAT-selective genes.

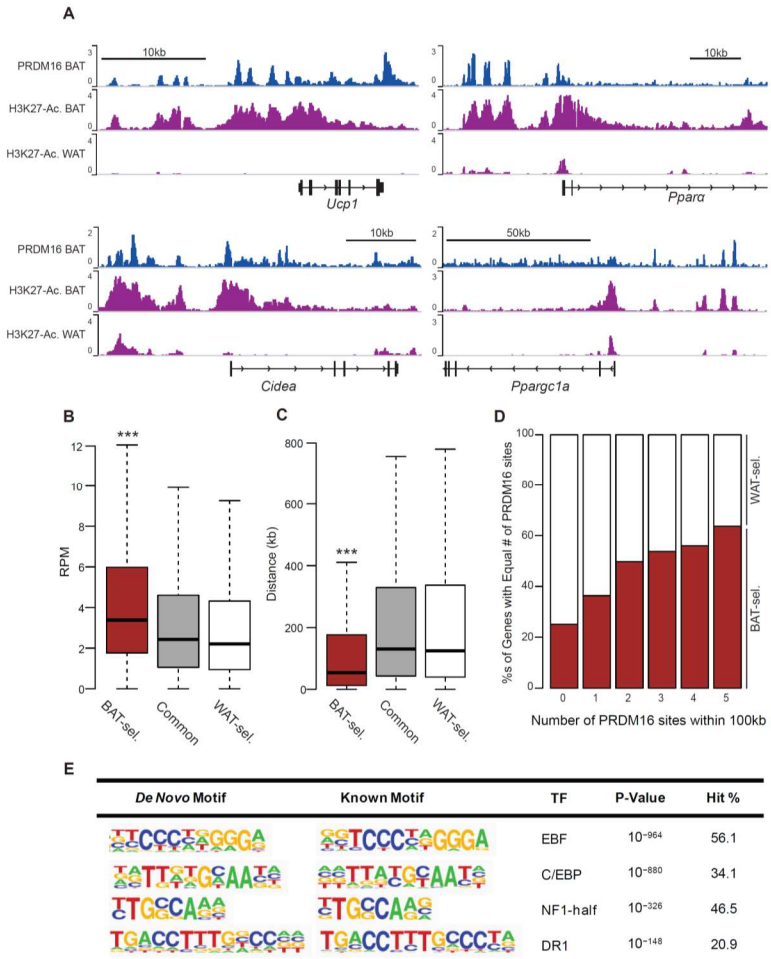

Figure 1. PRDM16 binding is enriched at BAT-selective genes
(A) ChIP-seq profiles in reads per million (RPM) for PRDM16 in BAT and H3K27-Ac in BAT and WAT at *Ucp1*, *Pparα*, *Cidea* and *Ppargc1a*. **(B)** Box plot comparing PRDM16 ChIP signal (RPM) around BAT-selective (BAT-sel.), common and WAT-selective (WAT-sel.) genes (***$p < 10^{-20}$). **(C)** Box plot comparing the distance (kb) of the closest PRDM16 binding site from the transcriptional start site (TSS) of BAT-sel., common or WAT-sel. genes (***$p < 10^{-25}$). **(D)** Proportion (%) of BAT and WAT-selective genes grouped by number of PRDM16 binding sites within 100 kb of the TSS. **(E)** *De novo* motif analysis of PRDM16-binding sites.

An important question is whether PRDM16 binds to DNA directly or is recruited to the genome by other factors. *De novo* motif analyses showed that consensus sequences for EBF, C/EBP and PPAR (DR1 motif) were enriched at PRDM16 binding sites (Figure 1E). By contrast, the putative PRDM16/PRDM3 binding motif [217] was poorly represented in the full set of PRDM16-binding regions. These results suggest that PRDM16 is recruited to chromatin in BAT through its interaction with DNA-binding partners, including C/EBPβ and PPARy [13,90]. This is consistent with earlier mutational studies which indicated that the DNA-binding activity of PRDM16 was dispensable for much of its action in fat cells [87].

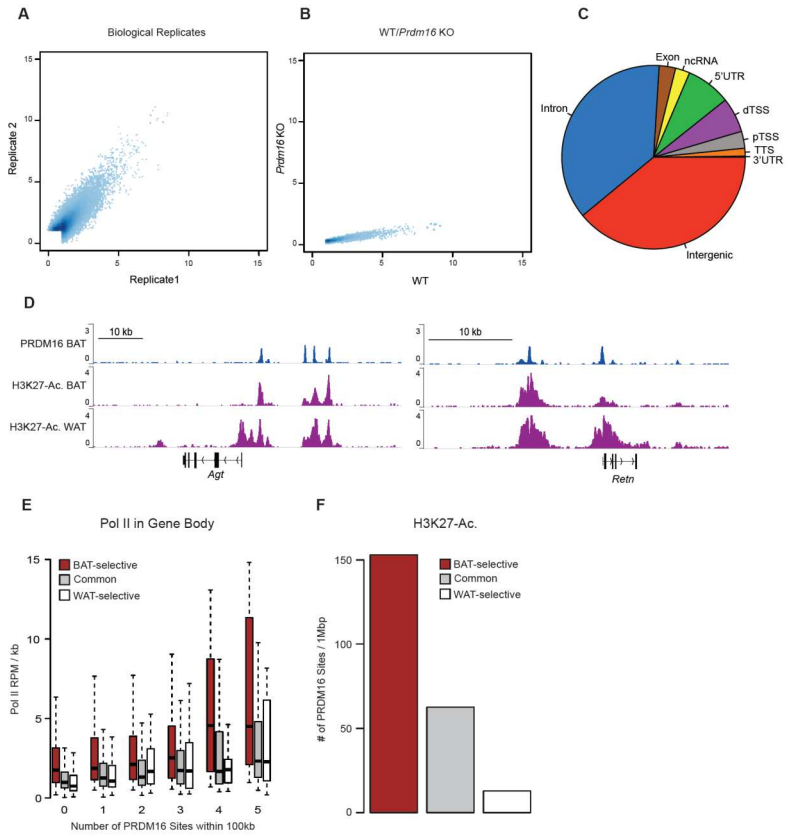

Figure S1. PRDM16 is preferentially bound to BAT-selective genes

(A) Scatter plot comparing PRDM16 ChIP-seq data from independent biological replicates **(B)** Scatter plot comparing PRDM16 ChIP-seq signal in wildtype (WT) and *Prdm16* KO BAT using pooled replicates. **(C)** Pie chart portraying the relative enrichment of PRDM16 in different genomic regions **(D)** ChIP-seq stack-height profiles in reads per million (RPM) for PRDM16 in BAT and H3K27-Ac. in BAT and WAT at the *Agt* and *Retn* loci.**(E)** Box plot comparing Pol II (RPM/kb) within gene bodies of BAT-sel., common and WAT-sel. genes with ncreasing number of proximal PRDM16 binding sites **(F)** Average number of PRDM16 binding sites (per 1Mbp) at BAT-sel., common and WAT-sel. regions of H3K27-Ac. enrichment

PRDM16 recruits MED1 to BAT-selective genes

Prdm16-deficiency causes a severe loss of BAT function in adult mice [214]. At a global scale, *Prdm16*-deficiency reduced the expression levels of BAT-selective genes, increased WAT-selective gene levels, and had no effect on the expression of common genes (Figure 2A). RNA Pol II binding was significantly reduced at BAT-selective genes in KO relative to WT BAT, suggesting that PRDM16 determines mRNA expression levels by affecting transcription (Figure 2B). We first postulated that PRDM16 may act to stabilize the association of its direct DNA-binding partners, PPARy and C/EBPβ [13,90] with chromatin. However, ChIP-PCR experiments revealed no difference between WT and KO in the binding levels of PPARy or C/EBPβ at BAT-selective genes (Figure S1A,B). Moreover, PRDM16-deficiency caused only a modest, albeit significant, reduction in H3K27-Ac levels at BAT-selective genes (Figure 2C).

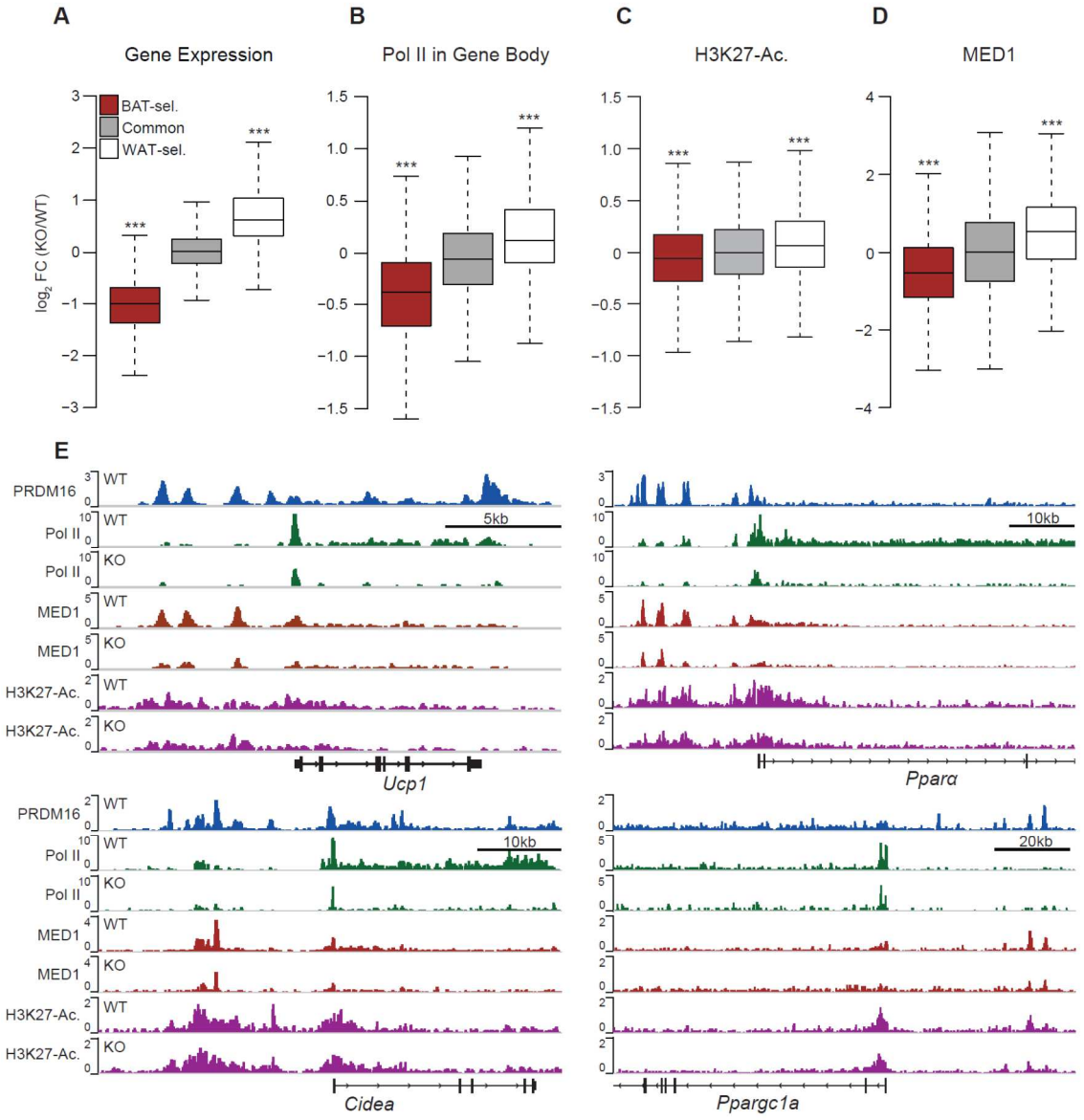

Figure 2. PRDM16-deficiency reduces MED1 levels at BAT-selective genes

(A) Box plot depicting changes in gene expression of BAT-sel. genes (red), common genes (gray) and WAT-sel. genes (white) in PRDM16 knockout (KO)/Wildtype (WT) BAT (***$p < 10^{-100}$). **(B)** Box plot showing changes in Pol II levels within the gene body of BAT-sel., common and WAT-sel. genes in *Prdm16* KO/WT BAT (***$p < 10^{-70}$). **(C)** Box plot showing H3K27-Ac levels within 100kb of the transcriptional start site (TSS) of BAT-sel., common and WAT-sel. genes in *Prdm16* KO/WT BAT. **(D)** Box plot depicting MED1 occupancy within 100kb of the TSS of BAT-sel., common, and WAT-sel. genes in *Prdm16* KO/WT BAT (***$p < 10^{-15}$). **(E)** ChIP-seq profiles for: PRDM16 (blue), Pol II in WT and KO BAT (green), MED1 in WT and KO BAT (red) and H3K27-Ac in WT and KO BAT (magenta).

The Mediator complex plays a crucial role in regulating transcription, in part through bridging of the transcription factor-bound enhancer regions with the general transcriptional machinery and RNA Pol II [218]. Of particular interest, the MED1 subunit of Mediator regulates the function of important transcription factors in adipocytes, including PPARy, PPARGC1a, C/EBPβ and Thyroid Receptor (TR) [219]; which, themselves, also cooperate with PRDM16. ChIP-seq analyses revealed a striking reduction in MED1 levels at BAT-selective, PRDM16-target sites in KO relative to WT BAT (Figure 2D, S2C). For example, there was diminished MED1 (and Pol II) binding with only modest decreases in H3K27-Ac levels at *Ucp1*, *Pparα*, *Cidea* and *Ppargc1a* (Figure 2E, S2D).

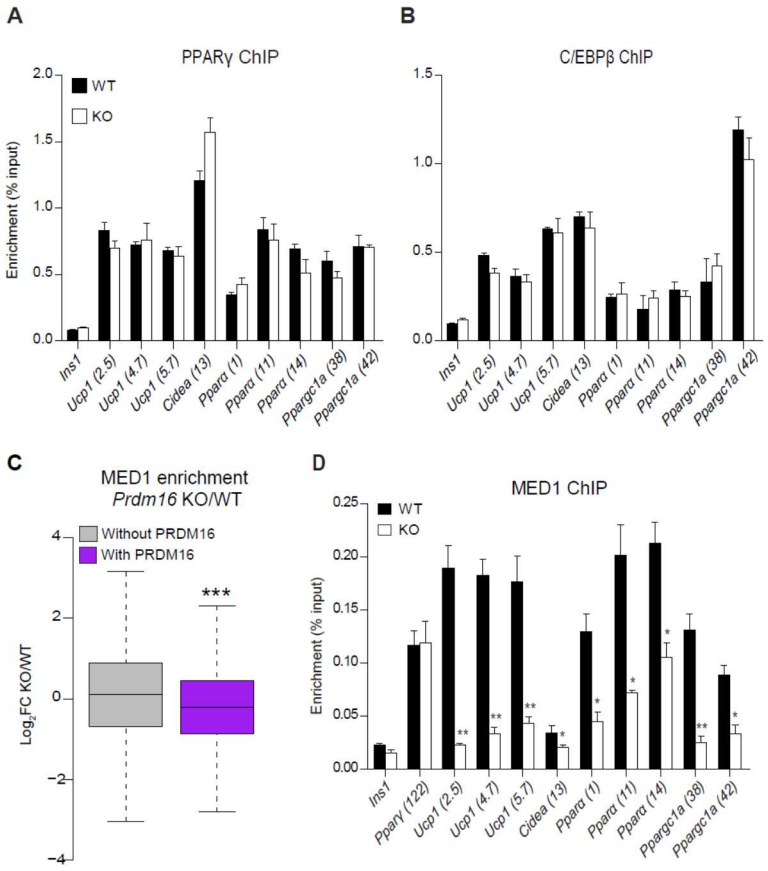

Figure S2. Loss of PRDM16 does not affect PPARγ or C/EBPβ binding levels at BAT-selective genes

(A) ChIP-qPCR analysis of PPARy binding at BAT-sel. genes in WT and *Prdm16* KO BAT(mean ± SEM; n = 3; *p < 0.05) **(B)** ChIP-qPCR analysis of C/EBPβ binding at BAT-sel. genes in WT and *Prdm16* KO BAT(mean ± SEM; n = 3; *p < 0.05) **(C)** Box plot comparing MED1 occupancy changes upon *Prdm16* KO in BAT at sites that possess or lack PRDM16 binding (***p < 10−10) **(D)** ChIP-qPCR analysis of MED1 levels at BAT-sel. genes in WT and *Prdm16* KO BAT (mean ± SEM; n = 3; *p < 0.05,**p<0.01)

We next tested whether PRDM16 could increase the recruitment of MED1 to BAT-selective genes. To do this, we transduced *Prdm16* KO brown adipocytes with PRDM16-expressing or control retrovirus. *Prdm16* KO adipocytes, while expressing normal levels of general adipogenic genes, displayed reduced binding levels of MED1 to BAT-selective genes (*Ucp1*, *Cidea* and *Pparα*) and a corresponding decrease in the expression levels of these genes (Figure S3A)[214]. Ectopic expression of PRDM16 in KO cells promoted the binding of MED1 to BAT-selective genes and activated the expression of these genes (Figure 3A, S3B). To determine whether MED1 was required for the expression of BAT-selective genes, we acutely knocked-down MED1 in mature brown adipocytes using siRNA. The depletion of MED1 caused a sharp decrease in the expression of BAT-selective genes while also reducing the expression levels of some common adipocyte genes (Figure S3C).

The PRDM16-dependent binding of MED1 to BAT-selective genes raised the question of whether PRDM16 physically interacts with MED1. Using co-immunoprecipitation assays, we detected a robust interaction between MED1 and PRDM16 in brown adipocytes (Figure 3B). *In vitro* binding studies using bacterially purified GST-PRDM16 protein fragments revealed that MED1 interacts with the two zinc finger domains of PRDM16 (242-454 and 881-1038) (Figure 3C, S3D). Taken together, these data demonstrate that PRDM16 plays a critical role in physically recruiting MED1 to BAT-selective target genes in adipocytes.

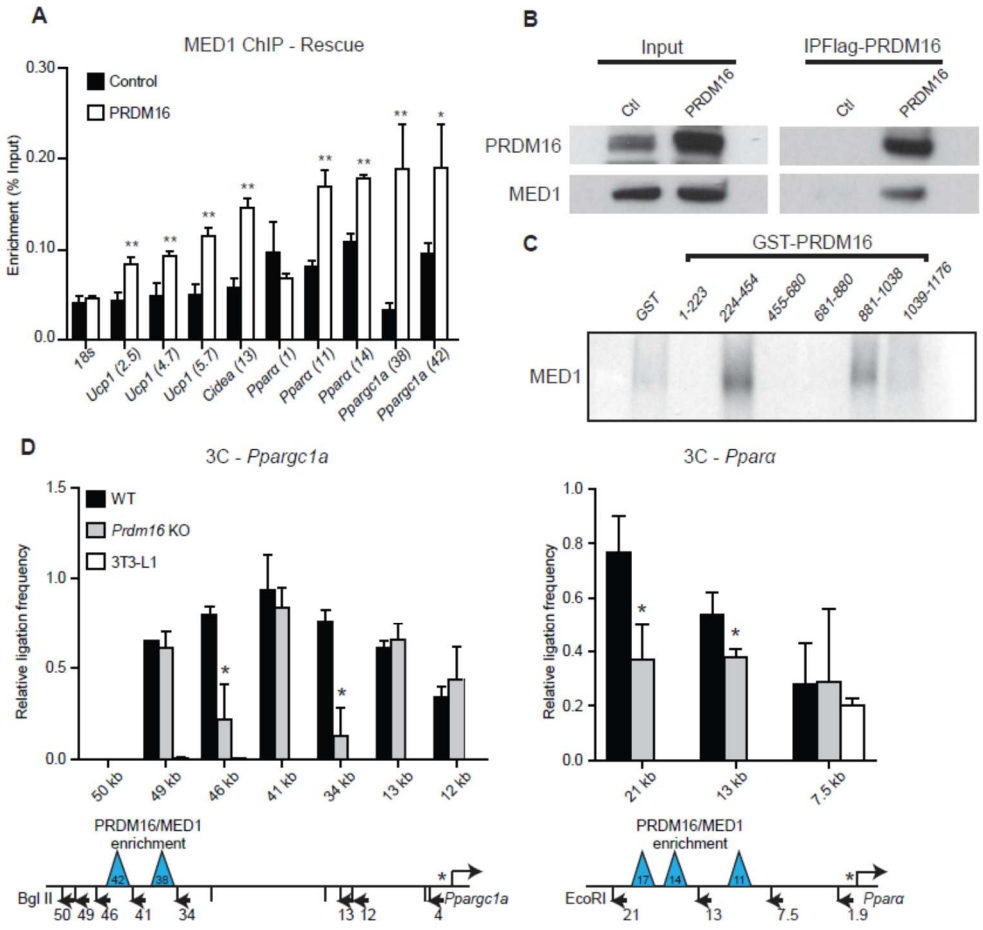

Figure 3. PRDM16 binds to MED1 and recruits it to BAT-selective genes

(A) ChIP-qPCR analysis of MED1 binding at BAT-selective genes in *Prdm16* KO adipocytes that express PRDM16 or a control (puro) virus. *18s* was used as a non-specific binding site (mean ± Stdev; n = 3; *p < 0.05, **p<0.01). **(B)** Co-immunoprecipitation of MED1 and PRDM16 in brown adipocytes that express control or Flag-PRDM16. **(C)** Fluorography of GST fusion proteins containing different regions of PRDM16 that had been incubated with *in vitro* translated and S^{35}-labeled MED1. **(D)** 3C analysis of the *Ppargc1a* and *Pparα* loci in WT and *Prdm16* KO brown adipocytes and 3T3-L1 white adipocytes. Map of loci shows location of restriction sites and PCR primers used. *anchor primer which resides on a fragment containing the transcriptional start site (TSS) (mean ± Stdev; n = 3; *p < 0.05)

In young animals (< 2 months) PRDM3 compensates for the loss of PRDM16 to activate BAT-selective genes[214]. This suggested that PRDM3 may also bind and cooperate with MED1 at BAT genes. As hypothesized, PRDM3, like PRDM16, bound to

MED1 in brown preadipocytes (Figure S3E). Moreover, there were substantially lower levels of MED1 at BAT-selective PRDM16-target genes (*Ucp1*, *Cidea*, *Pparα* and *Pparc1a*) in *Prdm16*/*Prdm3* double-KO (dKO) BAT relative to WT or *Prdm16* KO BAT (Figure S3F). These results indicate that PRDM3 and/or PRDM16 can participate in the recruitment of MED1 to BAT-selective genes.

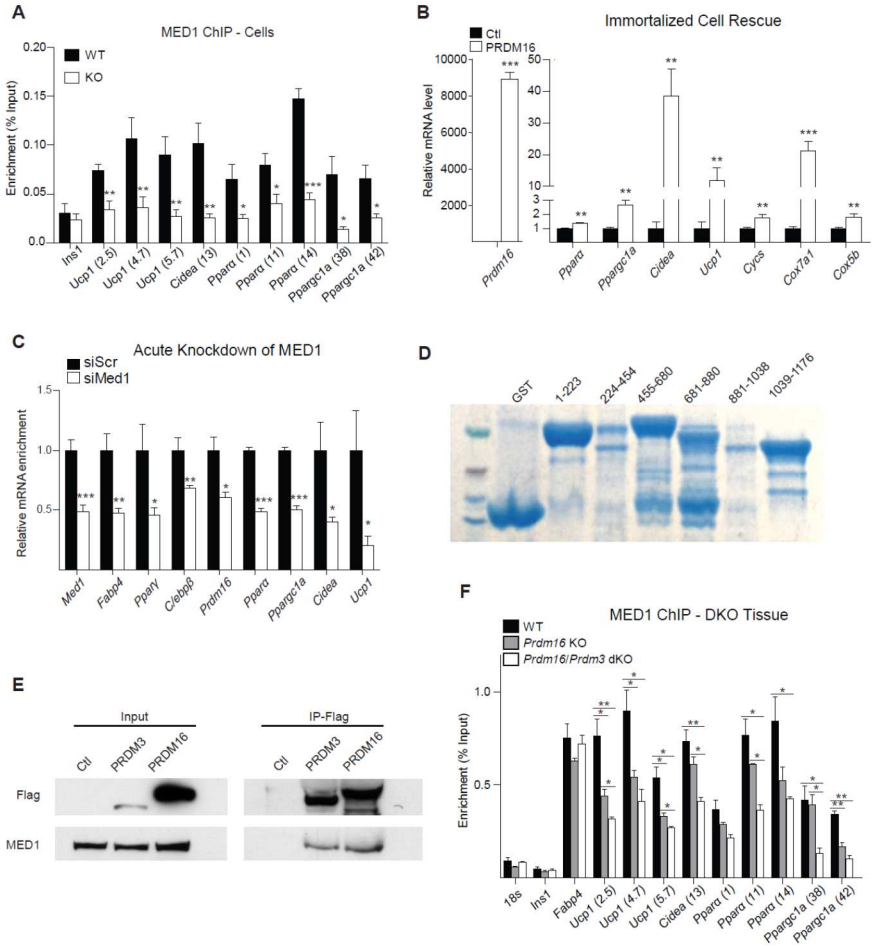

Figure S3. PRDM3 binds and recruits MED1 to BAT-selective loci

(A) ChIP-qPCR analysis of MED1 binding at BAT-selective genes in wildtype (WT) and PRDM16 knockout (KO) adipocytes. Ins1 was used as a non-specificbinding site (mean ± Stdev; n = 3; *p < 0.05, **p<0.01, ***p<0.001). **(B)** Relative mRNA levels of BAT-sel. genes in PRDM16-deficient brown adipocytes that were transduced with control or PRDM16 expressing virus. (mean ±Stdev; n = 3; *p < 0.05, **p<0.01, ***p<0.001) **(C)** Relative mRNA levels of adipogenic and BAT-sel. genes from differentiated primary brown adipocytes that were transfected with siScr or siMed1. (mean ± Stdev; n = 3; *p < 0.05, **p<0.01, ***p<0.001) **(D)** Commassie blue staining of GST and GST-PRDM16 fusion proteins **(E)** Co-immunopreciptation of MED1, PRDM16 and PRDM3 from PRDM16 deficient pre-adipocytes that express control, Flag-PRDM16 or Flag-PRDM3 **(F)** ChIP-qPCR analysis of MED1 binding at adipogenic and BAT-sel. genes in WT, *Prdm16* KO and *Prdm16*/*Prdm3* double KO (dKO) BAT. 18s and Ins1 were used as non-specific binding sites (mean ± SEM; n = 3; *p < 0.05, **p<0.01)

PRDM16 controls higher order chromatin structure

We hypothesized that PRDM16 was essential for promoting long range chromatin interactions between gene regulatory regions and their associated promoters. To test this, we used chromosome conformation capture (3C) assays to examine the effect of PRDM16 on the chromatin architecture at *Ppargc1a* and *Pparα*. At *Ppargc1a*, the region surrounding two PRDM16/MED1 binding sites (-34 kb to -46 kb) interacts with the promoter in WT brown adipocytes but not in 3T3-L1 white adipocytes (Figure 3D). The interactions between the promoter and the -34 kb and -46 kb regions were significantly decreased in PRDM16 KO adipocytes, whereas the interaction between the promoter and the -41 kb region was unaffected. These results suggest PRDM16 regulates the assembly of an active chromatin hub. Similarly, at *Pparα*, there were higher levels of interaction between the promoter and 2 upstream regions (containing all three sites of PRDM16/MED1 enrichment) in WT relative to *Prdm16* KO adipocytes. (Figure 3D). Altogether, these results show that PRDM16 is required for the proper assembly of higher order (and active) chromatin structure at critical BAT genes.

Previous studies showed that PRDM16 binds and regulates the adipogenic transcription factors PPARγ and C/EBPβ [87,90]. Here, we noted that PRDM16 activity was not required to promote or stabilize the binding of these factors to BAT-selective genes. This implies that PRDM16 does not play a crucial role in making the chromatin competent for DNA-binding or for stabilizing transcription factor complexes at enhancers. Rather, our data argue that PRDM16, presumably through interacting with MED1/Mediator, regulates long range interactions between enhancer elements and promoters. In support of this, Mediator is known to bridge enhancer-bound

transcriptional complexes with the general transcriptional machinery and to promote the formation of pre-initiation complexes [218,220].

Prdm16 controls BAT-selective super-enhancers

Cell type-specific identity genes are often regulated by large enhancer regions called super-enhancers (SE) that are bound by master-transcription factors [216]. SE have higher levels of MED1 binding and multiple MED1 binding sites as compared to typical enhancers (TE) [216]. Given the role of PRDM16 in controlling BAT identity, we tested whether PRDM16 was associated with SE activity. We used the genome-wide binding profile of PPAR*y,* the master transcriptional regulator of white and brown adipocytes, to define a set of constituent enhancers. Then, using the previously described method [216], we identified 507 SE and 15,712 TE in BAT and assigned them to the nearest gene (Figure 4A). As anticipated, genes associated with a nearby SE were expressed at higher levels as reflected by higher levels of Pol II in gene bodies (Figure S4A). Many BAT-selective genes had a nearby SE, including *Prdm16*, *Pparα*, *Ppargc1a*, *Ucp1* and *Cidea*. Brown fat differentiation, fat cell differentiation, oxidative reduction and fatty acid metabolic process were identified by GO analysis as the top scoring gene categories associated with SE-linked genes in BAT (Figure S4B).

Remarkably, 78% of BAT SE contain at least one PRDM16 binding site and the strength of PRDM16 binding was higher at SE than at TE (Figure 4B,C). SE were much more sensitive than TE to the loss of PRDM16 (Figure 4D). Out of 507 SE in WT BAT, more than half of these (277) were lost (defined by reduction in MED1 levels) in PRDM16 KO BAT while only 15 SE were induced (Figure 4E). The lost SE were linked to genes that had reduced expression levels in *Prdm16* KO relative to WT BAT,

including *Ucp1*, *Pparα*, *Cidea* and *Ppargc1a* (Fig 4F). Globally, ~50% of the SE-linked BAT-selective genes had decreased levels in *Prdm16* KO BAT (Figure 4G).

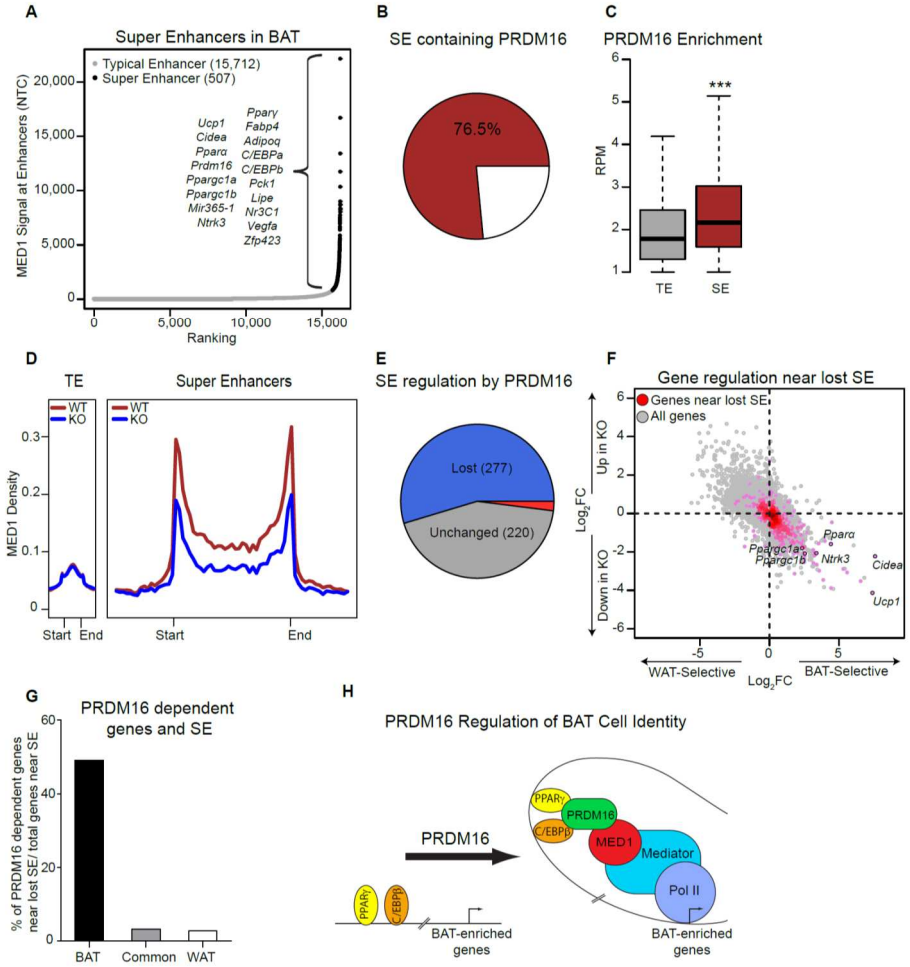

Figure 4. PRDM16 controls BAT-selective Super Enhancers

(A) MED1 ChIP-seq signal (normalized tag count) across 16,219 identified enhancers in BAT. **(B)** Pie chart showing the number of super enhancers (SE) that are bound by PRDM16. **(C)** Box plot comparing PRDM16 binding strength (RPM) at typical enhancers (TE) and SE (***p < 10−25). **(D)** Metagene representation of MED1 signal at TE and SE in Wildtype (WT) (red) and PRDM16 knockout (KO) (blue) BAT. X-axis schematizes the start and end of enhancers. The y-axis is the average signal in RPM. **(E)** Pie chart showing BAT SE that are lost (blue), induced (red) or unchanged (gray) by PRDM16-deficiency. Lost or induced was defined as ≥2 fold change of MED1 signal. **(F)** Scatter plot showing correlation between SE lost in PRDM16 KO BAT and gene expression levels in BAT versus WAT (X-axis) and PRDM16 KO versus WT BAT (Y-axis). **(G)** Proportion of BAT-sel., common or WAT-sel. genes that have reduced gene expression in PRDM16 KO BAT and are associated with lost SE. **(H)** Model for PRDM16-mediated gene activation. PRDM16 interacts with enhancer regions at BAT-selective genes through C/EBPβ and PPAR*γ*. PRDM16 recruits MED1/Mediator to bridge enhancer-bound transcription factors with RNA Pol II/the general transcription machinery.

SE activity is regulated by BRD4, a bromodomain protein that interacts with Mediator [221]. To examine if the transcription of SE-linked, BAT-selective genes is dependent on BRD4 activity, we treated brown adipocytes with JQ1, an inactive analog (JQ1-), or vehicle control for 6 hours. We then measured the expression levels of the top eight BAT-selective genes that had a linked SE. The levels of 7/8 of these genes were decreased by JQ1, whereas several highly expressed TE-associated genes were unaffected (Figure S4C). These results suggest that PRDM16-activated genes in BAT depend on BRD4 function and are thus likely controlled by SE.

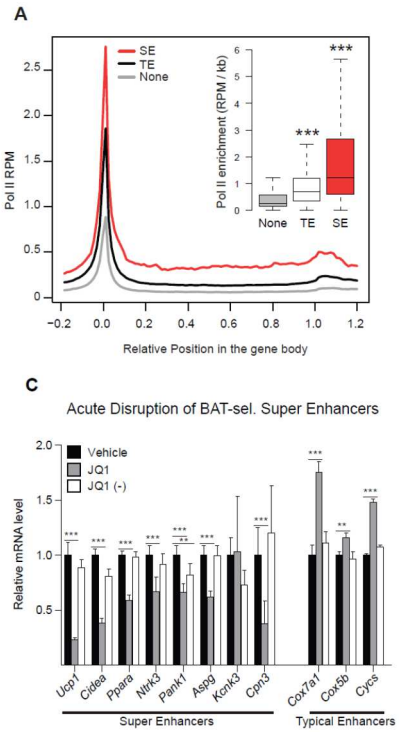

B

GO analysis for genes near SE

Rank	Term	P-Value
1	brown fat cell differentiation	1.92E-13
2	fat cell differentiation	2.22E-10
3	oxidation reduction	4.86E-09
4	fatty acid metabolic process	7.50E-09
5	generation of precursor metabolites and energy	4.84E-08
6	energy derivation by oxidation of organic compounds	5.25E-08
7	organic ether metabolic process	6.73E-07
8	glycerol ether metabolic process	2.94E-06
9	glycerolipid metabolic process	2.96E-06
10	coenzyme metabolic process	2.97E-06

Figure S4. PRDM16 regulates Super Enhancers in BAT

(A) Average Pol II profile (RPM) around gene bodies of genes associated with super enhancers (red), typical enhancers (black), or genes without proximal MED1 occupancy (grey). Insert – box plot representation of Pol II signal (RPM/kb) of same data (***p < 10−50) **(B)** DAVID gene ontology (GO) analysis for super enhancer-associated genes in WT BAT **(C)** Relative mRNA levels of genes marked by SE or TE in differentiated primary brown adipocytes that were treated with either vehicle, JQ1 or an inert JQ1 analog (JQ1(-)) (mean ± Stdev; n = 6; *p < 0.05, **p<0.01, ***p<0.001)

In summary, our data suggests that PRDM16 binds to chromatin at BAT-selective genes via PPARγ and C/EBPβ (and likely other factors) where it acts to recruit MED1/Mediator (Figure 4H). In our model, the chromatin-bound PRDM16/MED1 enhances transcription by: (1) establishing interactions between promoters and SE; and (2) increasing Pol II and promoting pre-initiation complex assembly at promoter regions.

Materials and Methods

Animals

Myf5^{Cre} mice (stock number 010529) were obtained from the Jackson Laboratory. *Prdm16*^{flox} and *Prdm3*^{flox} were previously described [199,214]. Adult *Prdm16* KO mice were studied at ≥ 9 months of age. All animal experiments were approved by the University of Pennsylvania's Institutional Animal Care and Use Committee.

Cell Culture

WT and *Prdm16* KO brown adipocytes were cultured and differentiated as described before [214]. siMed1 (Dharmacon L-040964-01) was electroporated into primary brown adipocytes at 6 days of differentiation using the Lonza Amaxa Nucleofector II (program A-033) and nucleofector kit V (VCA-1003). Brown adipocytes were treated with 500 nM of JQ1 and its inert analog JQ1(-) for 6 hr.

Real-Time qPCR

Total RNA was extracted by TRIzol (Invitrogen) followed by purification using PureLink RNA columns (Invitrogen). Isolated mRNA was reverse transcribed using the High-Capacity cDNA Synthesis kit (Applied Biosystems) and used in real-time qPCR reactions with SYBR Green master mix (Applied Biosystems) on a 7900 HT (Applied Biosystems). *Tata-binding protein* (*Tbp*) was used as an internal normalization control.

Chromatin Immunoprecipitation

ChIP was performed as previously described [214,222].

ChIP-seq data processing

ChIP-seq reads for Prdm16, H3K27-Ac, Pol II, and Med1 were aligned to mouse genome (mm9) using Bowtiee with options, '-k 1 -m 1 --best --strata' [223]. All redundant

reads were discarded except one per genomic position. Peak-calling for PRDM16 and MED1 was performed using Homer [224]. After initial calling, all peaks were resized to 200 bp, and a 1 RPM cut-off was applied. PRDM16 binding sites were more rigorously defined as follows. After initial peak-calling, reproducibility of replicates was assessed by scatter plot before pooling. Final peak-calling was performed for pooled WT using pooled KO samples as background control. For H3K27-Ac analysis, we performed differential peak-calling for BAT and WAT samples using one depot as a ChIP sample and the other as a control, and vice-versa. In all cases, any genomic regions that overlapped with ENCODE blacklist regions [225] were eliminated. *De novo* motif search was done within 200 bp region around peak centers using Homer.

Genome-wide analysis comparing depot-selective genes

'Bedtools' [226] was used for genomic region handling. When comparing PRDM16 signal around depot-selective genes, we used Fat Pad DNase hypersensitive (DHS) sites downloaded from ENCODE [225] as an unbiased set of regulatory elements, and PRDM16 ChIP-seq signals at DHS within 100 kb of TSS were summed for each gene. H3K27-Ac levels were also compared between depot-selective genes anchoring on DHS sites, where H3K27-Ac ChIP-seq signal was measured in 2 kb window around DHS. Gene transcriptional changes were measured as Pol II ChIP-seq signal in gene bodies excluding first 500bp from TSS. To compare MED1 occupancy changes, two sets of MED1 peaks from WT and KO were pooled and any overlapping peaks whose center-to-center distance is < 100bp were merged into a single peak.

Super enhancer (SE) analysis

Previously published PPARy ChIP-seq data in BAT was downloaded from GEO [156]. ROSE [221,227] was used for SE calling, where enhancers were ranked by MED1 signal. A

gene was associated with enhancers (typical or super) within 100 kb region around TSS, where multiple associations were allowed. Gene ontology analysis was done using DAVID [228].

Chromatin Conformation Capture (3C)

The 3C procedure was performed as described [229] using WT and *Prdm16* KO brown adipocytes or 3T3-L1 adipocytes at day 8 of differentiation. Briefly, 20 µg of fixed nuclei was digested with Bgl II (*Ppargc1a*) or EcoR1 (*Pparα*). Half (10 µg) of the digested chromatin was used for the ligation while the other half was set up identically, but without T4 DNA ligase. The PCR products were separated on 1.5% agarose gels, stained with SYBR Gold, imaged with the Typhoon Phosphorimager system (GE Healthcare) and quantified using ImagerQuant TL (GE Healthcare). The ligation efficiency was calculated as the ratio of ligated products to the corresponding random ligation of a mouse BAC clone; this was normalized to 3C analysis at a housekeeping locus (*Ercc3*) [230].

Protein Interaction Analyses

Protein interactions were assayed as previously described [13,215]. Protein extracts were prepared in a buffer containing 20mM Tris, 10% glycerol, 200mM NaCl, 2mM EDTA, 0.1% NP-40, 10mM NaF and protease inhibitors. Flag-M2 beads (Sigma A2220) were added to the lysate and subsequently washed 5 times. Proteins were separated in 4%–12% Bis-Tris NuPAGE gels (Invitrogen) and transferred to PVDF membranes. Primary antibodies were anti-PRDM16 [87], MED1 (Bethyl A300-793A) and M2-HRP (Sigma A8592). For *In vitro* binding assays, GST-PRDM16 fragments were prepared as described [215]. S^{35} labeled MED1 was prepared using the TNT reticulocyte lysate kit (Promega L5020). Equal amounts of GST-PRDM16 proteins were incubated overnight at 4°C with *in vitro* translated MED1 in a buffer containing 20mM HEPES pH 7.6, 150mM

KCl, 2.5mM MgCl2, 0.05% NP40 and 10% glycerol. GST beads were washed three times. Bound proteins were separated in 4%–12% Bis-Tris NuPAGE gels (Invitrogen), soaked in a solution containing 4% glycerol, 46% MeOH and 10% acetic acid for 30 minutes, followed by soaking in Amplify (GE/Amersham NAMP 100) for 30 minutes. The gel was dried and analyzed via fluorography.

Statistical Analysis

All ChIP-qPCR data derived from tissue is reported as mean ± SEM. Data from cell lines and primary cells is reported as mean ± SD. Student's t test was used to calculate significance in ChIP-qPCR and tissue culture experiments (*$p < 0.05$, **$p<0.01$, ***$p<0.001$) using Excel.

Primers used for real-time qPCR and ChIP-qPCR analysis

mRNA	Fwd	Rev
Aspg	ATTGCCTTCAGG GGCTGTGAC	CTGGCCCAGCACATAGGACAGT
C/ebpβ	ACGACTTCCTCTCCGACCTCT	CGAGGCTCACGTAACCGTAGT
Cidea	TGCTCTTCTGTATCGCCCAGT	GCCGTGTTAAGGAATCTGCTG
Cox5b	GCTGCATCTGTGAAGAGGACAAC	CAGCTTGTAATGGGTTCCACAGT
Cox7a1	CAGCGTCATGGTCAGTCTGT	AGAAAACCGTGTGGCAGAGA
Cpn3	GCCGACATCCCTCCGGACATC	TCCAGGTGACGGACCTGAGTGT
Cycs	GCAAGCATAAGACTGGACCAAA	TTGTTGGCATCTGTGTAAGAGAATC
Fabp4	ACACCGAGATTTCCTTCAAACTG	CCATCTAGGGTTATGATGCTCTTCA
Kcnk3	GCTTCGCCG GCTCCTTCTACTT	CTAGTGTGAGCGGGATGCCCAG
Med1	TGCTTGGAAAATTCCTCAAAA	GATGTCAAAGTGGCTCACCA
Ntrk3	ATGCGAGCCCTACACCTCCTA	GACTGCTATGGACACCCCAAA
Pank1	CGCTGTTCGCCCAGCATGATTC	CAGCTTAACCAGGGTTCCACCGA
Ppargc1a	CCCTGCCATTGTTAAGACC	TGCTGCTGTTCCTGTTTTC
Pparα	GCGTACGGCAATGGCTTTAT	GAACGGCTTCCTCAGGTTCTT
Pparγ2	TGGCATCTCTGTGTCAACCATG	GCATGGTGCCTTCGCTGA
Prdm16	CAGCACGGTGAAGCCATTC	GCGTGCATCCGCTTGTG
Tbp	GAAGCTGCGGTACAATTCCAG	CCCCTTGTACCCTTCACCAAT
Ucp1	ACTGCCACACCTCCAGTCATT	CTTTGCCTCACTCAGGATTGG

ChIP	**Fwd**	**Rev**
18s	AGTCCCTGCCCTTTGTACACA	CGATCCGAGGGCCTCACT
Cidea (13)	GGCCACTTGAGGAGCCAACCA	TGGGCACTGGCCTTGTAGCTG
Fabp4	GACAAAGGCAGAAATGCACA	AATGTCAGGCATCTGGGAAC
Ins1	GGACCCACAAGTGGAACAAC	GTGCAGCACTGATCCACAAT
Ppargc1a (38)	TCCGAGTTTCCCTGCTGTGGC	AGGGACTTGCAGCTGTGGTGG
Ppargc1a (42)	GAGGTGGCACCAGGACACCAG	CCCAAGCTCGAGACTCCGCTC
Pparα (1)	GGGGCATGTGCATTCCGTGAC	CACTGGGGCTCTGCCAACTGA
Pparα (11)	AAGAGCATGGGACAGTGGCCG	TGGCCAGCTGAAGGTCACCAC
Pparα (14)	CCTGCCCCATAGGCAGTATGGTC	ACAGGGGCAGAAGCCAAGCTG
Pparγ (122)	AGCTTTGCTGGCTAGAGGTG	TTTCGCAGAACTGAGGTTGA
Ucp1 (2.5)	CAAATGGTGACCGGGTGCCCT	GGGTGACTGACCCTCTGTGACG
Ucp1 (4.7)	CCCCACTGCCTGTCACGTTCA	GAAGCTGCCGAATGGTGCGTC
Ucp1 (5.7)	ACCACACCATTTGGAGCCTGAC	TGAGTTTGCAGGGAGGATGGGC

Author Contributions

M.J.H, Y.H, S.S., J.I., S.R., D.J.S performed experiments and analyzed data. H-W.L. and K-J.W. performed computational analyses of ChIPseq and mRNA expression datasets. D.J.S. and M.A.L. provided ChIP-seq datasets for integrated analysis. M.J.H., H-W.L., K-J.W. designed experiments. M.J.H. and P.S. wrote the manuscript.

Acknowledgments

We thank Samantha Falk for technical help. We are also grateful to the Functional Genomics Core of the Penn Diabetes and Endocrinology Research Center (DK19525) for high throughput sequencing. This work was supported by NIGMS/NIH award DP2OD007288 and by a Searle Scholars Award to P.S. and by NIDDK R01 DK49780 and the JPB Foundation to M.A.L.

Discussion and Future Directions

Taken together, my work reveals new insights into the mechanistic function of PRDM16. We have shown that PRDM16 is critically required to maintain BAT identity and this requirement appears to be linked to the recruitment of MED1/the Mediator complex to control chromatin architecture. However, a number of salient questions remain to be addressed.

One of our most surprising results is that mice with poor brown fat functionality (adult PRDM16 KO mice) are not predisposed to weight gain. This suggests that in mice, while brown fat is required to acutely defend body temperature against a cold challenge, it is the thermogenic adipocytes in white fat (beige adipocytes) which mediate diet-induced thermogenesis and regulate body weight. In direct support of this hypothesis, the Spiegelman lab found that mice lacking *Prdm16* in all adipose tissues, thus ablating beige adipocytes, gained more weight than wild type controls[188]. Indeed, the data from Table 1 which displays mouse models that are resistant to weight gain indicates that most of the mouse models that have decreased weight gain have an activation of both brown and beige fat, or only beige fat without a concurrent activation of brown fat. Only a small number of genetic models resistant to obesity have an increase in brown fat activity without an increase in beige[187]. Taken together, this suggests that hyperstimulating brown fat can be a way to suppress weight gain, however the loss of brown fat doesn't necessarily predispose to weight gain.

Although *Prdm16* deficient BAT eventually loses its brown fat character, the expression of WAT-selective genes are elevated in BAT at any age post-weaning. This has presented us with a number of interesting questions. The most obvious being, is

PRDM16 predominantly a repressor, and has secondary activating effects on BAT-selective genes? This would explain why/how the brown fat is able to develop in PRDM16 KO mice. However, our results in chapter 2 refute this hypothesis. Using genome-wide data of PRDM16 occupancy we find that PRDM16 is more strongly associated with BAT genes, indicating that PRDM16 more directly regulates the activation and expression of BAT-selective genes.

We do not preclude the possibility that PRDM16 also acts on certain WAT genes directly. Indeed we show ChIP-seq tracks for PRDM16 at *Angiotensinogen* and *Resistin* showing a number of binding sites proximal to the respective genes TSS. These data suggest that PRDM16 directly regulates some WAT genes, while the others are consequential. Interestingly, PRDM16, but not PRDM3 is required to repress a WAT program. When we have assessed PRDM3 KO BAT, there is no increase in the expression of the WAT-selective gene set (data not shown). Furthermore the PRDM16/PRDM3 dKO BAT does not have further elevated expression of this WAT expression signature beyond that is seen in PRDM16 KO BAT. Thus the function of PRDM16 in the repression of WAT genes is unique. In the future it will be important to determine why PRDM16 represses these genes. Given the dramatic rise in expression of such a large number of WAT-selective genes, one would expect that some fundamental aspect of adipocyte biology has been altered. However, using metabolic cages and acutely activating BAT, we detected no change in thermogenic function in young PRDM16 KO mice that have elevated expression of WAT-selective genes but not BAT-selective genes (data not shown). It would be prudent to look at other measures of BAT function such as cold intolerance to determine if the up-regulation of these WAT-selective genes is sufficient to alter BAT function and impart a white adipocyte function.

Additionally, we will address if the aforementioned *Adiponectin-Cre Prdm16*$^{flox/flox}$ mice have elevated expression of these genes in the subcutaneous and visceral WAT. It is possible that PRDM16 has conserved mechanistic function in both tissues, but the repression of the WAT program in the browning of WAT has more physiological significance. To assess this hypothesis mutations in PRDM16 that prevent the binding of CtBP and fail to repress WAT-selective genes could be employed[231]. White adipocytes isolated from inguinal fat could be transduced with WT or PRDM16ΔCtBP virus and differentiated in culture, allowing us to see if PRDM16ΔCtBP is unable to repress WAT-selective genes in this cell type. If this mutation is revealed to be critical in this cell type, transgenic mice that contain the ΔCtBP mutation in all adipocytes could be generated and tested for metabolic/thermogenic defects.

One possible explanation for the broad rise in the expression of WAT-selective genes is that PRDM16 KO BAT has a significant increase in the expression and protein levels of PPARγ, the master regulator of adipogenesis. This increase is consistently observed in BAT in our studies using a *Myf5-Cre* driver and the Spiegelman group, who used *Adiponectin-Cre*[188]. It is conceivable that a slight elevation of PPARγ pushes a WAT transcriptional profile. To test this we could use existing genome-wide binding data of PPARγ in BAT[208]. We could take the list of genes that are up-regulated in PRDM16 KO mice and select proximal enhancers based on PPARγ binding. We could then assess if these genes have more PPARγ at enhancers in the PRDM16 KO mice relative to WT. Alternatively, PPARγ ChIP-seq can be performed on PRDM16 KO BAT and WT controls to look at changes in PPARγ binding in an unbiased way. Lastly, we could take WT brown adipocytes and virally overexpress PPARγ to asses if this is capable of inducing the expression of these genes.

An element of PRDM16 biology that remains unanswered is how PRDM16 is differentially recruited to activate BAT genes while repress certain WAT genes. PRDM16 can bind to canonically activating transcription factors and co-activators including PPARγ, PPARα, C/EBPs and PPARGC1a and with repressors including CtBP1/2 and EHMT1[87,90,231,232]. A mechanism has even been proposed that PPARGC1A and CtBP compete for binding with PRDM16[231]. Regardless, PRDM16 apparently works as an activator at certain loci, while at a repressor as others. Given the fact that PRDM16 contains zinc-fingers that are able to directly bind DNA, one hypothesis is that PRDM16 binds chromatin indirectly at BAT genes (as we have suggested in Chapter 2) while directly at WAT genes that it regulates, which could lead to differential recruitment of activating vs repressive complexes. However, in our analysis we did not pick up a highly enriched PRDM16 motif at WAT or BAT genes. One possibility is that when we assessed PRDM16 binding in mature brown adipocytes, our analysis was not amenable to capturing a unique “repressive” motif. Interestingly, over-expression of Prdm16 in PRDM16 KO brown pre-adipocytes leads to the repression of *Agt* and other WAT-selective gene expression, and it binds prominently proximal to *Agt* and *Retn* (data not shown). These binding sites are found in mature adipocytes, but interestingly, a number of additional PRDM16 binding sites found in mature tissue around these genes are not present in the preadipocyte state. Furthermore, these changes in gene expression are occurring in a preadipocyte state when PPARγ is not yet expressed. This indicates that PRDM16 is being recruited to these sites in a manner that differs from activating BAT-selective genes. Performing *de novo* motif analysis under areas of PRDM16 enrichment in preadipocytes – proximal to these effected WAT genes may reveal a novel binding signature.

PRDM16 is documented to control lineage specificity between brown fat and skeletal muscle cells[13]. Lineage tracing indicates that brown fat and skeletal muscle come from a common progenitor population, and that adenoviral delivery of siRNAs targeted against *Prdm16* results in an increase in the expression of muscle enriched genes. Indeed, mice that are whole body knockout for PRDM16 are embryonic lethal, but have an increase in the expression of certain skeletal muscle genes in their BAT. Surprisingly, despite this strong evidence in support of PRDM16 controlling lineage specificity, the mice used in both chapters above do not show any increase in a muscle signature at any time point that we have assessed. A number of possibilities exist that may explain the difference in results. One appealing argument is that the *Myf5-Cre* we used to drive recombination was expressed too late in development – that at the time *Myf5* is expressed brown adipocyte cell identity has already been determined. Little research has explored exactly when PRDM16 is expressed in developing mesoderm. It is possible that *Prdm16* could be expressed earlier than is currently imagined perhaps even coincident with *Myf5*. Given that PRDM16 powerfully shuts down a myogenic program in cell assays, it is conceivable that any expression of PRDM16 would be sufficient to permanently direct a cell towards an adipogenic lineage. To address this hypothesis an embryonic time course should be conducted looking for the earliest expression of PRDM16 in the mesoderm that develops into BAT. By assessing at what embryonic stage *Prdm16* is expressed we would be better informed to determine if issues with recombination timing are influencing our results. An alternative approach would be to cross our *Prdm16*$^{flox/flox}$ with another promoter driven-Cre that is expressed in the somatic mesoderm including *Pax7,* Pax3 and *Engrailed-1.*

Another possibility is that the siRNA directed against PRDM16 could have had off target effects that somehow made the cells more dependent on PRDM16. As we have seen with PRDM3 there is at least one instance where another factor is poised to compensate for the loss of PRDM16. In a developmental context, PRDM3 does not compensate since PRDM16/PRDM3 dKO BAT does not express a myogenic gene signature. However, there are numerous zinc finger proteins that share a highly conserved zinc finger motif in PRDM16; a segment of the protein which is critical for PRDM16 function. Indeed, by assessing the level of the 5 most closely related proteins to PRDM16, three of them have transcript levels that are reduced in siPrdm16 infected cells (data not shown). Two of these factors are enriched in BAT relative to WAT, as well as BAT relative to skeletal muscle (data not shown). Further analysis of these proteins and the consequence of their loss of function may shed light on this issue. It will also be of interest to determine when these unknown function are expressed *in vivo* and during the course of *in vitro* differentiation.

It is interesting to note that when the histone methyl transferase EHMT1 is knocked out *in vivo* using *Myf5-Cre* there in an increase in the expression of myogenic genes. This protein has been shown to interact directly with PRDM16 and mediate the PRDM16-action at least in cells[190]. The difference in the phenotype of the *Myf5-Cre Prdm16*$^{flox/flox}$ and *Myf5-Cre Ehmt1*$^{flox/flox}$ mice is consistent with the existence of a PRDM16-compensating factor. These data suggest that the compensating factor may also able to interact with EHMT1 and recruit EHMT1 to muscle genes. It would be interesting to perform mass spectrometry in order to identify EHMT1-interacting factors in brown adipocytes and look for other PRDM16-like zinc finger proteins. Or alternatively, if any of the putative compensating factors described in the section above

appear to be promising, assessing the interaction between the zinc finger protein and EHMT1 could lead to mechanistic insight.

The issue of compensating factors could potentially explain a number of unexpected results in the PRDM16 KO mice. One very curious observation is the difference in PRDM16 KO adipocytes *in vitro* versus *in vivo.* In culture, upon differentiation, *Prdm16*-deficient adipocytes have a substantial defect in the expression of a BAT-selective program. However this cell autonomus *in vitro* phenotype happens regardless of the age of the mice from which the cells were isolated, including embryonic day 18, a time in which the tissue displays no defects. One possible explanation for this is the observation that PRDM3 levels precipitously decline after plating primary cells (data not shown). This could mean that PRDM16 KO cells are functionally the same as double KO cells, when studied *ex vivo*. In the future it will be important to isolate primary cells from double KO mice and compare the results of differentiation to PRDM16 KO cells. Additionally PRDM3 should be virally overexpressed in PRDM16 KO cells to determine if this is sufficient to rescue the thermogenic program. Lastly, it will be interesting to assess if any of the other related zinc finger proteins also have levels that decline in culture.

Given that the phenotype in the PRDM16 KO mice is associated with age, it is possible that the phenotype is due to tissue turnover and incorporation of new adipocytes that are unable to induce a thermogenic program. Our isolation of primary cells from BAT involves enriching for the undifferentiated stem cell population while removing mature adipocytes. Our data from primary cells clearly shows that when PRDM16 KO cells are cultured they have a severe loss of BAT-selective gene expression. These data could imply that as the tissue turns over naturally, thermogenic-

defective adult stem cells are incorporated into the BAT yielding the progressive loss of BAT character that we observe. How PRDM16-deficient embryonic BAT is able to develop normally is unclear. It is possible that two pools of brown adipocyte precursors exist; one population could be responsible for embryonic tissue development and is PRDM16 independent, while another adult population maintains tissue mass and function through the animal's life and is PRDM16 dependent.

Interestingly, the PRDM16/PRDM3 dKO mice have what appears to be an accelerated phenotype, however we do not believe this is due to increased tissue turnover (data not shown). It is possible that in the dKO mice, although the incorporation of defective adipocytes plays a role, the accelerated phenotype is due to mature adipocytes requiring PRDM16 or PRDM3. This hypothesis implies that PRDM16/PRDM3 independent pathways are able to preserve BAT function in the dKO mice until 4-6 weeks. Future studies need to address which pathways and stimuli are PRDM16/PRDM3 independent, and if this knowledge can help explain the sudden phenotype onset in the dKO mice.

How and why PRDM3 is able to compensate in post embryonic BAT, and what causes it to no longer be sufficient in PRDM16 KO mice remains unclear. One explanation is the fact that as mice age from weaning to 6 months of age *Prdm3* mRNA levels decline (data not shown). However the mechanism responsible for decreasing the expression of *Prdm3* is not clear. It is unknown if the changes in expression are due to cell-autonomous regulation or systemic influences. One of the most obvious places to look is the effect that cold has on the regulation of PRDM3. However, housing and rearing WT and PRDM16 KO mice at thermoneutrality does accelerate the loss of

thermogenic function, indicating that cold stimulation does not keep PRDM3 levels elevated (data not shown).

Another avenue to explore is the fact that even in the dKO mice we see no phenotype until after weaning. One possibility is that suckling or dames' milk is able to rescue/maintain BAT identity through PRDM16/PRDM3 independent pathways. For example it is well established that milk/suckling induces the expression of FGF21 and PPARα in BAT, both which have been shown to be required for functional BAT[172,173,175]. To address this, dKO mice could be weaned slightly early from their mother (at 2 weeks of age) and fed a hydrogel diet. If this results in an interesting effect mice can be weaned earlier and fed manually with formula. For an *in vitro* approach we could assess if treating PRDM16 KO adipocytes with FGF21 or a PPARα activator is sufficient to rescue the phenotype.

Although the mechanism is currently unclear, it is highly probable that additional factors are able to compensate for the loss of PRDM16/PRDM3 to ensure the proper development of BAT. In the future I propose to do a small screen using CRISPR technology to delete structurally similar zinc-finger proteins (as mentioned above) as well as the remaining PRDM family members. Using this system in PRDM16 KO or PRDM16/PRDM3 dKO adipocytes we would be able to look for factors, or combinations of factors that either inhibit adipogenesis or increase the expression of myogenic factors. Any hits that reveal interesting phenotypes will have their patterns of expression assessed during the course of adipogenesis, during BAT development, and determine where they bind genome-wide at a stage in which they are found to be critical for BAT development. Lastly we will determine if any candidates are able to interact with MED1, possibly revealing mechanistic insight into the function of these proteins. As an

alternative approach we could interrogate the same factors but with a gain of function approach. In these experiments the factors would be virally overexpressed in C2C12 myoblasts, allowing us to assess which factors are competent to reprogram these cells into adipocytes like PRDM16 and PRDM3 can.

We have shown that PRDM16 recruits MED1/mediator to brown fat-selective genes and that loss of PRDM16 results in change of higher-order chromatic architecture. Furthermore our super enhancer analysis gives insight into how PRDM16 controls genes essential for BAT identity. Taken together, these results increase our understanding of PRDM16 function by allowing us to think of PRDM16 as a hub for higher-order chromatin structure. Acting as a hub PRDM16 is able to integrate the binding of master transcription factors such as PPARγ and C/EBPβ from multiple enhancers and allow these activators to come in contact with the TSS to activate the transcriptional machinery. Despite our increased understanding, a number of questions remain about how PRDM16 is able to organize chromatin. One of the most obvious questions is to what degree does PRDM16 affect chromatin structure genome-wide? To address this I would perform HiC, a genome-wide approach to assess chromatin interactions in WT and KO adipocytes. Using this technique we would be able to observe the full extent of the changes due to the loss of PRDM16. This data could also help us discern functional enhancers. For example at the *Ppargc1a* loci we detect changes in the loss at one of the two enhancers but not the other. This could imply that the enhancer which is lost is more critically required. Given that PPARGC1a is critical for mitochondrial formation and brown fat function, this type of information could be critical for therapeutics that wish to boost the expression of this gene or others like it. Furthermore, through this technique and defining functional PRDM16 binding sites we could perform additional computation

analysis such as motif analysis under these peaks of interest. A similar approach investigating chromatin organization could be informative for better understanding PRDM16s role in development. It would be interesting to infect C2C12 myoblasts with PRDM16 and do a time course with HiC. This would give us a detailed understanding of the temporal changes to chromatin that affect cell identity.

Another interesting fact is that in the BAT of *Adiponectin-Cre Prdm16* $^{flox/flox}$ mice, which only express Cre in differentiated adipocytes, there is no change in the expression of BAT-selective genes such as *Ucp1, Ppargc1a* or *Cidea*, even at three months of age, a time point that our data would suggest the mice should have a phenotype. This data from the Spiegelman lab lies in agreement with unpublished data that the acute knockdown of PRDM16 in differentiated brown adipocytes has a very subtle effect on the expression of BAT-selective genes. Together this implies that PRDM16 is required for chromatin hub formation, but not necessarily hub stabilization. In this model PRDM16 brings the enhancers into contact with the TSS, but once the interaction is formed it may be stabilized through other mechanisms. One appealing hypothesis is that the structural cohesin proteins, which are well documented to interact with MED1, are additionally recruited with the enhancers to the TSS by PRDM16. Once PRDM16 has established a thermogenic chromatin architecture they stabilize the chromatin loops. To test this, we should determine if there is cohesin at/near BAT selective loci. We can then compare cohesin enrichment at WT, PRDM16-acute KO, and KO adipocytes.

In our model PRDM16 is required to recruit MED1 to connect distal enhancers with the transcriptional start site (TSS) of BAT-selective genes to drive gene expression[218,220]. Our data also implies that PRDM3 and possibly other related zinc-finger transcription factors are also able to do the same in the absence of PRDM16. In

our PRDM16 KO mice, the understanding is that a connection between distal enhancers and the TSS was initially formed but lost over time. This implies that although other factors have the capacity to form a connection between enhancers and the TSS in the absence of PRDM16, PRDM16 is uniquely required for the maintenance of the chromatin conformation and BAT identity.

Another point to consider is that in our model PRDM16 recruits MED1 to BAT-selective loci. However, PPARγ and C/EBP both interact with MED1[219] and are bound at these enhancers, so why is PRDM16 required at all? It would appear that either in brown adipocytes or at BAT-selective enhancers PPARγ and C/EBP do not, or are unable to interact with MED1. Perhaps the binding patterns at BAT-selective genes are unique and sterically prevent the interaction with MED1. For example infecting C2C12 muscle cells with PPARγ will induce an adipogenic program presumably through the recruitment of MED1[233]. However, no brown fat genes will be turned on. These observations give exciting insight into the unique functions that PRDM16 is able to perform.

Lastly, all of our ChIP assays have been performed in fully differentiated brown adipocytes. It would be interesting to determine if our analysis of “steady state” BAT recapitulates development. It is highly possible PRDM16 binding patterns change and differ throughout out the course of differentiation. In support of this notion, in undifferentiated adipocytes that over express PRDM16, we find no enrichment at enhancers proximal to Ucp1. To further explore the dynamic regulation and recruitment of PRDM16, I would perform ChIP-Seq on WT brown adipocytes throughout their differentiation.

In conclusion, my studies have revealed new insight into the developmental and transcriptional regulation of BAT through PRDM16. I have found that PRDM16 is critically required to maintain BAT identity and functionality in adult mice. However, BAT is able to develop normally in the absence of PRDM16, suggesting that related factors may compensate for its loss. We found that indeed, PRDM3 is able to compensate for the loss of PRDM16. Mechanistically we found that PRDM16s ability to control brown adipocyte cell identity is based upon the ability of PRDM16 to interact with MED1/the mediator complex, and recruit MED1 to BAT-selective genes to drive transcription. The insight garnered from these studies will be of use to future researchers that aim to recruit BAT in humans to decrease body weight. Any therapeutic approach that aims to increase BAT mass will have to affect PRDM16 directly or indirectly. Having a better understanding of when PRDM16 is required for BAT functionality and PRDM16s mechanism of action will be of benefit when designing weight loss strategies.

References

1. Lloyd-Jones, D.*, et al.* Heart disease and stroke statistics--2009 update: a report from the American Heart Association Statistics Committee and Stroke Statistics Subcommittee. *Circulation* **119**, e21-181 (2009).
2. Bornfeldt, K.E. & Tabas, I. Insulin resistance, hyperglycemia, and atherosclerosis. *Cell Metab* **14**, 575-585 (2011).
3. Cai, L., Lubitz, J., Flegal, K.M. & Pamuk, E.R. The predicted effects of chronic obesity in middle age on medicare costs and mortality. *Med Care* **48**, 510-517 (2010).
4. Hammond, R.A. & Levine, R. The economic impact of obesity in the United States. *Diabetes Metab Syndr Obes* **3**, 285-295 (2010).
5. Olshansky, S.J.*, et al.* A potential decline in life expectancy in the United States in the 21st century. *N Engl J Med* **352**, 1138-1145 (2005).
6. Ricquier, D. Uncoupling protein 1 of brown adipocytes, the only uncoupler: a historical perspective. *Frontiers in endocrinology* **2**, 85 (2012).
7. Vitali, A.*, et al.* The adipose organ of obesity-prone C57BL/6J mice is composed of mixed white and brown adipocytes. *J Lipid Res* **53**, 619-629 (2012).
8. Petrovic, N.*, et al.* Chronic peroxisome proliferator-activated receptor gamma (PPARgamma) activation of epididymally derived white adipocyte cultures reveals a population of thermogenically competent, UCP1-containing adipocytes molecularly distinct from classic brown adipocytes. *J Biol Chem* **285**, 7153-7164 (2010).
9. Jespersen, N.Z.*, et al.* A classical brown adipose tissue mRNA signature partly overlaps with brite in the supraclavicular region of adult humans. *Cell metabolism* **17**, 798-805 (2013).
10. Wu, J.*, et al.* Beige adipocytes are a distinct type of thermogenic fat cell in mouse and human. *Cell* **150**, 366-376 (2012).
11. Sharp, L.Z.*, et al.* Human BAT possesses molecular signatures that resemble beige/brite cells. *PLoS One* **7**, e49452 (2012).
12. Lidell, M.E.*, et al.* Evidence for two types of brown adipose tissue in humans. *Nat Med* (2013).
13. Seale, P.*, et al.* PRDM16 controls a brown fat/skeletal muscle switch. *Nature* **454**, 961-967 (2008).
14. Xue, B.*, et al.* Genetic variability affects the development of brown adipocytes in white fat but not in interscapular brown fat. *J Lipid Res* **48**, 41-51 (2007).
15. Wu, J., Cohen, P. & Spiegelman, B.M. Adaptive thermogenesis in adipocytes: is beige the new brown? *Genes Dev* **27**, 234-250 (2013).
16. Cypess, A.M.*, et al.* Identification and importance of brown adipose tissue in adult humans. *N Engl J Med* **360**, 1509-1517 (2009).
17. Nedergaard, J., Bengtsson, T. & Cannon, B. Unexpected evidence for active brown adipose tissue in adult humans. *Am J Physiol Endocrinol Metab* **293**, E444-452 (2007).
18. Saito, M.*, et al.* High incidence of metabolically active brown adipose tissue in healthy adult humans: effects of cold exposure and adiposity. *Diabetes* **58**, 1526-1531 (2009).
19. van Marken Lichtenbelt, W.D.*, et al.* Cold-activated brown adipose tissue in healthy men. *N Engl J Med* **360**, 1500-1508 (2009).

20. Virtanen, K.A.*, et al.* Functional brown adipose tissue in healthy adults. *N Engl J Med* **360**, 1518-1525 (2009).
21. Harper, J.A., Dickinson, K. & Brand, M.D. Mitochondrial uncoupling as a target for drug development for the treatment of obesity. *Obes Rev* **2**, 255-265 (2001).
22. Vegiopoulos, A.*, et al.* Cyclooxygenase-2 controls energy homeostasis in mice by de novo recruitment of brown adipocytes. *Science* **328**, 1158-1161 (2010).
23. Cederberg, A.*, et al.* FOXC2 is a winged helix gene that counteracts obesity, hypertriglyceridemia, and diet-induced insulin resistance. *Cell* **106**, 563-573 (2001).
24. Dahle, M.K.*, et al.* Mechanisms of FOXC2- and FOXD1-mediated regulation of the RI alpha subunit of cAMP-dependent protein kinase include release of transcriptional repression and activation by protein kinase B alpha and cAMP. *J Biol Chem* **277**, 22902-22908 (2002).
25. Kim, J.K.*, et al.* Adipocyte-specific overexpression of FOXC2 prevents diet-induced increases in intramuscular fatty acyl CoA and insulin resistance. *Diabetes* **54**, 1657-1663 (2005).
26. Seale, P.*, et al.* Prdm16 determines the thermogenic program of subcutaneous white adipose tissue in mice. *J Clin Invest* **121**, 96-105 (2011).
27. Ortega-Molina, A.*, et al.* Pten positively regulates brown adipose function, energy expenditure, and longevity. *Cell Metab* **15**, 382-394 (2012).
28. Kopecky, J., Clarke, G., Enerback, S., Spiegelman, B. & Kozak, L.P. Expression of the mitochondrial uncoupling protein gene from the aP2 gene promoter prevents genetic obesity. *J Clin Invest* **96**, 2914-2923 (1995).
29. Stefl, B.*, et al.* Brown fat is essential for cold-induced thermogenesis but not for obesity resistance in aP2-Ucp mice. *Am J Physiol* **274**, E527-533 (1998).
30. Tsukiyama-Kohara, K.*, et al.* Adipose tissue reduction in mice lacking the translational inhibitor 4E-BP1. *Nat Med* **7**, 1128-1132 (2001).
31. Yu, X.X.*, et al.* Reduced adiposity and improved insulin sensitivity in obese mice with antisense suppression of 4E-BP2 expression. *American journal of physiology. Endocrinology and metabolism* **294**, E530-539 (2008).
32. Fournier, B.*, et al.* Blockade of the activin receptor IIb activates functional brown adipogenesis and thermogenesis by inducing mitochondrial oxidative metabolism. *Mol Cell Biol* **32**, 2871-2879 (2012).
33. Koncarevic, A.*, et al.* A novel therapeutic approach to treating obesity through modulation of TGFbeta signaling. *Endocrinology* **153**, 3133-3146 (2012).
34. Kiefer, F.W.*, et al.* Retinaldehyde dehydrogenase 1 regulates a thermogenic program in white adipose tissue. *Nat Med* (2012).
35. Patwari, P.*, et al.* The arrestin domain-containing 3 protein regulates body mass and energy expenditure. *Cell Metab* **14**, 671-683 (2011).
36. Singh, R.*, et al.* Autophagy regulates adipose mass and differentiation in mice. *J Clin Invest* **119**, 3329-3339 (2009).
37. Wang, C.*, et al.* ATF4 regulates lipid metabolism and thermogenesis. *Cell Res* **20**, 174-184 (2010).
38. Meakin, P.J.*, et al.* Reduction in BACE1 decreases body weight, protects against diet-induced obesity and enhances insulin sensitivity in mice. *Biochem J* **441**, 285-296 (2012).

39. Zhou, Z.*, et al.* Cidea-deficient mice have lean phenotype and are resistant to obesity. *Nature genetics* **35**, 49-56 (2003).
40. Perwitz, N.*, et al.* Cannabinoid type 1 receptor blockade induces transdifferentiation towards a brown fat phenotype in white adipocytes. *Diabetes Obes Metab* **12**, 158-166 (2010).
41. Bale, T.L.*, et al.* Corticotropin-releasing factor receptor-2-deficient mice display abnormal homeostatic responses to challenges of increased dietary fat and cold. *Endocrinology* **144**, 2580-2587 (2003).
42. Bjursell, M.*, et al.* Improved glucose control and reduced body fat mass in free fatty acid receptor 2-deficient mice fed a high-fat diet. *American journal of physiology. Endocrinology and metabolism* **300**, E211-220 (2011).
43. Nakae, J.*, et al.* Forkhead transcription factor FoxO1 in adipose tissue regulates energy storage and expenditure. *Diabetes* **57**, 563-576 (2008).
44. Toh, S.Y.*, et al.* Up-regulation of mitochondrial activity and acquirement of brown adipose tissue-like property in the white adipose tissue of fsp27 deficient mice. *PLoS One* **3**, e2890 (2008).
45. Lin, L.*, et al.* Ablation of ghrelin receptor reduces adiposity and improves insulin sensitivity during aging by regulating fat metabolism in white and brown adipose tissues. *Aging Cell* **10**, 996-1010 (2011).
46. Vila-Bedmar, R.*, et al.* GRK2 contribution to the regulation of energy expenditure and brown fat function. *FASEB J* (2012).
47. Satyanarayana, A., Klarmann, K.D., Gavrilova, O. & Keller, J.R. Ablation of the transcriptional regulator Id1 enhances energy expenditure, increases insulin sensitivity, and protects against age and diet induced insulin resistance, and hepatosteatosis. *FASEB journal : official publication of the Federation of American Societies for Experimental Biology* **26**, 309-323 (2012).
48. Chiang, S.H.*, et al.* The protein kinase IKKepsilon regulates energy balance in obese mice. *Cell* **138**, 961-975 (2009).
49. Strom, K.*, et al.* Attainment of brown adipocyte features in white adipocytes of hormone-sensitive lipase null mice. *PLoS One* **3**, e1793 (2008).
50. Liu, W.*, et al.* Low density lipoprotein (LDL) receptor-related protein 6 (LRP6) regulates body fat and glucose homeostasis by modulating nutrient sensing pathways and mitochondrial energy expenditure. *J Biol Chem* **287**, 7213-7223 (2012).
51. Wang, H.*, et al.* Liver X receptor alpha is a transcriptional repressor of the uncoupling protein 1 gene and the brown fat phenotype. *Mol Cell Biol* **28**, 2187-2200 (2008).
52. Zhang, C.*, et al.* Inhibition of myostatin protects against diet-induced obesity by enhancing fatty acid oxidation and promoting a brown adipose phenotype in mice. *Diabetologia* **55**, 183-193 (2012).
53. Bordicchia, M.*, et al.* Cardiac natriuretic peptides act via p38 MAPK to induce the brown fat thermogenic program in mouse and human adipocytes. *J Clin Invest* **122**, 1022-1036 (2012).
54. Czyzyk, T.A.*, et al.* Mice lacking delta-opioid receptors resist the development of diet-induced obesity. *FASEB J* (2012).
55. Scime, A.*, et al.* Rb and p107 regulate preadipocyte differentiation into white versus brown fat through repression of PGC-1alpha. *Cell Metab* **2**, 283-295 (2005).

56. Kang, H.W.*, et al.* Mice lacking Pctp /StarD2 exhibit increased adaptive thermogenesis and enlarged mitochondria in brown adipose tissue. *J Lipid Res* **50**, 2212-2221 (2009).
57. Hansen, J.B.*, et al.* Retinoblastoma protein functions as a molecular switch determining white versus brown adipocyte differentiation. *Proc Natl Acad Sci U S A* **101**, 4112-4117 (2004).
58. Armengol, J.*, et al.* Pref-1 in brown adipose tissue: specific involvement in brown adipocyte differentiation and regulatory role of C/EBPdelta. *Biochem J* **443**, 799-810 (2012).
59. Cummings, D.E.*, et al.* Genetically lean mice result from targeted disruption of the RII beta subunit of protein kinase A. *Nature* **382**, 622-626 (1996).
60. Huang, W., Bansode, R.R., Bal, N.C., Mehta, M. & Mehta, K.D. Protein kinase Cbeta deficiency attenuates obesity syndrome of ob/ob mice by promoting white adipose tissue remodeling. *J Lipid Res* **53**, 368-378 (2012).
61. Auffret, J.*, et al.* Beige differentiation of adipose depots in mice lacking prolactin receptor protects against high-fat-diet-induced obesity. *FASEB J* (2012).
62. Christian, M.*, et al.* RIP140-targeted repression of gene expression in adipocytes. *Mol Cell Biol* **25**, 9383-9391 (2005).
63. Leonardsson, G.*, et al.* Nuclear receptor corepressor RIP140 regulates fat accumulation. *Proc Natl Acad Sci U S A* **101**, 8437-8442 (2004).
64. Powelka, A.M.*, et al.* Suppression of oxidative metabolism and mitochondrial biogenesis by the transcriptional corepressor RIP140 in mouse adipocytes. *J Clin Invest* **116**, 125-136 (2006).
65. Sampath, H.*, et al.* Skin-specific deletion of stearoyl-CoA desaturase-1 alters skin lipid composition and protects mice from high fat diet-induced obesity. *J Biol Chem* **284**, 19961-19973 (2009).
66. Mori, H.*, et al.* Secreted frizzled-related protein 5 suppresses adipocyte mitochondrial metabolism through WNT inhibition. *J Clin Invest* **122**, 2405-2416 (2012).
67. Yadav, H.*, et al.* Protection from obesity and diabetes by blockade of TGF-beta/Smad3 signaling. *Cell Metab* **14**, 67-79 (2011).
68. Picard, F.*, et al.* SRC-1 and TIF2 control energy balance between white and brown adipose tissues. *Cell* **111**, 931-941 (2002).
69. Romanatto, T.*, et al.* Deletion of tumor necrosis factor-alpha receptor 1 (TNFR1) protects against diet-induced obesity by means of increased thermogenesis. *J Biol Chem* **284**, 36213-36222 (2009).
70. Ye, L.*, et al.* TRPV4 is a regulator of adipose oxidative metabolism, inflammation, and energy homeostasis. *Cell* **151**, 96-110 (2012).
71. Pan, D., Fujimoto, M., Lopes, A. & Wang, Y.X. Twist-1 is a PPARdelta-inducible, negative-feedback regulator of PGC-1alpha in brown fat metabolism. *Cell* **137**, 73-86 (2009).
72. Lu, X.*, et al.* Resistance to obesity by repression of VEGF gene expression through induction of brown-like adipocyte differentiation. *Endocrinology* **153**, 3123-3132 (2012).
73. Watson, E.*, et al.* Analysis of knockout mice suggests a role for VGF in the control of fat storage and energy expenditure. *BMC Physiol* **9**, 19 (2009).
74. Heaton, J.M. The distribution of brown adipose tissue in the human. *J Anat* **112**, 35-39 (1972).

75. Sanchez-Gurmaches, J.*, et al.* PTEN loss in the Myf5 lineage redistributes body fat and reveals subsets of white adipocytes that arise from Myf5 precursors. *Cell Metab* **16**, 348-362 (2012).
76. Lepper, C. & Fan, C.M. Inducible lineage tracing of Pax7-descendant cells reveals embryonic origin of adult satellite cells. *Genesis* **48**, 424-436 (2010).
77. Timmons, J.A.*, et al.* Myogenic gene expression signature establishes that brown and white adipocytes originate from distinct cell lineages. *Proc Natl Acad Sci U S A* **104**, 4401-4406 (2007).
78. Forner, F.*, et al.* Proteome differences between brown and white fat mitochondria reveal specialized metabolic functions. *Cell metabolism* **10**, 324-335 (2009).
79. Himms-Hagen, J.*, et al.* Multilocular fat cells in WAT of CL-316243-treated rats derive directly from white adipocytes. *Am J Physiol Cell Physiol* **279**, C670-681 (2000).
80. Wang Q, T.C., Gupta RK, Scherer PE. Tracking adipogenesis during white adipose tissue development, expansion and regeneration. *Cell Metabolism* (2013).
81. Rosenwald, M., Perdikari, A., Rulicke, T. & Wolfrum, C. Bi-directional interconversion of brite and white adipocytes. *Nat Cell Biol* (2013).
82. Barbatelli, G.*, et al.* The emergence of cold-induced brown adipocytes in mouse white fat depots is determined predominantly by white to brown adipocyte transdifferentiation. *Am J Physiol Endocrinol Metab* **298**, E1244-1253 (2010).
83. Lee, Y.H., Petkova, A.P., Mottillo, E.P. & Granneman, J.G. In vivo identification of bipotential adipocyte progenitors recruited by beta3-adrenoceptor activation and high-fat feeding. *Cell Metab* **15**, 480-491 (2012).
84. Berry, R. & Rodeheffer, M.S. Characterization of the adipocyte cellular lineage in vivo. *Nat Cell Biol* **15**, 302-308 (2013).
85. Elabd, C.*, et al.* Human multipotent adipose-derived stem cells differentiate into functional brown adipocytes. *Stem cells* **27**, 2753-2760 (2009).
86. Cypess, A.M.*, et al.* Anatomical localization, gene expression profiling and functional characterization of adult human neck brown fat. *Nat Med* (2013).
87. Seale, P.*, et al.* Transcriptional control of brown fat determination by PRDM16. *Cell Metab* **6**, 38-54 (2007).
88. Lee, P.*, et al.* High prevalence of brown adipose tissue in adult humans. *J Clin Endocrinol Metab* **96**, 2450-2455 (2011).
89. Hondares, E.*, et al.* Thiazolidinediones and rexinoids induce peroxisome proliferator-activated receptor-coactivator (PGC)-1alpha gene transcription: an autoregulatory loop controls PGC-1alpha expression in adipocytes via peroxisome proliferator-activated receptor-gamma coactivation. *Endocrinology* **147**, 2829-2838 (2006).
90. Kajimura, S.*, et al.* Initiation of myoblast to brown fat switch by a PRDM16-C/EBP-beta transcriptional complex. *Nature* **460**, 1154-1158 (2009).
91. Ohno, H., Shinoda, K., Spiegelman, B.M. & Kajimura, S. PPARgamma agonists induce a white-to-brown fat conversion through stabilization of PRDM16 protein. *Cell Metab* **15**, 395-404 (2012).
92. Tseng, Y.H.*, et al.* New role of bone morphogenetic protein 7 in brown adipogenesis and energy expenditure. *Nature* **454**, 1000-1004 (2008).
93. Schulz, T.J.*, et al.* Identification of inducible brown adipocyte progenitors residing in skeletal muscle and white fat. *Proc Natl Acad Sci U S A* **108**, 143-148 (2011).

94. Schulz, T.J.*, et al.* Brown-fat paucity due to impaired BMP signalling induces compensatory browning of white fat. *Nature* **495**, 379-383 (2013).
95. Trajkovski, M., Ahmed, K., Esau, C.C. & Stoffel, M. MyomiR-133 regulates brown fat differentiation through Prdm16. *Nat Cell Biol* **14**, 1330-1335 (2012).
96. Liu, W.*, et al.* miR-133a Regulates Adipocyte Browning In Vivo. *PLoS genetics* **9**, e1003626 (2013).
97. Yin, H.*, et al.* MicroRNA-133 controls brown adipose determination in skeletal muscle satellite cells by targeting Prdm16. *Cell Metab* **17**, 210-224 (2013).
98. Rothwell, N.J. & Stock, M.J. A role for brown adipose tissue in diet-induced thermogenesis. *Nature* **281**, 31-35 (1979).
99. Lowell, B.B.*, et al.* Development of obesity in transgenic mice after genetic ablation of brown adipose tissue. *Nature* **366**, 740-742 (1993).
100. Enerback, S.*, et al.* Mice lacking mitochondrial uncoupling protein are cold-sensitive but not obese. *Nature* **387**, 90-94 (1997).
101. Feldmann, H.M., Golozoubova, V., Cannon, B. & Nedergaard, J. UCP1 ablation induces obesity and abolishes diet-induced thermogenesis in mice exempt from thermal stress by living at thermoneutrality. *Cell Metab* **9**, 203-209 (2009).
102. Anunciado-Koza, R.P.*, et al.* Inactivation of the mitochondrial carrier SLC25A25 (ATP-Mg2+/Pi transporter) reduces physical endurance and metabolic efficiency in mice. *The Journal of biological chemistry* **286**, 11659-11671 (2011).
103. Bal, N.C.*, et al.* Sarcolipin is a newly identified regulator of muscle-based thermogenesis in mammals. *Nat Med* **18**, 1575-1579 (2012).
104. Kontani, Y.*, et al.* UCP1 deficiency increases susceptibility to diet-induced obesity with age. *Aging cell* **4**, 147-155 (2005).
105. Ma, S.W., Foster, D.O., Nadeau, B.E. & Triandafillou, J. Absence of increased oxygen consumption in brown adipose tissue of rats exhibiting "cafeteria" diet-induced thermogenesis. *Canadian journal of physiology and pharmacology* **66**, 1347-1354 (1988).
106. Anunciado-Koza, R., Ukropec, J., Koza, R.A. & Kozak, L.P. Inactivation of UCP1 and the glycerol phosphate cycle synergistically increases energy expenditure to resist diet-induced obesity. *J Biol Chem* **283**, 27688-27697 (2008).
107. Fromme, T. & Klingenspor, M. Uncoupling protein 1 expression and high-fat diets. *American journal of physiology. Regulatory, integrative and comparative physiology* **300**, R1-8 (2011).
108. Bostrom, P.*, et al.* A PGC1-alpha-dependent myokine that drives brown-fat-like development of white fat and thermogenesis. *Nature* **481**, 463-468 (2012).
109. Collins, S., Daniel, K.W., Petro, A.E. & Surwit, R.S. Strain-specific response to beta 3-adrenergic receptor agonist treatment of diet-induced obesity in mice. *Endocrinology* **138**, 405-413 (1997).
110. Guerra, C., Koza, R.A., Yamashita, H., Walsh, K. & Kozak, L.P. Emergence of brown adipocytes in white fat in mice is under genetic control. Effects on body weight and adiposity. *J Clin Invest* **102**, 412-420 (1998).
111. Stanford, K.I.*, et al.* Brown adipose tissue regulates glucose homeostasis and insulin sensitivity. *J Clin Invest* **123**, 215-223 (2013).

112. Qiang, L.*, et al.* Brown remodeling of white adipose tissue by SirT1-dependent deacetylation of Ppargamma. *Cell* **150**, 620-632 (2012).
113. Bartelt, A.*, et al.* Brown adipose tissue activity controls triglyceride clearance. *Nat Med* **17**, 200-205 (2011).
114. Chang, L.*, et al.* Loss of perivascular adipose tissue on peroxisome proliferator-activated receptor-gamma deletion in smooth muscle cells impairs intravascular thermoregulation and enhances atherosclerosis. *Circulation* **126**, 1067-1078 (2012).
115. Morrison, S.F., Madden, C.J. & Tupone, D. Central control of brown adipose tissue thermogenesis. *Front Endocrinol (Lausanne)* **3**(2012).
116. Nguyen, K.D.*, et al.* Alternatively activated macrophages produce catecholamines to sustain adaptive thermogenesis. *Nature* **480**, 104-108 (2011).
117. Collins, S. beta-Adrenoceptor Signaling Networks in Adipocytes for Recruiting Stored Fat and Energy Expenditure. *Frontiers in endocrinology* **2**, 102 (2012).
118. Bukowiecki, L., Collet, A.J., Follea, N., Guay, G. & Jahjah, L. Brown adipose tissue hyperplasia: a fundamental mechanism of adaptation to cold and hyperphagia. *Am J Physiol* **242**, E353-359 (1982).
119. Desautels, M., Dulos, R.A. & Mozaffari, B. Selective loss of uncoupling protein from mitochondria of surgically denervated brown adipose tissue of cold-acclimated mice. *Biochemistry and cell biology = Biochimie et biologie cellulaire* **64**, 1125-1134 (1986).
120. Cannon, B. & Nedergaard, J. Brown adipose tissue: function and physiological significance. *Physiol Rev* **84**, 277-359 (2004).
121. Nicholls, D.G. The physiological regulation of uncoupling proteins. *Biochimica et biophysica acta* **1757**, 459-466 (2006).
122. Fedorenko, A., Lishko, P.V. & Kirichok, Y. Mechanism of fatty-acid-dependent UCP1 uncoupling in brown fat mitochondria. *Cell* **151**, 400-413 (2012).
123. Jastroch, M., Hirschberg, V. & Klingenspor, M. Functional characterization of UCP1 in mammalian HEK293 cells excludes mitochondrial uncoupling artefacts and reveals no contribution to basal proton leak. *Biochimica et biophysica acta* **1817**, 1660-1670 (2012).
124. Shabalina, I.G.*, et al.* Uncoupling protein-1 is not leaky. *Biochim Biophys Acta* **1797**, 773-784 (2010).
125. Barbatelli, G.*, et al.* The Emergence of Cold-Induced Brown Adipocytes in Mouse White Fat Depots Is Predominantly Determined by White to Brown Adipocyte Transdifferentiation. *American journal of physiology. Endocrinology and metabolism* **298**, E1244-E1253 (2010).
126. Cousin, B.*, et al.* Occurrence of brown adipocytes in rat white adipose tissue: molecular and morphological characterization. *Journal of cell science* **103 (Pt 4)**, 931-942 (1992).
127. Huttunen, P., Hirvonen, J. & Kinnula, V. The occurrence of brown adipose tissue in outdoor workers. *Eur J Appl Physiol Occup Physiol* **46**, 339-345 (1981).
128. Young, P., Arch, J.R. & Ashwell, M. Brown adipose tissue in the parametrial fat pad of the mouse. *FEBS Lett* **167**, 10-14 (1984).
129. Murano, I., Barbatelli, G., Giordano, A. & Cinti, S. Noradrenergic parenchymal nerve fiber branching after cold acclimatisation correlates with brown adipocyte density in mouse adipose organ. *J Anat* **214**, 171-178 (2009).

130. Xue, Y.*, et al.* FOXC2 controls Ang-2 expression and modulates angiogenesis, vascular patterning, remodeling, and functions in adipose tissue. *Proc Natl Acad Sci U S A* **105**, 10167-10172 (2008).
131. Lidell, M.E.*, et al.* The adipocyte-expressed forkhead transcription factor Foxc2 regulates metabolism through altered mitochondrial function. *Diabetes* **60**, 427-435 (2011).
132. Buemann, B., Toubro, S. & Astrup, A. Effects of the two beta3-agonists, ZD7114 and ZD2079 on 24 hour energy expenditure and respiratory quotient in obese subjects. *International journal of obesity and related metabolic disorders : journal of the International Association for the Study of Obesity* **24**, 1553-1560 (2000).
133. Arch, J.R. beta(3)-Adrenoceptor agonists: potential, pitfalls and progress. *European journal of pharmacology* **440**, 99-107 (2002).
134. Foster, D.O. & Frydman, M.L. Nonshivering thermogenesis in the rat. II. Measurements of blood flow with microspheres point to brown adipose tissue as the dominant site of the calorigenesis induced by noradrenaline. *Canadian journal of physiology and pharmacology* **56**, 110-122 (1978).
135. Xue, Y.*, et al.* Hypoxia-independent angiogenesis in adipose tissues during cold acclimation. *Cell Metab* **9**, 99-109 (2009).
136. Asano, A., Morimatsu, M., Nikami, H., Yoshida, T. & Saito, M. Adrenergic activation of vascular endothelial growth factor mRNA expression in rat brown adipose tissue: implication in cold-induced angiogenesis. *Biochem J* **328 (Pt 1)**, 179-183 (1997).
137. Tonello, C.*, et al.* Role of sympathetic activity in controlling the expression of vascular endothelial growth factor in brown fat cells of lean and genetically obese rats. *FEBS Lett* **442**, 167-172 (1999).
138. Bagchi, M.*, et al.* Vascular endothelial growth factor is important for brown adipose tissue development and maintenance. *FASEB J* **27**, 3257-3271 (2013).
139. Elias, I.*, et al.* Adipose tissue overexpression of vascular endothelial growth factor protects against diet-induced obesity and insulin resistance. *Diabetes* **61**, 1801-1813 (2012).
140. Sun, K.*, et al.* Dichotomous effects of VEGF-A on adipose tissue dysfunction. *Proc Natl Acad Sci U S A* **109**, 5874-5879 (2012).
141. Puigserver, P.*, et al.* A cold-inducible coactivator of nuclear receptors linked to adaptive thermogenesis. *Cell* **92**, 829-839 (1998).
142. Tiraby, C.*, et al.* Acquirement of brown fat cell features by human white adipocytes. *J Biol Chem* **278**, 33370-33376 (2003).
143. Lin, J.*, et al.* Defects in adaptive energy metabolism with CNS-linked hyperactivity in PGC-1alpha null mice. *Cell* **119**, 121-135 (2004).
144. Leone, T.C.*, et al.* PGC-1alpha deficiency causes multi-system energy metabolic derangements: muscle dysfunction, abnormal weight control and hepatic steatosis. *PLoS Biol* **3**, e101 (2005).
145. Uldry, M.*, et al.* Complementary action of the PGC-1 coactivators in mitochondrial biogenesis and brown fat differentiation. *Cell Metab* **3**, 333-341 (2006).
146. Kleiner, S.*, et al.* Development of insulin resistance in mice lacking PGC-1alpha in adipose tissues. *Proc Natl Acad Sci U S A* **109**, 9635-9640 (2012).
147. Cao, W.*, et al.* p38 mitogen-activated protein kinase is the central regulator of cyclic AMP-dependent transcription of the brown fat uncoupling protein 1 gene. *Mol Cell Biol* **24**, 3057-3067 (2004).

148. Cao, W., Medvedev, A.V., Daniel, K.W. & Collins, S. beta-Adrenergic activation of p38 MAP kinase in adipocytes: cAMP induction of the uncoupling protein 1 (UCP1) gene requires p38 MAP kinase. *J Biol Chem* **276**, 27077-27082 (2001).
149. Hallberg, M.*, et al.* A functional interaction between RIP140 and PGC-1alpha regulates the expression of the lipid droplet protein CIDEA. *Mol Cell Biol* **28**, 6785-6795 (2008).
150. Rosen, E.D. & MacDougald, O.A. Adipocyte differentiation from the inside out. *Nat Rev Mol Cell Biol* **7**, 885-896 (2006).
151. Mori, M., Nakagami, H., Rodriguez-Araujo, G., Nimura, K. & Kaneda, Y. Essential role for miR-196a in brown adipogenesis of white fat progenitor cells. *PLoS Biol* **10**, e1001314 (2012).
152. Carmona, M.C.*, et al.* Defective thermoregulation, impaired lipid metabolism, but preserved adrenergic induction of gene expression in brown fat of mice lacking C/EBPbeta. *Biochem J* **389**, 47-56 (2005).
153. Karamanlidis, G., Karamitri, A., Docherty, K., Hazlerigg, D.G. & Lomax, M.A. C/EBPbeta reprograms white 3T3-L1 preadipocytes to a Brown adipocyte pattern of gene expression. *J Biol Chem* **282**, 24660-24669 (2007).
154. Tanaka, T., Yoshida, N., Kishimoto, T. & Akira, S. Defective adipocyte differentiation in mice lacking the C/EBPbeta and/or C/EBPdelta gene. *Embo J* **16**, 7432-7443 (1997).
155. Tai, T.A.*, et al.* Activation of the nuclear receptor peroxisome proliferator-activated receptor gamma promotes brown adipocyte differentiation. *J Biol Chem* **271**, 29909-29914 (1996).
156. Rajakumari, S.*, et al.* EBF2 Determines and Maintains Brown Adipocyte Identity. *Cell Metab* **17**, 562-574 (2013).
157. Siersbaek, M.S.*, et al.* Genome-wide profiling of PPARgamma in primary epididymal, inguinal, and brown adipocytes reveals depot-selective binding correlated with gene expression. *Mol Cell Biol* (2012).
158. Fukui, Y., Masui, S., Osada, S., Umesono, K. & Motojima, K. A new thiazolidinedione, NC-2100, which is a weak PPAR-gamma activator, exhibits potent antidiabetic effects and induces uncoupling protein 1 in white adipose tissue of KKAy obese mice. *Diabetes* **49**, 759-767 (2000).
159. Rong, J.X.*, et al.* Adipose mitochondrial biogenesis is suppressed in db/db and high-fat diet-fed mice and improved by rosiglitazone. *Diabetes* **56**, 1751-1760 (2007).
160. Sell, H.*, et al.* Peroxisome proliferator-activated receptor gamma agonism increases the capacity for sympathetically mediated thermogenesis in lean and ob/ob mice. *Endocrinology* **145**, 3925-3934 (2004).
161. Vernochet, C.*, et al.* C/EBPalpha and the corepressors CtBP1 and CtBP2 regulate repression of select visceral white adipose genes during induction of the brown phenotype in white adipocytes by peroxisome proliferator-activated receptor gamma agonists. *Mol Cell Biol* **29**, 4714-4728 (2009).
162. Wilson-Fritch, L.*, et al.* Mitochondrial remodeling in adipose tissue associated with obesity and treatment with rosiglitazone. *J Clin Invest* **114**, 1281-1289 (2004).
163. Digby, J.E.*, et al.* Thiazolidinedione exposure increases the expression of uncoupling protein 1 in cultured human preadipocytes. *Diabetes* **47**, 138-141 (1998).
164. Choi, J.H.*, et al.* Anti-diabetic drugs inhibit obesity-linked phosphorylation of PPARgamma by Cdk5. *Nature* **466**, 451-456 (2011).

165. Bakopanos, E. & Silva, J.E. Thiazolidinediones inhibit the expression of beta3-adrenergic receptors at a transcriptional level. *Diabetes* **49**, 2108-2115 (2000).
166. Festuccia, W.T.*, et al.* Peroxisome proliferator-activated receptor-gamma-mediated positive energy balance in the rat is associated with reduced sympathetic drive to adipose tissues and thyroid status. *Endocrinology* **149**, 2121-2130 (2008).
167. Bonet, M.L., Oliver, P. & Palou, A. Pharmacological and nutritional agents promoting browning of white adipose tissue. *Biochimica et biophysica acta* **1831**, 969-985 (2013).
168. Villarroya, F. & Vidal-Puig, A. Beyond the sympathetic tone: the new brown fat activators. *Cell metabolism* **17**, 638-643 (2013).
169. Lira, V.A., Benton, C.R., Yan, Z. & Bonen, A. PGC-1alpha regulation by exercise training and its influences on muscle function and insulin sensitivity. *Am J Physiol Endocrinol Metab* **299**, E145-161 (2010).
170. Wenz, T., Rossi, S.G., Rotundo, R.L., Spiegelman, B.M. & Moraes, C.T. Increased muscle PGC-1alpha expression protects from sarcopenia and metabolic disease during aging. *Proc Natl Acad Sci U S A* **106**, 20405-20410 (2009).
171. Chartoumpekis, D.V.*, et al.* Brown adipose tissue responds to cold and adrenergic stimulation by induction of FGF21. *Mol Med* **17**, 736-740 (2011).
172. Hondares, E.*, et al.* Thermogenic activation induces FGF21 expression and release in brown adipose tissue. *J Biol Chem* **286**, 12983-12990 (2011).
173. Hondares, E.*, et al.* Hepatic FGF21 expression is induced at birth via PPARalpha in response to milk intake and contributes to thermogenic activation of neonatal brown fat. *Cell Metab* **11**, 206-212 (2010).
174. Coskun, T.*, et al.* Fibroblast growth factor 21 corrects obesity in mice. *Endocrinology* **149**, 6018-6027 (2008).
175. Fisher, F.M.*, et al.* FGF21 regulates PGC-1alpha and browning of white adipose tissues in adaptive thermogenesis. *Genes Dev* **26**, 271-281 (2012).
176. Kharitonenkov, A.*, et al.* FGF-21 as a novel metabolic regulator. *J Clin Invest* **115**, 1627-1635 (2005).
177. Xu, J.*, et al.* Fibroblast growth factor 21 reverses hepatic steatosis, increases energy expenditure, and improves insulin sensitivity in diet-induced obese mice. *Diabetes* **58**, 250-259 (2009).
178. Wei, W.*, et al.* Fibroblast growth factor 21 promotes bone loss by potentiating the effects of peroxisome proliferator-activated receptor gamma. *Proc Natl Acad Sci U S A* **109**, 3143-3148 (2012).
179. Chainani-Wu, N.*, et al.* Relation of B-type natriuretic peptide levels to body mass index after comprehensive lifestyle changes. *Am J Cardiol* **105**, 1570-1576 (2010).
180. Sengenes, C., Berlan, M., De Glisezinski, I., Lafontan, M. & Galitzky, J. Natriuretic peptides: a new lipolytic pathway in human adipocytes. *FASEB journal : official publication of the Federation of American Societies for Experimental Biology* **14**, 1345-1351 (2000).
181. Whittle, A.J.*, et al.* BMP8B increases brown adipose tissue thermogenesis through both central and peripheral actions. *Cell* **149**, 871-885 (2012).
182. de Jesus, L.A.*, et al.* The type 2 iodothyronine deiodinase is essential for adaptive thermogenesis in brown adipose tissue. *J Clin Invest* **108**, 1379-1385 (2001).

183. Lopez, M.*, et al.* Hypothalamic AMPK and fatty acid metabolism mediate thyroid regulation of energy balance. *Nature medicine* **16**, 1001-1008 (2010).
184. Silva, J.E. Thermogenic mechanisms and their hormonal regulation. *Physiological reviews* **86**, 435-464 (2006).
185. Sellayah, D., Bharaj, P. & Sikder, D. Orexin is required for brown adipose tissue development, differentiation and function. *Cell Metab* (2011).
186. Zhang, W.*, et al.* Orexin neurons are indispensable for stress-induced thermogenesis in mice. *J Physiol* **588**, 4117-4129 (2010).
187. Harms, M. & Seale, P. Brown and beige fat: development, function and therapeutic potential. *Nat Med* **19**, 1252-1263 (2013).
188. Cohen, P.*, et al.* Ablation of PRDM16 and Beige Adipose Causes Metabolic Dysfunction and a Subcutaneous to Visceral Fat Switch. *Cell* **156**, 304-316 (2014).
189. Atit, R.*, et al.* Beta-catenin activation is necessary and sufficient to specify the dorsal dermal fate in the mouse. *Developmental biology* **296**, 164-176 (2006).
190. Ohno, H., Shinoda, K., Ohyama, K., Sharp, L.Z. & Kajimura, S. EHMT1 controls brown adipose cell fate and thermogenesis through the PRDM16 complex. *Nature* (2013).
191. Sun, L.*, et al.* Mir193b-365 is essential for brown fat differentiation. *Nat Cell Biol* **13**, 958-965 (2011).
192. Tallquist, M.D., Weismann, K.E., Hellstrom, M. & Soriano, P. Early myotome specification regulates PDGFA expression and axial skeleton development. *Development* **127**, 5059-5070 (2000).
193. Wang, W.*, et al.* Ebf2 is a selective marker of brown and beige adipogenic precursor cells. *Proc Natl Acad Sci U S A* **111**, 14466-14471 (2014).
194. Uezumi, A., Fukada, S., Yamamoto, N., Takeda, S. & Tsuchida, K. Mesenchymal progenitors distinct from satellite cells contribute to ectopic fat cell formation in skeletal muscle. *Nat Cell Biol* **12**, 143-152 (2010).
195. Cannon, B. & Nedergaard, J. Nonshivering thermogenesis and its adequate measurement in metabolic studies. *The Journal of experimental biology* **214**, 242-253 (2011).
196. Golozoubova, V., Cannon, B. & Nedergaard, J. UCP1 is essential for adaptive adrenergic nonshivering thermogenesis. *American journal of physiology. Endocrinology and metabolism* **291**, E350-357 (2006).
197. Hohenauer, T. & Moore, A.W. The Prdm family: expanding roles in stem cells and development. *Development* **139**, 2267-2282 (2012).
198. Ishibashi, J.*, et al.* An Evi1-C/EBPbeta complex controls peroxisome proliferator-activated receptor gamma2 gene expression to initiate white fat cell differentiation. *Mol Cell Biol* **32**, 2289-2299 (2012).
199. Goyama, S.*, et al.* Evi-1 is a critical regulator for hematopoietic stem cells and transformed leukemic cells. *Cell stem cell* **3**, 207-220 (2008).
200. Derecka, M.*, et al.* Tyk2 and Stat3 Regulate Brown Adipose Tissue Differentiation and Obesity. *Cell Metab* **16**, 814-824 (2012).
201. Park, J.H.*, et al.* A multifunctional protein, EWS, is essential for early brown fat lineage determination. *Developmental cell* **26**, 393-404 (2013).

202. Yin, H.*, et al.* MicroRNA-133 controls brown adipose determination in skeletal muscle satellite cells by targeting Prdm16. *Cell Metab* **17**, 210-224 (2013).
203. Connolly, E., Morrisey, R.D. & Carnie, J.A. The effect of interscapular brown adipose tissue removal on body-weight and cold response in the mouse. *Br J Nutr* **47**, 653-658 (1982).
204. Rothwell, N.J. & Stock, M.J. Surgical removal of brown fat results in rapid and complete compensation by other depots. *Am J Physiol* **257**, R253-258 (1989).
205. Motyl, K.J. & Rosen, C.J. Temperatures rising: brown fat and bone. *Discovery medicine* **11**, 179-185 (2011).
206. Daubas, P.*, et al.* The regulatory mechanisms that underlie inappropriate transcription of the myogenic determination gene Myf5 in the central nervous system. *Developmental biology* **327**, 71-82 (2009).
207. Tajbakhsh, S. & Buckingham, M.E. Lineage restriction of the myogenic conversion factor myf-5 in the brain. *Development* **121**, 4077-4083 (1995).
208. Rajakumari, S.*, et al.* EBF2 determines and maintains brown adipocyte identity. *Cell Metab* **17**, 562-574 (2013).
209. Smyth, G.K., Michaud, J. & Scott, H.S. Use of within-array replicate spots for assessing differential expression in microarray experiments. *Bioinformatics* **21**, 2067-2075 (2005).
210. Mullner, D. fastcluster: Fast Hierarchical, Agglomerative Clustering Routines for R and Python. *Journal of Statistical Software* **53**, 1-18 (2013).
211. Heinz, S.*, et al.* Simple combinations of lineage-determining transcription factors prime cis-regulatory elements required for macrophage and B cell identities. *Molecular cell* **38**, 576-589 (2010).
212. Amthor, H.*, et al.* Lack of myostatin results in excessive muscle growth but impaired force generation. *Proc Natl Acad Sci U S A* **104**, 1835-1840 (2007).
213. Pinheiro, I.*, et al.* Prdm3 and Prdm16 are H3K9me1 methyltransferases required for mammalian heterochromatin integrity. *Cell* **150**, 948-960 (2012).
214. Harms, M.J.*, et al.* Prdm16 is required for the maintenance of brown adipocyte identity and function in adult mice. *Cell Metab* **19**, 593-604 (2014).
215. Kajimura, S.*, et al.* Regulation of the brown and white fat gene programs through a PRDM16/CtBP transcriptional complex *Genes Dev* **22**(2008).
216. Whyte, W.A.*, et al.* Master transcription factors and mediator establish super-enhancers at key cell identity genes. *Cell* **153**, 307-319 (2013).
217. Nishikata, I.*, et al.* A novel EVI1 gene family, MEL1, lacking a PR domain (MEL1S) is expressed mainly in t(1;3)(p36;q21)-positive AML and blocks G-CSF-induced myeloid differentiation. *Blood* **102**, 3323-3332 (2003).
218. Malik, S. & Roeder, R.G. The metazoan Mediator co-activator complex as an integrative hub for transcriptional regulation. *Nature reviews. Genetics* **11**, 761-772 (2010).
219. Borggrefe, T. & Yue, X. Interactions between subunits of the Mediator complex with gene-specific transcription factors. *Seminars in cell & developmental biology* **22**, 759-768 (2011).
220. Malik, S. & Roeder, R.G. Dynamic regulation of pol II transcription by the mammalian Mediator complex. *Trends in biochemical sciences* **30**, 256-263 (2005).
221. Loven, J.*, et al.* Selective inhibition of tumor oncogenes by disruption of super-enhancers. *Cell* **153**, 320-334 (2013).

222. Siersbaek, R.*, et al.* Transcription factor cooperativity in early adipogenic hotspots and super-enhancers. *Cell reports* **7**, 1443-1455 (2014).
223. Langmead, B., Trapnell, C., Pop, M. & Salzberg, S.L. Ultrafast and memory-efficient alignment of short DNA sequences to the human genome. in *Genome Biology*, Vol. 10 (BioMed Central Ltd, 2009).
224. Heinz, S.*, et al.* Simple Combinations of Lineage-Determining Transcription Factors Prime cis-Regulatory Elements Required for Macrophage and B Cell Identities. *Molecular Cell* **38**, 576-589 (2010).
225. Bernstein, B.E.*, et al.* An integrated encyclopedia of DNA elements in the human genome. *Nature* **489**, 57-74 (2012).
226. Quinlan, A.R. & Hall, I.M. BEDTools: a flexible suite of utilities for comparing genomic features. *Bioinformatics* **26**, 841-842 (2010).
227. Hnisz, D.*, et al.* Super-enhancers in the control of cell identity and disease. *Cell* **155**, 934-947 (2013).
228. Huang, D., Sherman, B. & Lempicki, R. Systematic and integrative analysis of large gene lists using DAVID bioinformatics resources. *Nature Protocols* **4**, 44-57 (2009).
229. Ho, Y., Shewchuk, B.M., Liebhaber, S.A. & Cooke, N.E. Distinct chromatin configurations regulate the initiation and the maintenance of hGH gene expression. *Mol Cell Biol* **33**, 1723-1734 (2013).
230. Ho, Y., Tadevosyan, A., Liebhaber, S.A. & Cooke, N.E. The juxtaposition of a promoter with a locus control region transcriptional domain activates gene expression. *EMBO reports* **9**, 891-898 (2008).
231. Kajimura, S.*, et al.* Regulation of the brown and white fat gene programs through a PRDM16/CtBP transcriptional complex. *Genes Dev* **22**, 1397-1409 (2008).
232. Ohno, H., Shinoda, K., Ohyama, K., Sharp, L.Z. & Kajimura, S. EHMT1 controls brown adipose cell fate and thermogenesis through the PRDM16 complex. *Nature* **504**, 163-167 (2013).
233. Hu, E., Tontonoz, P. & Spiegelman, B.M. Transdifferentiation of myoblasts by the adipogenic transcription factors PPAR gamma and C/EBP alpha. *Proc Natl Acad Sci U S A* **92**, 9856-9860. (1995).